THE REACTIVITY OF NEW ZEALAND ILMENITES

JAMES BERNARD METSON

Submitted for the degree of

Doctor of Philosophy in Chemistry

at Victoria University of Wellington,

New Zealand, October 1980.

ACKNOWLEDGEMENTS

The author would like to thank Professor J. F. Duncan for his continued interest and assistance during the course of this work. The assistance and helpful advice of Dr J. H. Johnston is also gratefully acknowledged.

The author is also grateful to the Industrial Processing Division of DSIR through Mr T. Marshall and Mr B. Judd for both financial support and continued interest and assistance in the course of this work.

My thanks are also due to those who provided advice or technical assistance, particularly Dr S. R. McConnel, Fertilizer Manufacturers Research Association, Auckland N.Z., Dr J. Cole, Geology Department, Victoria University of Wellington, Mr M. Loper, Electron Microscope Laboratory, V.U.W., Mr K. Calder, Geology Department, V.U.W., Mr K. Palmer, Analytical Facility, V.U.W., Mrs J. Benfield, Photographic section, Zoology Department, V.U.W. and my fellow PhD students Mr D. Nelson, Mr K. Morgan and Mr P. Graham.

Mrs M. R. Singleton has my gratitude for her patience and skill in typing this thesis.

My sincere thanks also to Ms J. M. Daniell and my family for their unfailing support.

ABSTRACT

The dissolution of West Coast, South Island, New Zealand ilmenite in acid solutions was studied under a variety of conditions, including concentrations approaching those used industrially. The major dissolution medium considered was hydrochloric acid (1→10 M), at temperatures of 50→80 °C. The series of experiments undertaken sought to establish the factors affecting the reactivity of the ilmenite samples.

Concentrations of dissolved components of the ilmenite were followed by Atomic Absorption spectrometry and the structure and composition of the residual ilmenite was examined by X-ray powder diffraction, X-ray fluorescence, electron microprobe and scanning electron microscopy.

Evidence for the rapid dissolution of an iron-rich surface phase was observed, but the dominant feature of early reaction is selective attack along zones parallel to the basal plane of the ilmenite structure. After the initial phase of rapid dissolution, reaction rate declines and an extended period of concentration/time linearity follows. This decline in rate appears to relate to polymerisation and transport of dissolved titanium within the porous solid.

The addition of phosphate and fluoride to the system, has been shown to seriously affect the properties and transport of dissolved titanium. The effects of other interfering reagents such as additional titanium and iron were also considered.

The observed behaviour of these ilmenites in dissolution, was related to the pattern of natural weathering identified in other ilmenite concentrates. The structure and composition of a range of these materials was examined by X-ray diffraction, Electron microprobe and Mössbauer spectroscopy.

CONTENTS

Chapter 1

INTRODUCTION

1.1 Titanium Dioxide Pigment Production

There are three stable dioxides of titanium, rutile, anatase and brookite. Of these, rutile and anatase have significant pigmenting properties and have almost replaced other white pigments in paints, plastics, enamels and paper. World production of TiO_2 pigments is presently running in excess of two million tonnes per year. The raw materials for the manufacture of these pigments, are the naturally occurring titanium ores rutile (TiO_2) and ilmenite ($FeTiO_3$). Depletion of rutile reserves has meant that the world's considerable deposits of ilmenite (exceeding one billion [US] tonnes outside the USSR and China) have become increasingly attractive as a raw material. Ilmenite occurs in a broad compositional range often enriched in titanium. Enrichment depends on the degree of natural weathering and alteration. Australian ilmenites for example range in composition from close to stoichiometric (52% TiO_2) to very titanium rich (>80% TiO_2). The eventual product of alteration is mineral rutile and Australia also supplies in excess of 90% of the world's natural rutile.

Commercial pigment production utilizes two main methods, the traditional sulphuric acid route and the more recently developed chloride route. The two processes are outlined in figure 1.1.

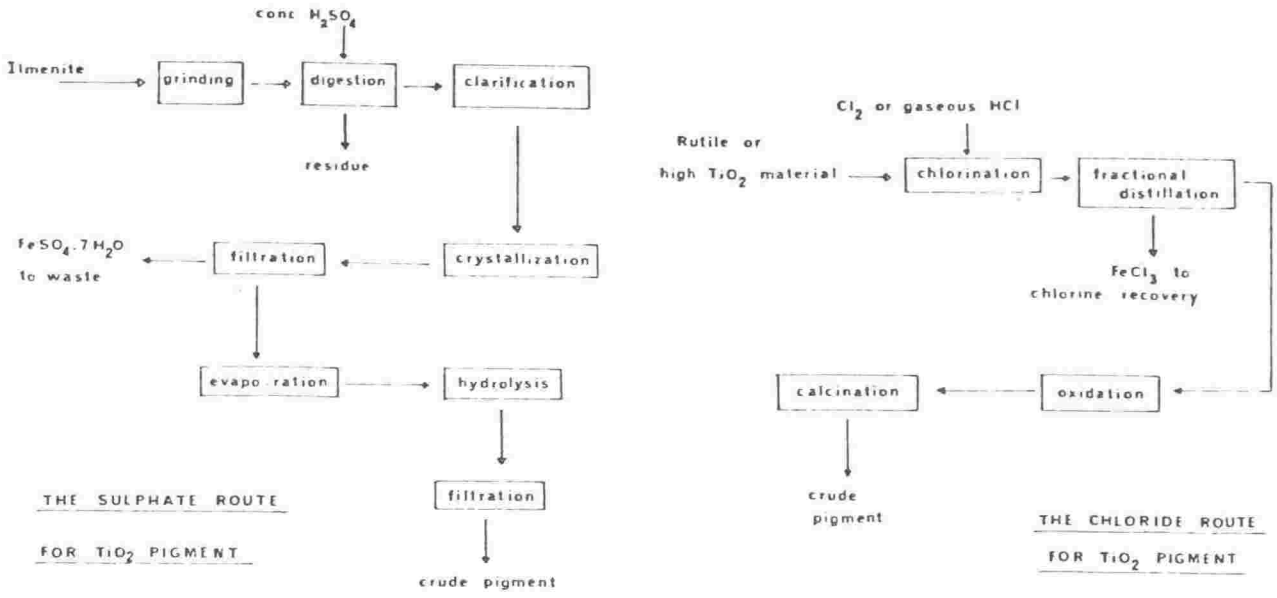

Fig. 1.1 Simplified flowcharts for the sulphuric acid (sulphate) and chloride routes to TiO_2 pigment.

The sulphate route involves direct dissolution of ilmenite in strong acid, typically 95% constant boiling H_2SO_4. The resulting exothermic reaction leaves a sponge of soluble sulphates which are then dissolved in water. Concentration and extraction of the iron by precipitation as ferrous sulphate are followed by carefully controlled hydrolysis of the almost pure titanium solution to give a slurry which is calcined to yield the crude pigment.

The chloride process utilizes rutile or a material upgraded to a high titanium content, for fluidised bed chlorination at 800 → 1000 °C

followed by purification by fractional distillation and oxidation to titanium dioxide.

Much effort has been directed into investigations of the most efficient and economical methods of upgrading "altered" ilmenites to high titanium materials (≈95% TiO_2), suitable as rutile substitutes for the chloride process. The major impetus for developing such materials is the high cost of sulphate plants, both in building and in effluent disposal.

1.2 The New Zealand Situation

New Zealand is fortunate in having considerable reserves of ilmenite. The West Coast of the South Island has huge beachsand deposits, possibly of the order of 80 million tonnes (Martin 1955, Nicholson et al 1958). There are also considerable deposits on the West Coast of the North Island, centred around Waikato North Head. The possibility of New Zealand processing its own raw material as an alternative to importing pigment, or as a saleable high-titanium product, has led to a number of investigations, mainly by the Department of Scientific and Industrial Research (DSIR). As early as 1967, Walker (1967) predicted,

> "It was concluded that these materials would be attractive raw materials for use in a titanium dioxide plant using the sulphate route. Studies of projected market demand indicated that the New Zealand market could support a plant producing 12,000 tons/yr of titanium dioxide by 1980."

Conditions have changed significantly since then, both in New Zealand and in the world pigment market. A New Zealand plant is not yet planned, although investigations are continuing.

1.3 New Zealand Ilmenites

West Coast South Island ilmenite is a relatively low grade ore in terms of titanium content (see Table 1.1). However the high ferrous analysis is paralleled by high acid reactivity (Walker 1967). The concentrate is a geologically "young" beachsand material showing little weathering or alteration and makes up from 5 to 40% by weight of the sand deposits, the largest of which lie around Westport. The geology of the Westport deposits is described by McPherson (1978).

Ilmenites occur in lesser quantities along the West Coast of the North Island, interspersed with titanomagnetite sands. This concentrate shows higher iron and a higher ferric content than the South Island material (see Table 1.1) and is less homogeneous, making it less attractive as a raw material either for pigment production or upgrading to a high-titanium material.

A number of studies have been carried out on extraction (Nicholson et al 1966), smelting (Marshall and Finch 1967), processing in sulphuric acid (Walker 1967, Judd and Palmer 1973, Walker et al 1975) and hydrochloric acid dissolution (Judd 1977) of New Zealand ilmenites. The critical factor in the dissolution studies has been balancing the economies of acid consumption with the quantity of ilmenite dissolved. The disposal of large volumes of high acid waste also presents major problems particularly if a sulphuric acid route is used.

1.4 This Study

The purpose of this study was to examine the mechanism of acid attack on New Zealand ilmenites. Although reviews, patents and texts

TABLE 1.1 - Analysis of New Zealand and Overseas Titaniferous Ores

Material	South Island Ilmenite Concentrate	North Island Ilmenite Concentrate	Australian Ilmenite Concentrate*	Indian Ilmenite Concentrate†	Norwegian Hard rock Ilmenite+
Source	Tauranga Bay	Hamiltons Gap	Capel W. Australia	Orissa India	
TiO_2 %	46.3	39.5	55.2	53.2	43.9
Fe_2O_3	3.0	23.0	17.8	12.5	13.1
FeO	37.8	31.5	23.4	33.1	34.0
MnO	1.6	1.1	1.6	-	0.3
MgO	1.5	2.4	-	-	3.7
Al_2O_3	2.6	1.1	0.2	0.6	0.8
CaO	1.2	0.4	-	-	0.2
Cr_2O_3	0.03*	0.01*	0.03	-	0.03
V_2O_5	0.04*	0.18*	0.05	-	0.2
SiO_2	4.4	1.0	0.5	0.6	3.3

* From Walker (1967) †From Jain and Jena (1977) +From Judd and Palmer (1973)

such as Barksdale (1949) have covered the technical aspects and efficiency improvements in the processing of ilmenite, there is comparatively little known about the way the dissolution reaction proceeds, particularly in concentrated solutions.

The ilmenite used, from Tauranga Bay, is typical of the West Coast, South Island beachsand ilmenites which have considerable promise as raw materials for a titanium dioxide industry. The reaction of this ilmenite in acid solutions in the 1 to 10 M range was studied at temperatures of 50 to 80 °C.

Chapter 2

THE REACTIVITY OF MINERAL ILMENITE

2.1 Crystal Structure

Ilmenite ($FeTiO_3$) lends its name to a class of crystal structures closely related to the corundum (α-Al_2O_3) structure. A hexagonally close-packed array of oxide ions has two thirds of the octahedral interstices occupied by cations, with the cations being of two different types in the ilmenite structure (Fig. 2.1).

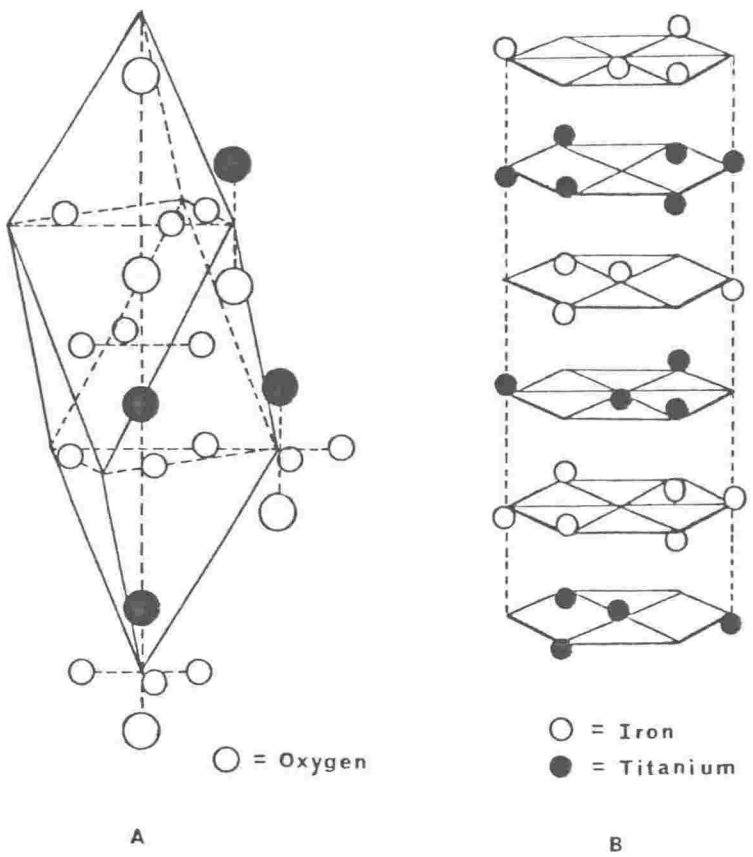

Fig. 2.1 The structure of $FeTiO_3$, showing A the rhombohedral and B the hexagonal unit cells.

This structure is adopted by ABO_3 oxides when the two cations A and B are of similar size and the sum of their charges equals six. The space group is $R\bar{3}$ if the Fe and Ti are ordered - Fe and Ti occupying alternate layers - or $R\bar{3}c$ if they are totally disordered (Raymond and Wenk 1971). However metal ion disorder is rarely encountered, even in quenched synthetic ilmenites (Shirane et al 1962).

Natural ilmenites are frequently found with small amounts of Mg and Mn substituted almost exclusively in the Fe^{II} sites but because of their size and charge similarity with the Fe^{2+} ion, no lattice distortion results. In the Tauranga Bay ilmenite used in the following work, MnO makes up 2→4% of the analysis of the ilmenite phase (see Table 4.1).

2.2 Natural Weathering

Mineral ilmenite is particularly resistant to natural weathering agents, however Lynd (1960) has shown that over many thousands of years, beachsand ilmenite deposits can be significantly enriched in titanium by the leaching of iron. A small proportion of the world's rutile reserves are assumed to have formed through ilmenite weathering. The process of natural weathering of ilmenite, is generally accepted to consist of oxidation and leaching of the iron with corresponding enrichment in titanium and initially at least, without major structural distortion (Lynd 1960, Temple 1966, Bailey et al 1956, Grey and Reid 1975).

This essentially continuous process gives rise to a problem of definition. A considerable number of names and formulae exist for alteration products falling between pure ilmenite ($FeTiO_3$) and rutile (TiO_2). These include pseudorutile (or arizonite as it has

been called) which is approximately $Fe_2Ti_3O_9$, amorphous iron-titanate and leucoxene, which is taken by some to represent any titanium-enriched product (Bailey et al 1956) and by others to describe "essentially TiO_2" (Temple 1966). There has also been some conflict in the literature over the nature of pseudorutile, with support for a distinct intermediate isotropic material with a narrow range of composition (Teufer and Temple 1966), while others propose an amorphous iron-titanium oxide or mechanical mixture of amorphous titanium oxide and iron oxide (Overholt et al 1950). Recent single crystal X-ray diffraction studies appear to have settled the matter in favour of the former (Grey and Reid 1975).

The pseudorutile composition marks an intermediate stage in the weathering process. The first stage involves progressive iron oxidation and leaching under the influence of seawater and weakly acidic rainwater and groundwater. Lynd (1960) has tested the effects of each of these factors on ilmenite weathering in laboratory experiments. He concludes:

> "...the most effective weathering agents of those likely to be present in rain and groundwater are humic acid (derived from rotted leaves) and sulphuric acid. Seawater and other weakly alkaline solutions did not attack ilmenite appreciably."

Iron has been shown to be removed along structural discontinuities by examination using electron microprobe and optical microscopy (Temple 1966). This supports an iron migration gradient initiated at the structural interfaces and maintained by progressive oxidation of ferrous iron. This diffusion process continues without oxygen removal until all ferrous iron has been oxidised or removed and the pseudorutile composition is reached. This process is represented as:

$$6Fe^{2+}TiO_3 + 3O_2 + 3H_2O \rightarrow 2Fe_2^{3+}Ti_3O_9 + 2Fe(OH)_3$$

Further leaching of iron must be accompanied by oxygen removal with disruption of the lattice. Grey and Reid (1975) suggest epitactic reprecipitation of the TiO_2 giving the final alteration product.

$$Fe_2Ti_3O_9 \rightarrow 3TiO_2 + \underbrace{2Fe^{3+} + 3O^{2-}}_{Fe_2O_3}$$

2.3 Acid Reactivity

Most commercial utilization of ilmenite is based on the dissolution of the mineral by rapid acid attack. The parameters governing maximum performance of digestors are well established, however most reviews do not include any detailed investigation of the mechanism of the dissolution process.

Imahashi and Takamatsu (1976) studied the dissolution of Japanese ilmenite and rutile in weak (0.03 → 1 M) hydrochloric and sulphuric acids. Their work supported the accepted conclusion that sulphuric acid is a better dissolution medium than the equivalent strength hydrochloric acid but they were uncertain as to the nature of the interaction between sulphate and/or bisulphate ions and the mineral.

Two distinct zones of conditions were identified in a temperature/acid concentration diagram (Fig. 2.2). In the higher acid strength region (A) the mole ratio of dissolved titanium to iron approached the stoichiometric (unity). However in the low strength, high temperature region (B), this ratio tended to become smaller with time. The mechanism proposed was one of changing surface area bringing about depression of the dissolution rate in region A and the involvement of an additional insoluble surface layer in region B.

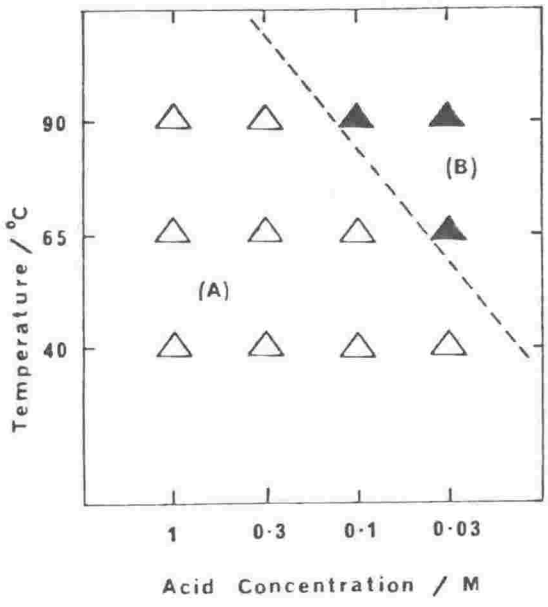

Fig. 2.2 Temperature and acid concentrations used in ilmenite dissolution (from Imahashi and Takamatsu 1976)

These reaction conditions are considerably milder than any possible commercial reaction and because of the low percentage conversion of the ilmenite in Imahashi and Takamatsu's work, any surface layer product such as TiO_2 was not detected by X-ray diffraction.

Jain and Jena (1977) studied the dissolution of Gopalpur ilmenite in hydrochloric acid of industrial strengths (4→10 M). In analysis, the raw material is not very different from typical New Zealand concentrates (Table 1.1). In view of its high ferrous content they proposed removing the iron values selectively by direct hydrochloric acid leaching under atmospheric pressure, without any pre-treatment of the mineral. Digestion was carried out in a reaction flask,or in an ilmenite packed column. The results were analysed in terms of % iron removed and the composition of the crude TiO_2 product, however they do not mention any titanium removal during the digestion. This makes the digestion efficiency

difficult to determine. If the iron alone is leached out with little or no accompanying titanium, a distinct iron containing phase would seem to be necessary. Jackson (1975) suggested that claimed selective leaching of iron from ilmenite using hydrochloric acid was really the result of concurrent precipitation of the titanium.

Remarkable efficiency in iron removal is achieved both in single stage (78-80% removed with boiling 20 wt% HCl in 50% excess of the stoichiometric requirement for dissolution) and multiple stage (88% with 24 wt% HCl, using four stages) extraction. Column reactors showed a tendency to clog with precipitated ferrous chloride, but the efficiency of iron removal was considerably better than in a flask.

Jain and Jena proposed that the initial reaction was a chemically controlled surface process resulting in rapid iron removal. The subsequent slowing of the reaction was due to:

(a) diffusion of acid into the pores of the particles, or

(b) less availability of iron(II) in the ilmenite, or

(c) lowering of acid concentration in the leachant and/or

(d) increased iron concentration in solution.

They concluded that partial reduction of the ilmenite followed by a column leach with 20 wt% HCl at 105→107 °C could provide a 92→93% TiO_2 product.

Jackson (1975) studied ilmenite dissolution in hydrochloric acid but in a unique mineral system. The Allard Lake concentrate used contained a typical ilmenite-hematite exsolution structure, so the reaction mechanism was unique to the system. The dissolution kinetics were studied with and without pre-treatment of the mineral, consisting of either partial oxidation or reduction. Jackson concluded the reaction showed a first order dependence on hydrogen ion activity and calculated activation

energies for the dissolution of the hematite rich and ilmenite rich phases (see Table 4.8).

Pre-reduction caused a marked increase in dissolution rate, but again approximately first order hydrogen ion activity dependence was observed.

One of the most interesting and recent views on the subject involved a new approach using a combination of particulate dissolution and rotating disk experiments on natural and synthetic ilmenites (McConnel 1978, Barton and McConnel 1979). The limitations of rotating disk surface area and roughening of the disk surface meant that only small degrees (1→2%) of conversion were followed by this technique, even using 9 M sulphuric acid over 28 hours at 65 °C. Together with the particulate dissolution studies, the rotating disk work yields some interesting conclusions. Firstly the dissolution rate is independent of rotation speed for both synthetic and natural ilmenites in sulphuric acid, implying chemically controlled reaction. Again iron leaves more rapidly than titanium in the early stages of reaction, but this does not occur in a carefully crystallised synthetic ilmenite. From temperature dependence of the reaction rate, Barton and McConnel calculate apparent activation energies for the rate determining step (see Table 4.8). These also support chemical control.

The particulate dissolution studies used a wide range of ilmenite concentrates of varying degrees of alteration, including West Coast and Tauranga Bay samples from New Zealand. The dissolution of specific size fractions in sulphuric acid up to 9 M was studied with emphasis on the role of altered phases. McConnel worked with unground ilmenite in a large excess of acid so solubility effects and hydrolysis could be minimized. He concluded that natural ilmenite dissolution initially

involves the removal of an altered surface high in ferric iron in the form of fine grained hematite. The bulk of the solid was then attacked. Thus the degree of alteration was a major factor in determining initial reactivity and later reaction depended on the composition of the bulk material.

McConnel then set out to simulate natural weathering using refluxed distilled water in a Soxhlet apparatus. After six months there was no significant crystallographic modification of the ilmenite, as determined by X-ray diffraction, but the solution contained appreciable concentrations of iron and titanium in the ratio of approximately 50:1.

To summarize briefly from the major studies of ilmenite dissolution, concentration/time plots are initially approximately linear under most acid conditions, and show first order dependence on hydrogen ion activity. This initial stage appears to be chemically controlled by the reaction at the ilmenite surface (McConnel 1978). Dissolution plots tend to curve and flatten out rapidly later in reaction, even in strongly acid solutions. In this region, processes such as acid diffusion, less availability of ferrous iron, lowering of acid concentration and increased concentration of iron in solution must be considered (Jain and Jena 1977).

2.4 Reactivity of New Zealand Ilmenites

West Coast South Island ilmenite, because of its high reactivity and moderate titanium content has always been the most attractive local material for acid digestion. Other titanium containing materials such as steel plant slags have been investigated with a view to obtaining a high-titanium upgrade material (Marshall and Finch 1967, Walker 1967), but none compare with West Coast ilmenite.

Judd and Palmer (1973) determined the effects of acid strength, acid/ilmenite ratio, temperature and hydrolysis conditions in achieving a satisfactory (>98%) TiO_2 material. The important features of the dissolution of this West Coast ilmenite were:

(a) because of its high reactivity, relatively dilute (<40% by weight) sulphuric acid can be used, making acid recovery from the hydrolysis filtrates technically feasible.

(b) A soluble mass of sulphates can be avoided in the initial digestion step because of the lower strength acid. Thus dissolution can be continuous with the reaction mixture fluid throughout the operation.

(c) There is very little ferric iron present in the raw ilmenite and as the dissolution is essentially non-oxidative, a reduction step is not required to prevent ferric iron interfering in later hydrolysis of the titanium solution.

Thus study led to experiments with a small batch run pilot plant using single stirred tanks for digestion and hydrolysis. The results were assessed economically together with plant and service costs for a pigment operation. Although tentative, this showed that the product could have a "small price advantage" over imported pigment.

Further work was carried out with a small mixer-cascade pilot plant set-up (Walker et al 1975). The plant consisted of six identical stages with acid and ilmenite running concurrently with gravity feed between stages. However the results were not encouraging by comparison with earlier batch work. The necessity of interstage acid addition and increased reaction times, made the economics of the continuous process unattractive.

Because of the difficulties of recovering and recycling sulphuric acid and problems in the disposal of large quantities of high acid ferrous sulphate waste (see Fig. 1.1), hydrochloric acid was considered for the digestion reaction. Although less reactive towards ilmenite, HCl has the following advantages:

(a) Well proven methods exist for acid recovery from moderate strength solutions.

(b) Acid recovery from iron-rich slurries produces iron oxide as the major by-product. This is readily saleable as a pigment or high grade ore.

In July 1977 Judd published a DSIR report "Production of Titanium Dioxide from Westland (West Coast) Ilmenite by Hydrochloric Acid Leaching". This report detailed laboratory experiments on batch digestion, clarification and the hydrolysis of the resulting titanium solutions. Judd showed that under favourable conditions, the digestion goes to completion, indicating that the reaction is not confined to leaching of iron from the ore (compare with Jain and Jena 1977).

Titanium solutions hydrolyse readily in hydrochloric acid so the temperature and acid/ilmenite ratio must be carefully regulated to delay hydrolysis until the digestion is at or near completion. The liquor can then be filtered to remove gangue minerals before the hydrolysis step. In fact small amounts of sulphuric acid were added to suppress hydrolysis in digestions carried out in boiling solutions. Judd proposed two distinct process designs based on hydrochloric acid digestion. The first utilized boiling acid and "in situ" hydrolysis while the second followed a more traditional route, using lower temperatures to delay hydrolysis until gangue minerals have been removed.

To summarize, ilmenite upgrading in New Zealand has been shown, through the work of DSIR, to be quite feasible on a technical basis either by a hydrochloric acid process or by a sulphuric acid route. The unmodified ore, although low grade in terms of titanium content, is unusually reactive towards acid dissolution, thus improving its processing possibilities. However, little of the mechanism of ilmenite dissolution is understood, particularly with these reactive concentrates. The observed behaviour at high acid/ilmenite ratios (McConnel 1978) in sulphuric acid, does not clarify the mechanism of dissolution in concentrated solutions, particularly in hydrochloric acid.

Chapter 3

EXPERIMENTAL

3.1 Introduction

The object of this work was to study the dissolution of ilmenite on a laboratory scale but under conditions close to those which might be used commercially. This meant concentrated solutions of high acidity and temperatures approaching boiling. The maximum acid strength used was 10 M HCl at an acid to ilmenite mole ratio of 10:1 (weight ratio 2.4:1). Judd (1977) in his investigation of commercial level digestions in hydrochloric acid used weight ratios between 2.36:1 and 0.65:1. Lesser emphasis was placed on sulphuric acid reactivity as this has been investigated in higher acid/ilmenite ratios by McConnel (1978), and in industrial concentrations in the work of Judd and Palmer (1973).

As well as the basic dissolution reactions, a variety of additives such as phosphoric acid, fluoride (as magnesium fluoride) and titanium (as potassium titanium oxalate) were introduced. Acid strength and temperature were the major parameters considered, with lesser emphasis on stirring rate and particle size. In one dissolution run an ultrasonic bath was used for "in situ" treatment of the ilmenite.

Experimental work involved three distinct aspects of the dissolution reaction:

(a) the reaction itself.

(b) the analysis of the resulting solutions.

(c) characterisation and analysis of the solid at different stages of reaction.

The following sections describe the instruments and methods used in studying the reaction.

3.2 Dissolution

Ilmenite samples were obtained from the Industrial Processing Division, DSIR, as concentrates from standard mineral dressing procedures. Australian samples were provided by Dr Ian Grey of the Division of Mineral Chemistry, CSIRO, Australia. The major raw material used was ilmenite from Tauranga Bay near Westport on the West Coast of the South Island. The size distribution of ground and unground fractions used in this work is detailed in table 3.1.

TABLE 3.1 Particle size distribution of ground and unground Tauranga Bay ilmenite samples used in the course of this work

fraction (μm)	unground (% by weight)	ground (A)	ground (B)
125 +	3.6	0.9	0.7
106-125	36.6	4.8	4.8
90-106	52.8	28.3	8.1
75-90	5.6	34.2	11.2
63-75	0.3	20.1	14.2
50-63*	0.1	6.6	9.4
37-50*	-	1.7	14.0
-37*	-	2.5	36.1
	99.0	99.1	98.5

*from Sedigraph analysis - see section 3.4.7.

Ilmenite was added to stirred acid solutions in a reaction flask suspended in a thermostated water bath and fitted with a reflux condenser (Fig. 3.1). Temperature control was better than ±0.25 °C. Acids used were analytical grade 95-98% H_2SO_5 and 33⅓% HCl diluted

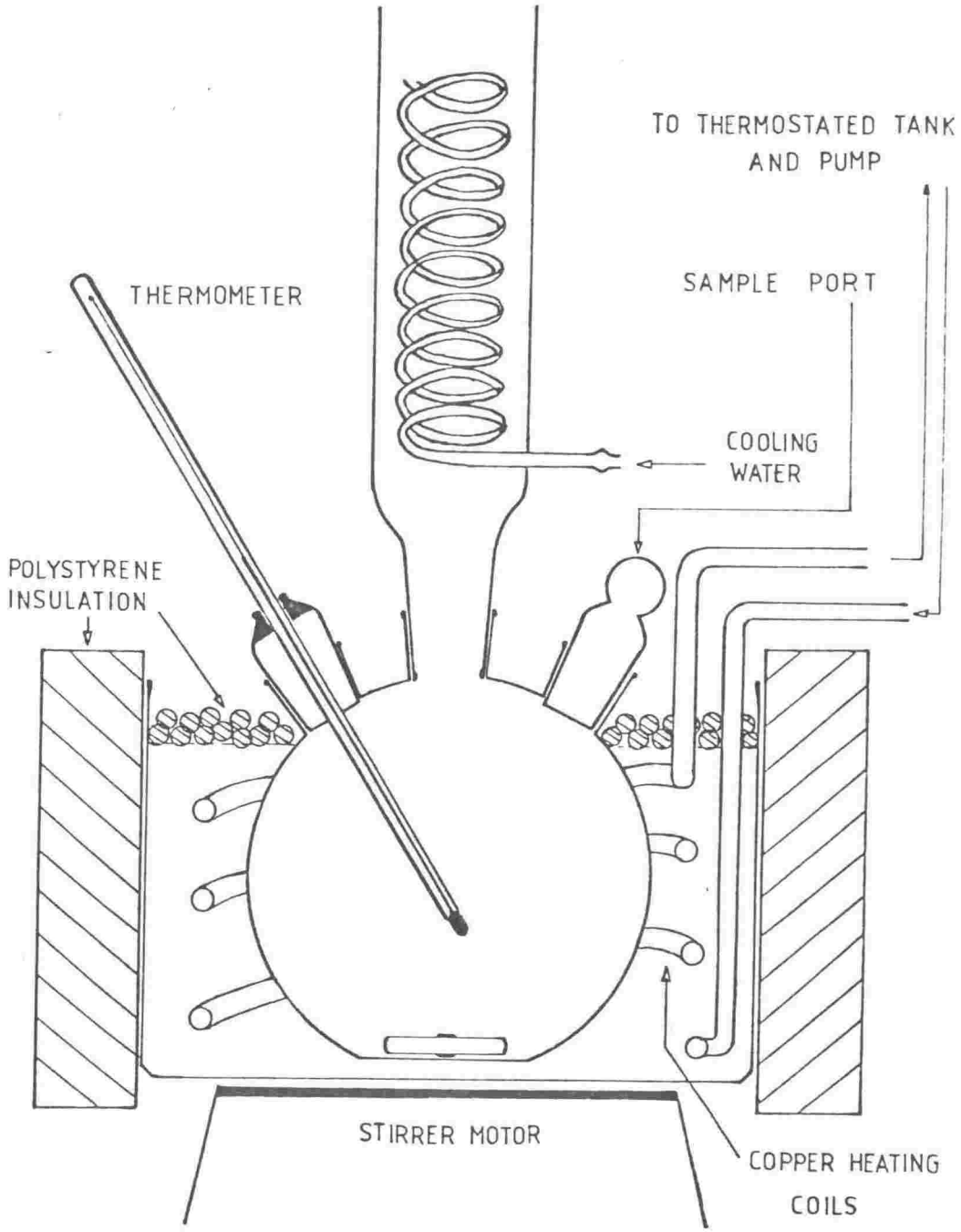

Fig. 3.1 Apparatus used in dissolution experiments.

to the appropriate strength. Samples were removed from the flask at intervals during each digestion, the typical duration of runs being eight to ten hours. The assembly (see Fig. 3.1) was found to be stable under the strongly acid conditions with insignificant loss of acid by fuming. Occasional troubles were encountered with the physical nature of the slurry, especially with finely divided samples which showed a tendency to cake and line the walls of the flask. A temperature range of 50→80 °C was used, the upper limit being determined by the rapid hydrolysis of titanium chloride solutions above this temperature (see section 4.2.2).

Samples were extracted by syringe pipette from the middle of the stirred slurry. They contained both solid and liquid thus avoiding variation in the solid/liquid ratio being introduced by sampling. After extraction, samples were centrifuged to drop temperature thus arresting reaction, and to separate the solid fraction. The 5 to 6 ml of clear liquid was then stored for analysis as was the washed and filtered solid.

In cases where interruption and washing of the undissolved ilmenite were necessary, the hot slurry was filtered through a Buchner funnel and the filtrate immediately returned to the thermostated flask. A wide variety of treatments were carried out on the solid including repeated washing in hot distilled water, washing in dilute acid and/or base etc. The solid was returned to the flask, usually after drying in a cool oven (40 °C) and the dissolution continued.

3.3 Analysis of the Liquor

Concentrations of iron, titanium and manganese in the solution were determined by Atomic Absorption spectroscopy using a Techtron AA4 instrument.

Titanium was measured at the 3643 A° resonance line and manganese at 2795 A°, both of these being the most sensitive resonance lines. However to avoid a separate set of dilutions, iron was measured at its next most sensitive line at 3720 A°.

Initially samples were doped with 2000 ppm potassium to suppress ionization, however this was determined to be unnecessary except in the absence of sulphuric acid. Matrix effects due to the viscosity of the sulphuric acid were encountered, necessitating the use of a standard 0.25 M sulphuric acid solution in all samples and standards. To keep samples in the range of the standards (25 → 200 ppm for Fe and Ti, 5 → 30 ppm for Mn) dilution by up to a factor of 200 was necessary.

Titanium analysis is considerably more difficult than either iron or manganese. A slightly rich nitrous oxide/acetylene flame is necessary and sensitivity is strongly dependent on the flame composition. The presence of iron in the solutions assists in overcoming common titanium interferences (Price 1972).

Iron response was tested for silica interference by a change of flame temperature, using nitrous oxide/acetylene in place of air/acetylene. No difference was detected and some accuracy was lost due to increased baseline instability.

Manganese, determined in an air/acetylene flame is also relatively free of interferences in the concentration ranges used.

Generally at least two dilutions of each sample were fitted into the concentration range of the standards. These rarely differed by more than four percent and average values were taken.

Ceric sulphate titration (Judd and Palmer 1973) was used on several of the early experimental runs to test the Atomic Absorption results. The accuracy of the method depends on a careful correction for dissolved

aluminium used to reduce the titanium and obtained by blank titration, and also on carrying out the first titration hot. The results for a typical reaction are shown in figure 3.2 together with comparative AA values. The method was found to be significantly more complicated than Atomic Absorption analysis and showed a marked loss in accuracy.

Acid consumption was determined by titration of the solution before and after dissolution with a standardised sodium hydroxide solution. The "after" titration was complicated by the presence of large concentrations of iron in the solution. Interference was minimised by dilution and the addition of EDTA which was corrected for by blank titration.

3.4 Analysis of the Ilmenite

3.4.1 X-ray Diffraction

Powder diffraction traces were run on a Philips PW 1025 diffractometer using Cu Kα radiation and a Xenon proportional counter. Initially peak positions were used in distinguishing possible reaction products such as pseudorutile, rutile and anatase. However apart from traces of rutile and anatase, no product phases were identified. Hydrated ferrous chloride was precipitated on cooling of the 10 M HCl digestion solution, however precipitation was not evident in the hot solution (70 °C).

The unit cell size of the ilmenite crystallites was determined from the nine major peaks of the powder diffraction pattern using a computer program based on the method of Appleton et al (1963). Peak positions were determined from traces run at $\frac{1}{2}°$ min^{-1} with "Analar" sodium or potassium chloride as an internal standard. No orientation or packing problems were encountered with the ground samples as positions rather than intensities or line widths were the critical parameters.

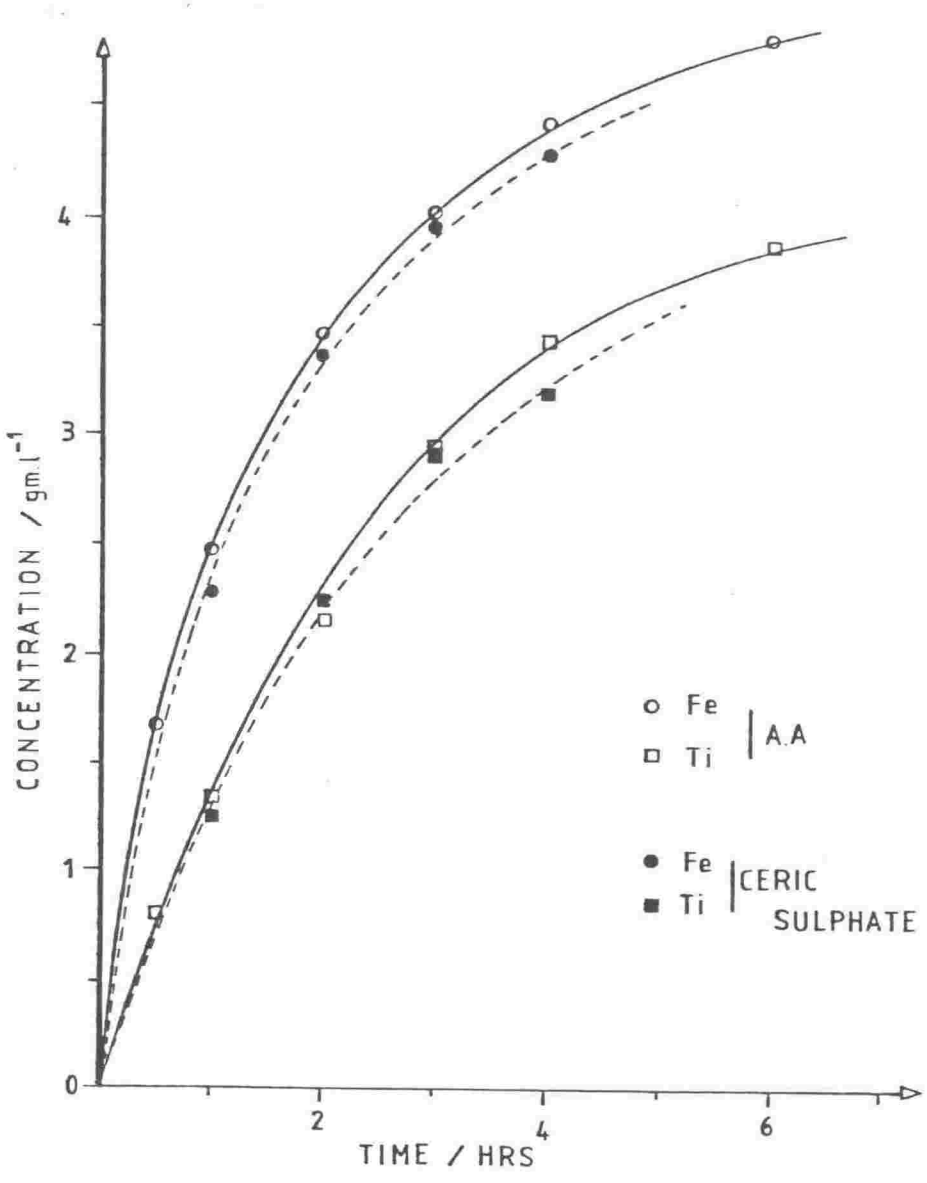

Fig. 3.2 Comparison of Ceric Sulphate and Atomic Absorption analysis for Iron and Titanium. 4 M H_2SO_4, 60 °C.

A major problem in X-ray diffraction work was the lack of resolution in attempting to distinguish reaction products. Several possible products have diffraction patterns similar to each other and to ilmenite. Pseudorutile is an example of this (Grey and Reid 1975).

3.4.2 X-ray Fluorescence

Major element analysis was carried out on fused discs of the ilmenite samples using a modified Norrish and Hutton method (Kennedy et al, in prepn.). A Siemens spectrometer fitted with a chromium X-ray tube was used to analyse discs prepared by fusing the sample with a spectroflux type 105 lithium tetraborate flux. Ilmenite is quite difficult to fuse and it was necessary to dope samples with up to 50% "spec-pure" silica. This introduces some additional error in the SiO_2 analyses in comparison to the other major elements. Iron totals must be corrected for the ferrous content which was determined by the standard dichromate titration method (Sarver 1927). Mass absorption effects from the high iron and titanium concentrations meant that standards with similar levels were required and some were manufactured by fusing mixtures of spec-pure TiO_2, Fe_2O_3 and SiO_2.

Samples which proved difficult to analyse were those from dissolution runs involving phosphoric acid addition to the solution (see section 4.2.7). These samples, which contained up to 14% P_2O_5, gave low totals and variable ignition losses. Remelting to improve disc homogeneity gave improved totals in some but not all cases. Table 4.1 shows a comparison of X-ray fluorescence analyses with those obtained from the electron microprobe and from wet chemical methods.

3.4.3 Scanning Electron Microscopy

SEM proved to be an extremely useful technique in observing the nature of the reaction on the ilmenite grains. Both whole grains and cross-sections were examined using a Cambridge Stereoscan 600 instrument. Whole grains were mounted on double sided adhesive tape on aluminium sample holders (see Fig. 3.3). These were then coated with a vapour deposited conducting layer of gold. For cross-sectional examination grains were set in "Araldite" mounts (Fig. 3.3) and polished on Struers polishing equipment, finishing with a 1 μm diamond paste to give a highly polished cross-sectional surface.

Because of the small grain sizes involved (<30 μm in many cases) a number of resins and impregnation techniques were tried. "Araldite D" was found to give satisfactory results because of its relatively low viscosity particularly when warmed. The Teflon mould and vacuum system used is shown in figure 3.4. Centrifuging the Araldite before injection and the use of reduced pressure (≃25 mm Hg) ensured a bubble-free mount with good adhesion to the grains and suitable polishing characteristics. These mounts were also used for electron-microprobe studies (see section 3.4.4).

The polished 2.5 cm diameter mounts were glued to aluminium stubs and coated as described earlier. The only problems encountered were again with the phosphate containing samples where surface coatings and precipitated material made resin adhesion poor and grains tended to break-out during polishing. The use of slight vacuum during impregnation as described above, was developed to overcome this difficulty.

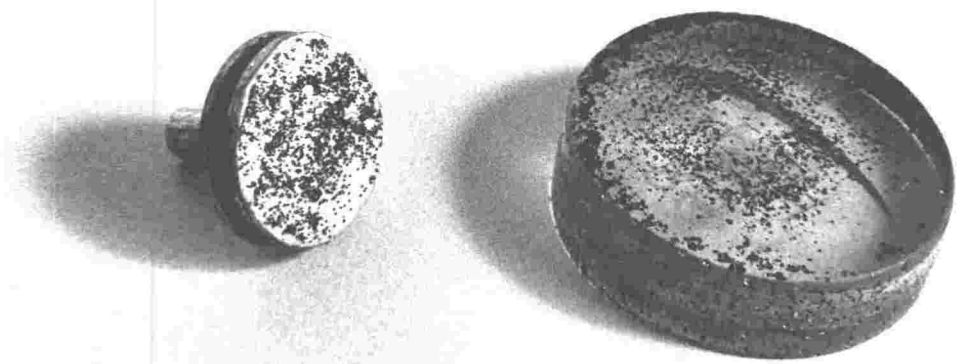

Fig. 3.3 Mounting stub used for whole grain examination by electron microscope and araldite mount used for cross-section examination by electron microscope and electron microprobe.

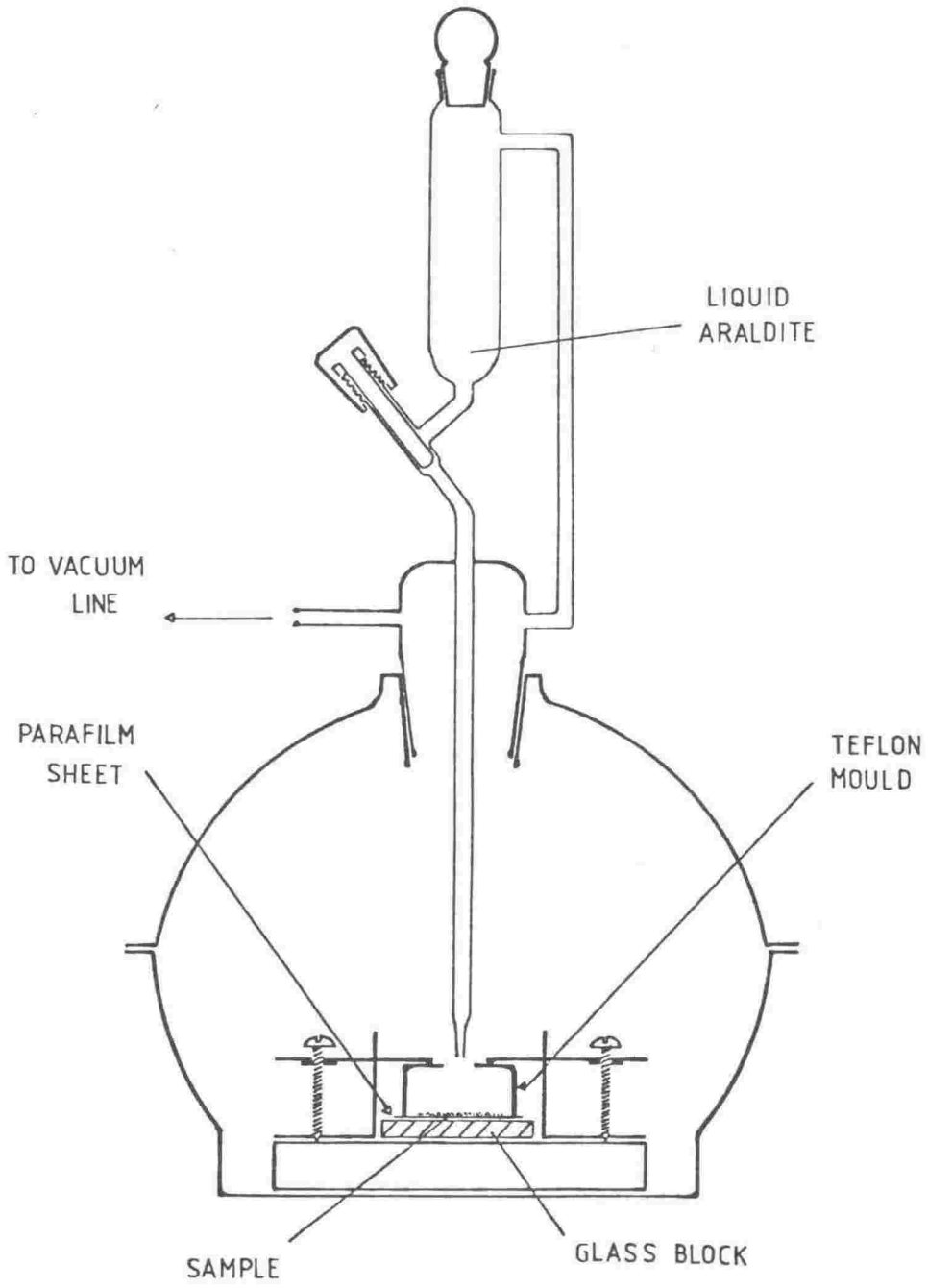

Fig. 3.4 Teflon mould and vacuum system used in the preparation of araldite sample mounts.

3.4.4 Electron Microprobe

The polished mounts constructed for SEM work (section 3.4.3) proved ideal for electron-microprobe analysis using the Victoria University Analytical Facilities JEOL 733 microprobe. The advantage of a focused beam probe is that point analysis can give the composition of discrete phases, assuming they can be distinguished either through the optical microscope or the SEM. Thus it was possible to look at the composition of the ilmenite phase as distinct from the bulk analysis and also to identify the inclusions. The elemental density mapping function was used to observe distributions of major elements, such as manganese which substitutes in the ilmenite phase. The instrument was usually used for major element analysis i.e. silica, titanium, iron, manganese, magnesium, aluminium, calcium, sodium and potassium. Barium, nickel, chromium and phosphorous were added to the program as required.

The normal accelerated voltage used for analysis was 15 kV with a probe current $\simeq 10^{-8}$ A. Beam diameter was between 2 and 5 μm depending on machine conditions and the nature of the region of interest. The complementary nature of bulk analysis by X-ray fluorescence and specific analysis of phases was extremely useful particularly in distinguishing which phases resisted attack.

Analysis totals were good (99±2%) in most cases, the exceptions were attributable to:

(a) overlap of phases not distinguished under the optical microscope,

(b) the excited region (Fig. 3.5) overlapping into resin material or

(c) surface contour causing scattering, particularly from partially dissolved samples.

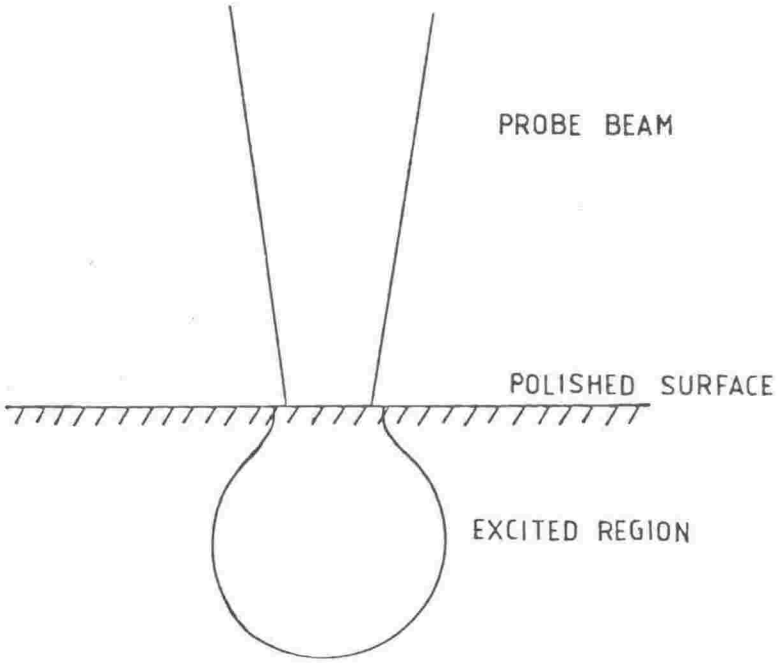

Fig. 3.5 The shape of the region of electron penetration and scatter, under a beam of low accelerating voltage. - From Bertin (1978).

The ferric content, although extremely small for Tauranga Bay ilmenite is appreciable for more weathered samples (see section 5.7), and must be considered in correcting low totals.

3.4.5 Optical Microscope

Optical microscopy was used on both whole grains and cross-sections but with limited success. The small particle size of the ilmenite meant viewing was restricted to clusters of grains under reflected light using the same polished mounts prepared for SEM and Probe work. Alteration was visible in Australian samples (see section 5.7) however in viewing Tauranga Bay ilmenite only occasional rings of exsolution hematite (Fig.4.5) were visible through the polariser. Ilmenite unfortunately reflects as subtle shades of grey (Deer, Howie and Zussman 1966) as do most of the inclusions. It was possible to distinguish three major phases in Tauranga Bay ilmenite consisting of the ilmenite, sodium rich feldspars and quartz.

The technique was of little use with partially dissolved materials, no reaction products were observed and resolution was not sufficient to study the mode of attack on the ilmenite grains.

3.4.6 Mössbauer Spectroscopy

Mössbauer spectroscopy is a particularly useful method of investigating the nearest neighbour environment of iron in the ilmenite lattice. Unlike X-ray diffraction, the technique is generally not particle size dependent. It is well suited to investigation of the iron population in non-equivalent sites and the oxidation state of iron in the lattice. The method utilizes the recoilless nuclear resonance absorption of the 14.4 keV gamma ray of ^{57}Fe (2.2% natural abundance) between the nuclear spin levels of I = 3/2 and I = 1/2 (Fig. 3.6). Refer to Bancroft (1973) or Goldanskii and Herber (1968) for a full discussion of the effect and its applications.

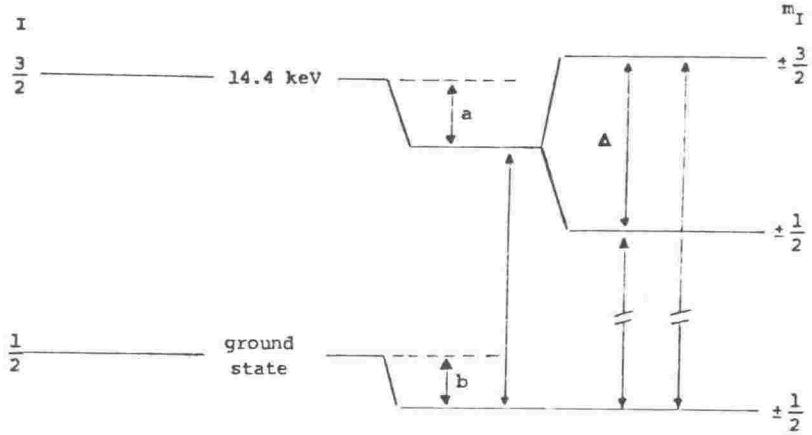

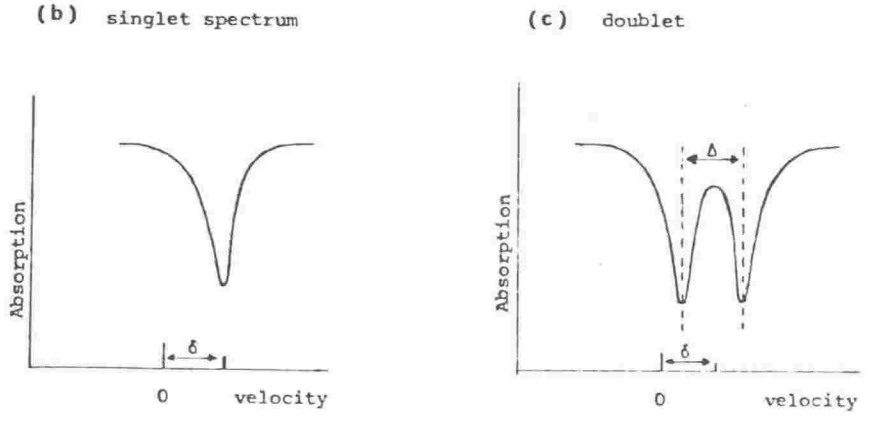

Fig. 3.6(a) The parameters of the Mössbauer spectrum.

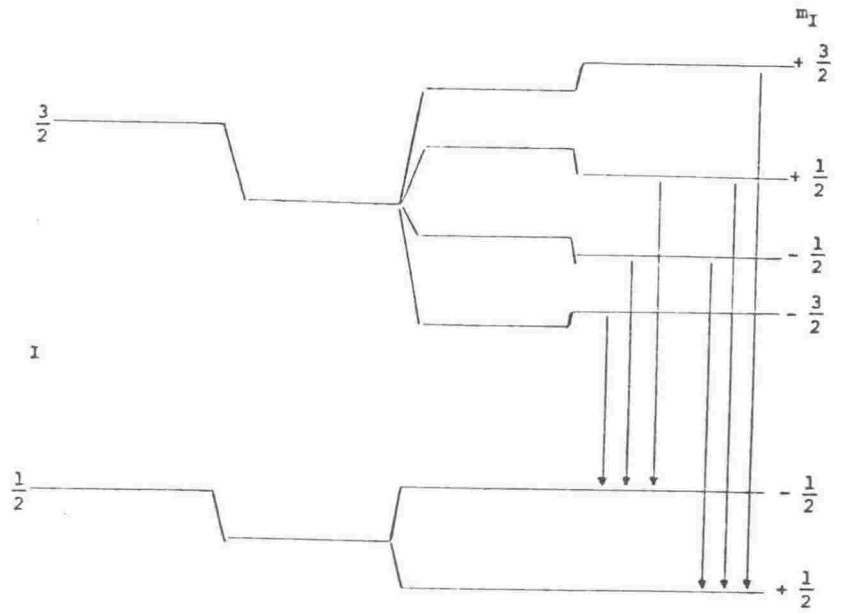

Magnetic hyperfine splitting of the nuclear levels of ^{57}Fe showing the allowed transitions observed by Mössbauer spectroscopy.

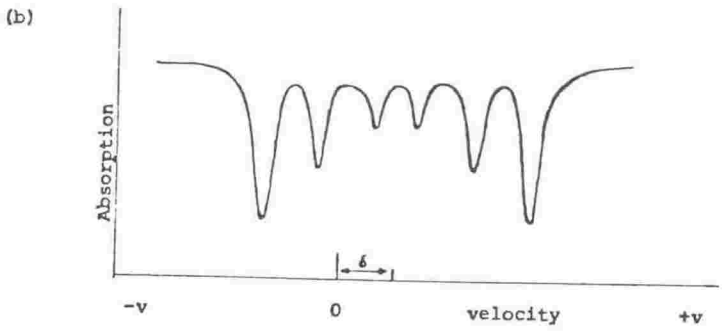

a typical six peak magnetic hyperfine split spectrum.

Fig. 3.6(b) Magnetic hyperfine splitting in the Mössbauer spectrum.

Spectra were recorded on a constant acceleration Mössbauer spectrometer (Johnston and Nixon 1971) at room temperature and over a velocity range of ± 2.2 mm s^{-1}. An approximately 10 mc ^{57}Co source annealed into a copper matrix was used, therefore all velocities are calculated relative to copper.

Calibration was carried out regularly using powdered sodium nitroprusside dihydrate. Computer fitting was carried out where possible using a modified version of the χ^2 minimisation program of Stone (1967).

Mössbauer spectra provided information on the natural alteration of ilmenites through a series of New Zealand and Australian samples but was of limited use in the investigation of dissolution mechanism. No significant oxidation or distortion of the ferrous site is apparent during dissolution of Tauranga Bay ilmenite (see section 4.4).

3.4.7 Particle Size Determination

Particle size and surface area effects were initially thought to have considerable influence on the reaction mechanism. Particle sizes were determined by a combination of sieving (down to a 63 μm mesh) and a Micromeritics Sedigraph 5000 D, used to measure distribution from approximately 60 μm down to 1 μm. The Sedigraph utilizes variation in settling rate with particle size. This rate is measured by an X-ray beam through a moving cell containing a suspension of the material under test. Critical parameters in setting up the instrument are the density and viscosity of the solvent used. Because of ilmenites density ($\simeq 4.5$ g/cm^3), water and light alcohols are unsatisfactory and a solution of 40% glycerol was used. The density and viscosity of this solution were taken from tables in the Handbook of Chemistry and Physics (1974). Determining the suitability of a solvent system involves calculating a settling velocity from the equation:

$$\text{Settling velocity} = \frac{D\ (\rho-\rho_o)980}{18\eta}$$

where D = the starting diameter (upper limit of particle size)

ρ = density of the solid

ρ_o = density of the solvent

η = viscosity of the solvent

From the settling velocity and the Reynolds number;

$$R = \frac{Dv\rho_o}{\eta} \qquad (v = \text{settling velocity}).$$

a rate setting is calculated for the instrument. If the rate does not lie in a specified range the solvent is unsatisfactory.

These calculations assume spherical particles, however this source of error can be minimised by using a relatively slow settling rate (a scan over 60 μm will take approximately 35 minutes). Tauranga Bay ilmenite even when ground shows a predominance of spherical particles under the SEM, so this assumption is justified.

One problem which was encountered in sedigraph analysis was consistently low readings in the initial stages of analysis i.e. close to 63 μm. This difficulty persisted despite careful sieving (to ensure a minimum of >63 μm diameter particles in the initial sample) and variations in stirring and pre-treatment in the ultrasonic bath. The problem was attributed to a calibration difficulty with the instrument and meant plots of particle size distribution were biased toward low particle sizes (see for example Fig. 4.25).

Chapter 4

REACTIONS OF TAURANGA BAY ILMENITE

4.1 The Composition of the Solid

4.1.1 Introduction

Tauranga Bay ilmenite, the major raw material used in this work, was extracted by tabling, magnetic and electrostatic separation from the beachsands of Tauranga Bay, West Coast, South Island, New Zealand. The origin and mineralogy of the ilmenite sands have been investigated by McPherson (1978) and the separation of ilmenite and accessory minerals by Nicholson et al (1966).

Analyses of the ilmenite concentrate by several methods are shown in Table 4.1. The ilmenite phase is close to stoichiometric ferrous titanate in composition, the difference in analysis between this phase (analysed by microprobe) and the bulk material (analysed by X-ray fluorescence) is due to a large number of small inclusions. Figure 4.1 shows electron photomicrographs of cross-sections of Tauranga Bay ilmenite grains. The major inclusions are identified by the probe as the feldspars albite and oligoclase, also quartz and lesser quantities of sphene, prehnite and apatite have been identified.

The ilmenite phase itself appears quite homogeneous from optical and electron microscopy, and microprobe studies (Fig. 4.1), and the probe shows little deviation from the analysis shown in Table 4.1. There is little evidence of the typical cross-hatched alteration zones visible in weathered ilmenites (Deer, Howie and Zussman 1966, El-Hinnawi 1969). Manganese, commonly substituted in the ferrous site in ilmenite (Elsdon 1975, Temple 1966) reports at 2 to 2.5% levels in the probe

Table 4.1 Analyses of Tauranga Bay ilmenite by X-ray fluorescence, Electron-microprobe and wet chemical methods.

	Electron microprobe[a]	X-ray fluorescence	Previous analysis[b]
TiO_2 %	52.44	46.5	46.5
FeO	45.60	37.8[c]	37.6
Fe_2O_3	na	3.0	3.2
MnO	2.04	1.6	1.7
MgO	0.06	1.5	1.2
CaO	0.02	1.2	1.4
Al_2O_3	0.04	2.6	2.8
Na_2O	0.02	1.7	na
K_2O	0.01	0.20	na
Cr_2O_3	0.00	na	0.03
P_2O_5	0.01	0.22	0.19[d]
SiO_2	0.04	4.4	4.1

(a) This is an average from a number of point analyses. The probe analyses refer specifically to the ilmenite phase, the other two methods provide analyses of the bulk concentrate.

(b) From Walker (1967).

(c) Determined by dichromate titration (see section 3.4.2).

(d) From Judd and Palmer (1973).

na = not analysed.

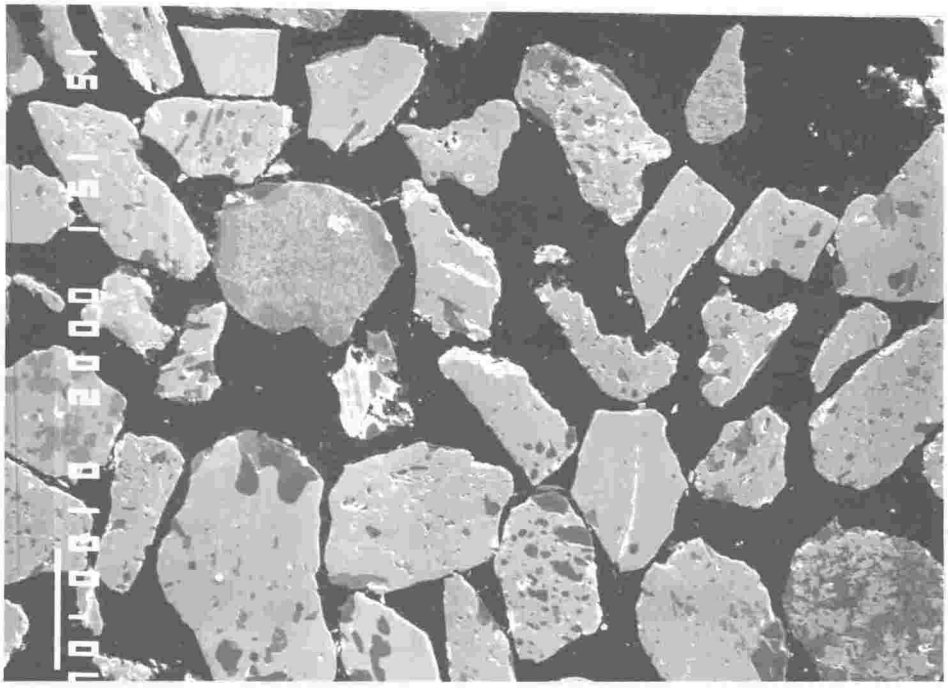

(a) Cross-section view of a cluster of grains - marker bar = 100 μm.

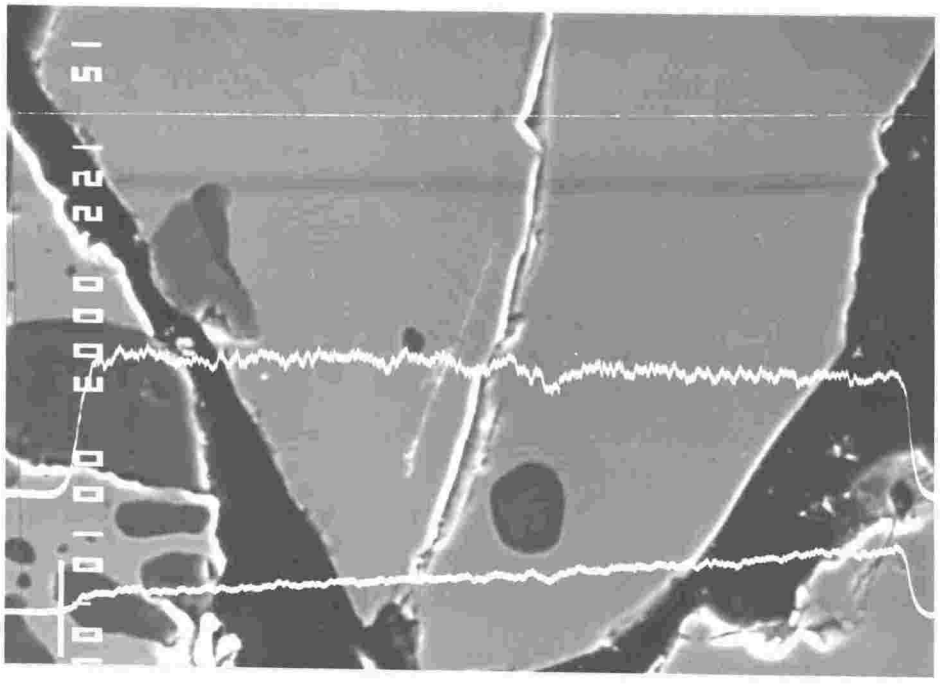

(b) Electron-probe line-scan for iron and titanium across a grain from the above photograph - marker bar = 10 μm.

Fig. 4.1 Electron microscope photographs of cross-sections from Tauranga Bay ilmenite.

analysis. Mapping of the manganese concentration using the electron microprobe shows an even distribution within the limits of resolution (mapping was carried out on a grid of 2 μm steps with a 2 μm beam diameter). A random distribution of manganese in the ferrous sites, is also supported by the observation that the rate of appearance of manganese in solution during dissolution, is directly proportional to that of iron (see section 4.2.1).

X-ray diffraction analysis of ground Tauranga Bay ilmenite reveals a very crystalline lattice conforming accurately to the ASTM peak positions - Table 4.2. Unit cell dimensions, calculated as described in section 3.4.1, show deviation of less than 0.3% from the ASTM reference material. Residual peaks can be attributed to the silicate inclusions with the strong quartz peak (3.34 A°) making a significant contribution.

4.1.2 Compositional Changes during Reaction

The quartz and feldspar inclusions are extremely acid resistant and are left as gangue material after dissolution. The accessible apatite however dissolves readily, as is shown by X-ray fluorescence analyses of solid residues from different stages of reaction (Fig. 4.2). Calcium and phosphorous levels in the solid decline rapidly within the first hour of reaction, whereas silica increases markedly over the same interval.

TABLE 4.2 X-ray diffraction data from Tauranga Bay ilmenite

Peak Å	I/I_o	Peak (ASTM)	I/I_o
3.733	30	3.73	50
3.333*	10		
3.196+	8		
2.748	100	2.74	100
2.542	50	2.54	85
2.346	10		
2.236	20	2.23	70
2.177	5		
1.865	20	1.86	85
1.724	50	1.72	100
1.636	10	1.63	50
1.506	30	1.50	85
1.471	25	1.47	85
1.342	40	1.34	70

Diffraction pattern calibrated with powdered 'Analar' NaCl.

*Quartz

+Albite

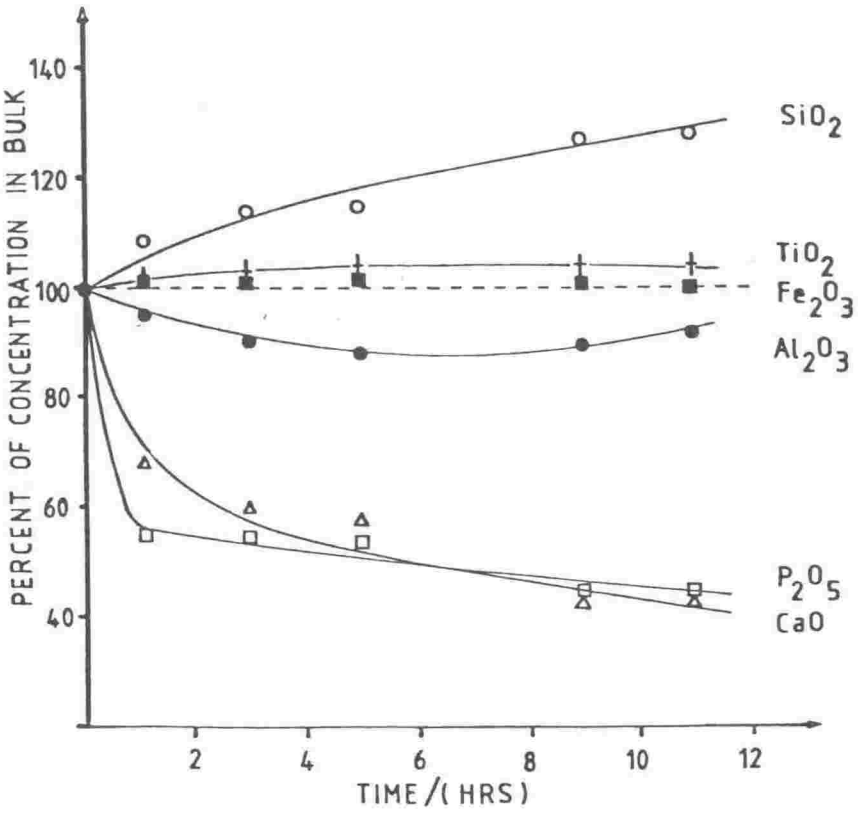

Fig. 4.2 Analyses of solid samples from dissolution in 6 M HCl 70 °C.

The bulk analysis shows, over the course of dissolution, only slight variation in the Fe:Ti ratio with enrichment in titanium relative to iron (Fig. 4.3). This is consistent with the direction of the concentration imbalance observed in the solution, but does not account for the magnitude of the solution imbalance. This is discussed further in section 5.3.3.

The reaction of unground ilmenite reveals irregularity in the early stages of iron dissolution. This is best illustrated in the Activation Energy experiments (see section 4.3) in which small degrees of dissolution are followed. The behaviour of iron in these low concentrations (see Fig. 4.6) is consistent with the dissolution of a surface layer rich in ferric iron. McConnel (1978) suggests fine grained hematite and supports this with ferric iron analyses in these

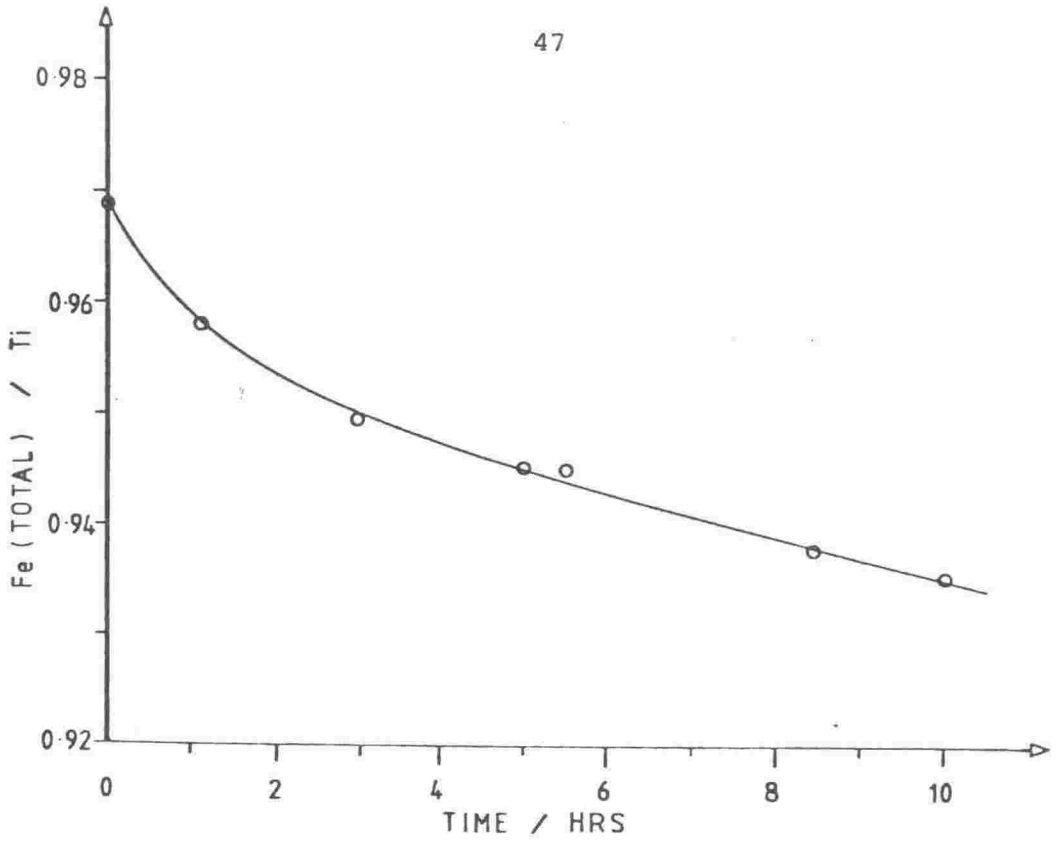

Fig. 4.3 Fe:Ti ratio from ilmenite samples - 6 M HCl 70 °C.

solutions (Fig. 4.4). Isolated occurrences of surface hematite are visible through the optical microscope (Fig. 4.5) and one occurrence of distinct hematite lamellae orientated parallel to the basal plane in an ilmenite grain was noted [see for example El-Hinnawai (1969) and Lally et al (1976) for a discussion of the ilmenite/hematite relationship]. Surface hematite is however not extensive and is not observed by X-ray diffraction even using unground samples, neither is it observed in the Mössbauer spectrum of Tauranga Bay ilmenite (see section 4.4).

If the plotted line for iron dissolution is projected back through the concentration axis, the intercept is seen to coincide for reactions at 60, 70 and 80 °C (Fig. 4.6) suggesting the concentration irregularity is proportional to the amount of ilmenite rather than the path of reaction.

Further evidence for such a layer can be seen in scanning electron photomicrographs of whole grains in the early stages of reaction (see Fig. 4.12).

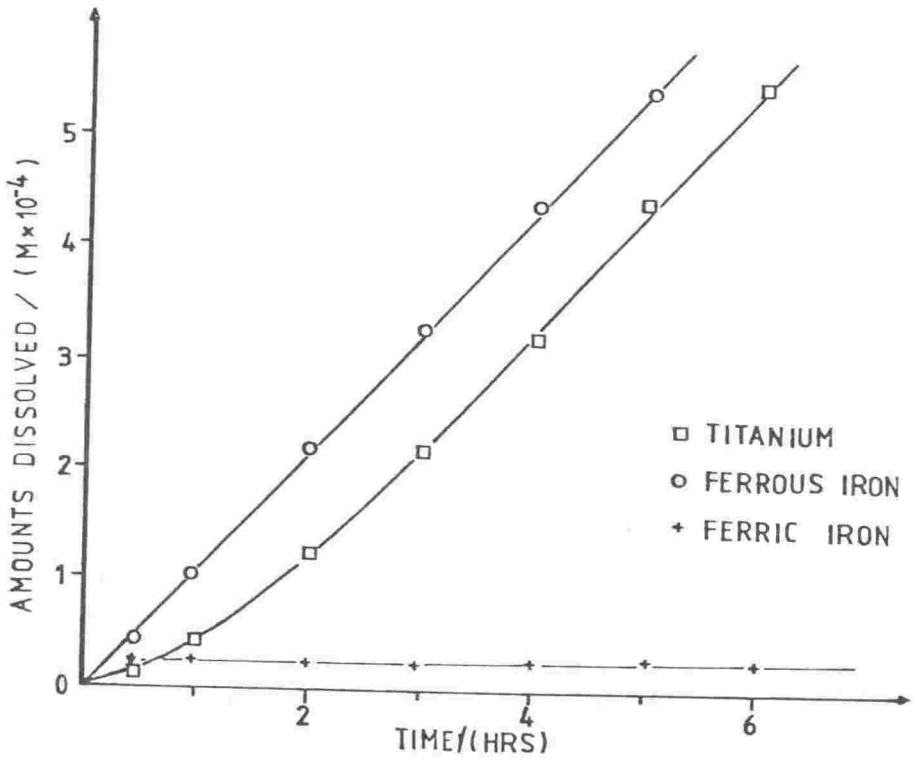

Fig. 4.4 The dissolution of titanium, ferrous iron and ferric iron from Tauranga Bay ilmenite - 9.02 M H_2SO_4 65 °C. (From McConnel 1978).

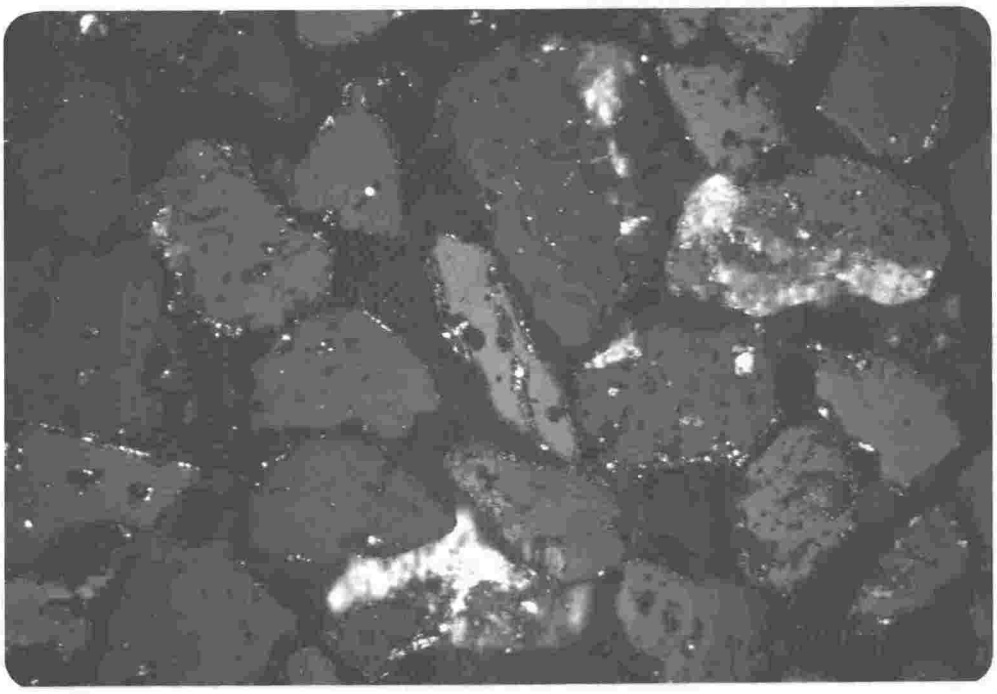

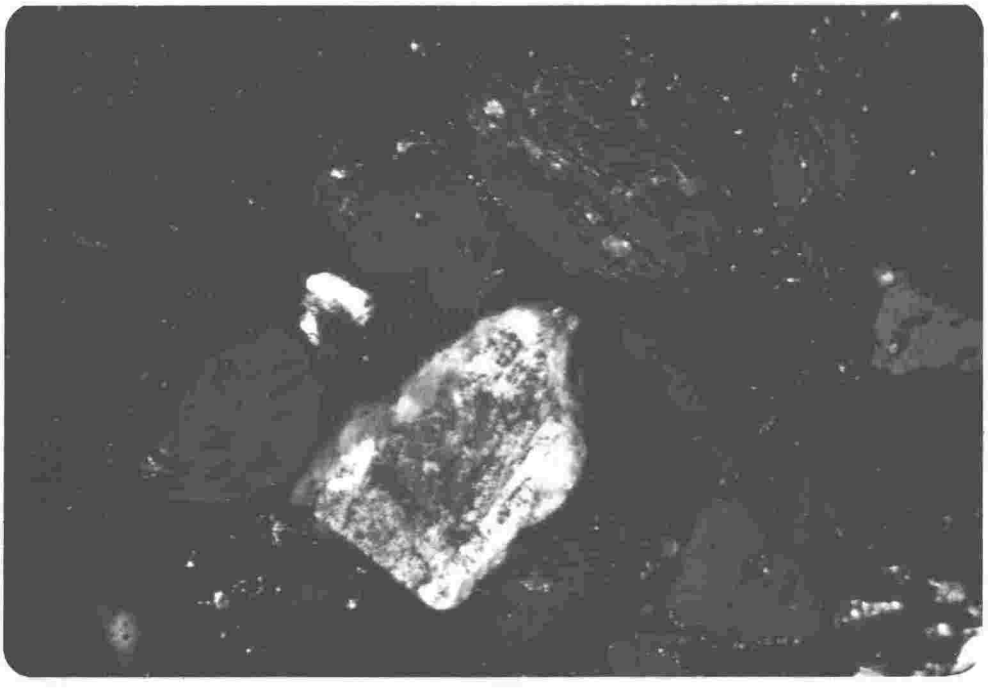

Fig. 4.5 Cross-section of Tauranga Bay ilmenite grains viewed under crossed-polarised light. Hematite appears as red-brown streaks. (Field of view = 420 μm).

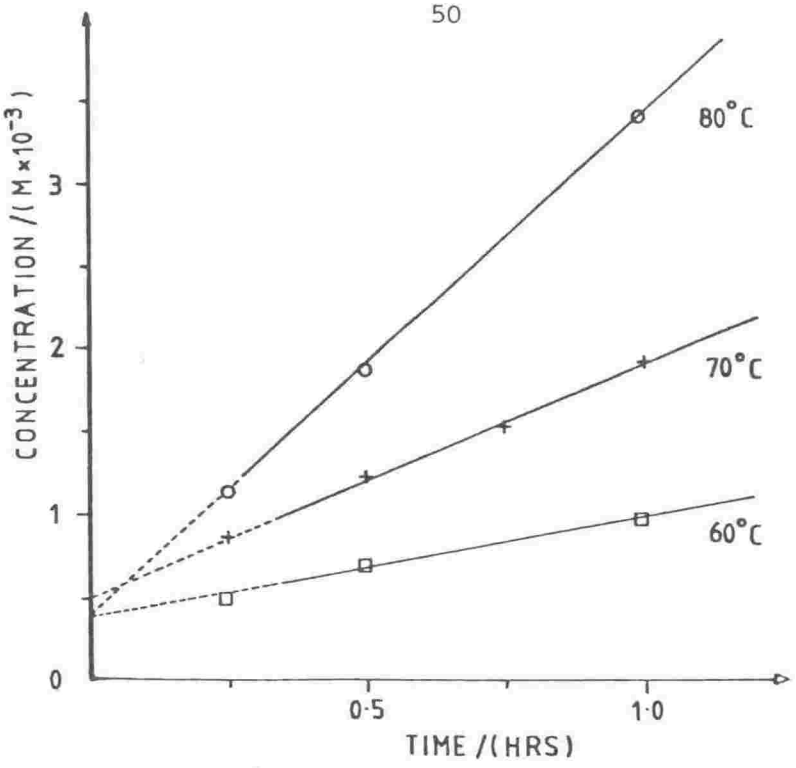

Fig. 4.6 Projection of plots of iron dissolution from activation energy determination (see section 4.3), back through the concentration axis, 6 M HCl, 75-125 μm ilmenite sample.

Unit cell parameters for the ilmenite crystallites were calculated as described in section 3.4.1. Figure 4.7 shows the variation in the parameters of Tauranga Bay samples after differing degrees of reaction and Table 4.3 lists these values in comparison with other ilmenites studied. The results indicate a slight shrinkage in the unit cell volume with progressive reaction (whether by acid dissolution or by natural weathering). Variation is similar in both the a and c axes of the hexagonal unit cell but is at less than 1% levels. This is consistent with a small degree of iron oxidation with no significant deformation of the unit cell.

4.1.3 Solid Products from the Reaction

X-ray diffraction analysis was used in attempting to identify product or intermediate phases in the dissolution. The intensity of the ilmenite diffraction pattern because of its highly crystalline nature, tends to mask peaks from a number of possible products which exhibit

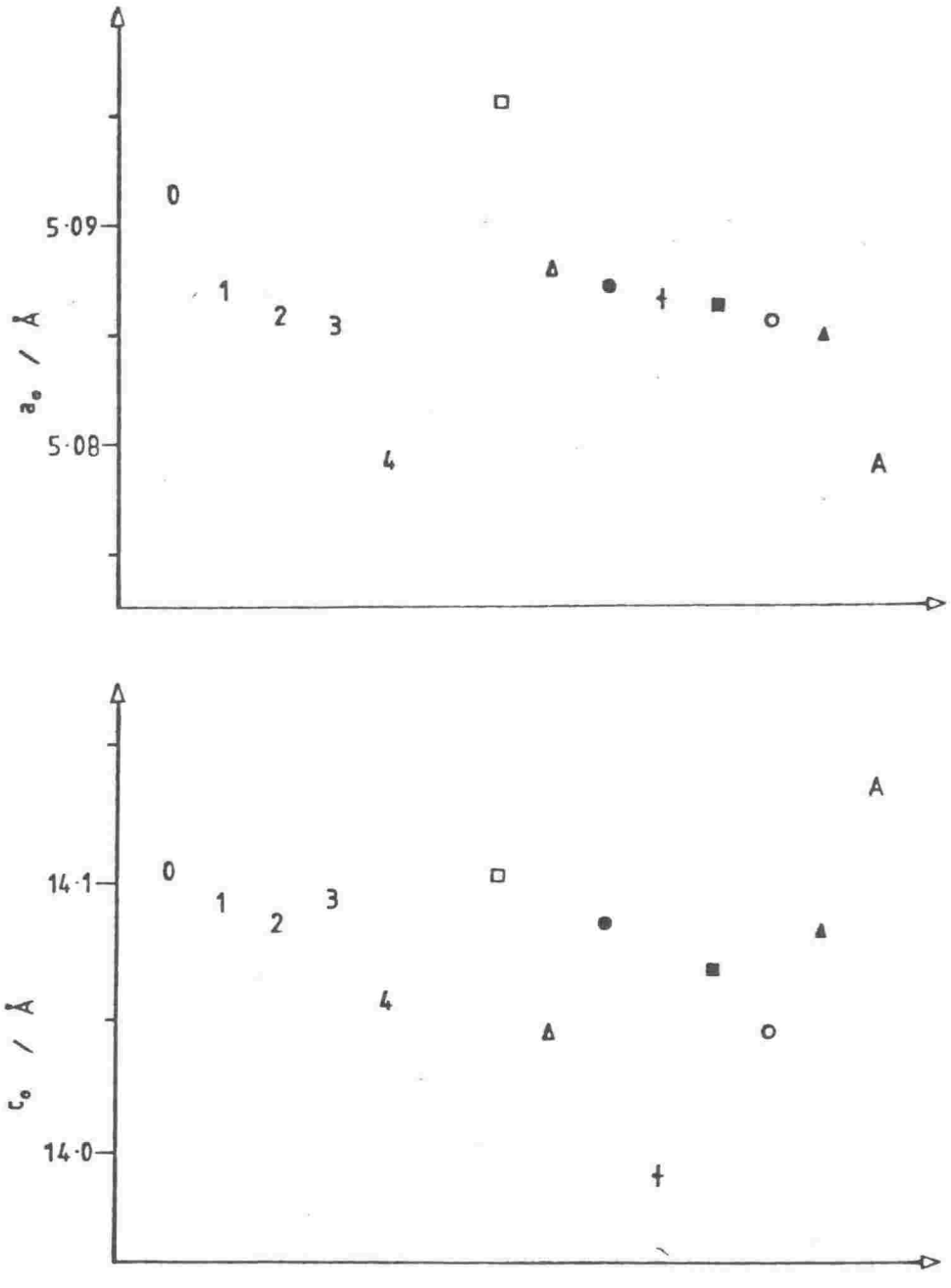

0 = TAURANGA BAY
1 = /4M H_2SO_4 10 HRS
2 = /8M HCl
3 = /10M HCl
4 = /4M H_2SO_4 36 HRS

□ = BARRYTOWN (WEST COAST)
Δ = MANUKAU (NTH ISLAND)
● = SYNTHETIC (SHIRANE ET AL 1962)
† = BOWENTOWN (NTH ISLAND)
■ = WESTRALIAN SANDS (AUST)
○ = HAMILTONS GAP (NTH ISLAND)
▲ = WESTERN TITANIUM (AUST)
A = ASTM VALUES

Fig. 4.7 Unit cell parameters (hexagonal unit cell) for ilmenites.

TABLE 4.3 Unit cell parameters* for ilmenites and related minerals

Sample	a_o (A°)	c_o (A°)	Volume
Tauranga Bay	5.092	14.102	316.6
/4 M H_2SO_4 10 hr	5.087	14.093	315.8
/8 M HCl	5.086	14.093	315.8
/10 M HCl	5.085	14.087	315.5
/4 M H_2SO_4 36 hr	5.079	14.057	314.0
Manukau	5.088	14.045	314.8
Western Titanium	5.085	14.082	315.3
Synthetic (Shirane et al 1962)	5.085	14.082	315.3
ASTM	5.079	14.135	315.8
Pseudorutile ($Fe_2Ti_3O_9$)	4.615	14.375	265.1
Hematite (α-Fe_2O_3)	5.034	13.752	301.8

*All unit cell parameters quoted in this work are based on the hexagonal unit cell, rather than the rhombohedral equivalent - see Fig. 2.1.

similar patterns e.g. pseudorutile ($Fe_2Ti_3O_9$) and rutile (TiO_2). However after extensive reaction (greater than 50% dissolution) product phases can be identified.

Figure 4.8 shows the diffraction pattern of the solid residue after 80% dissolution in 10 M HCl. The ilmenite pattern is still well defined, but is overshadowed by broad peaks from poorly crystalline

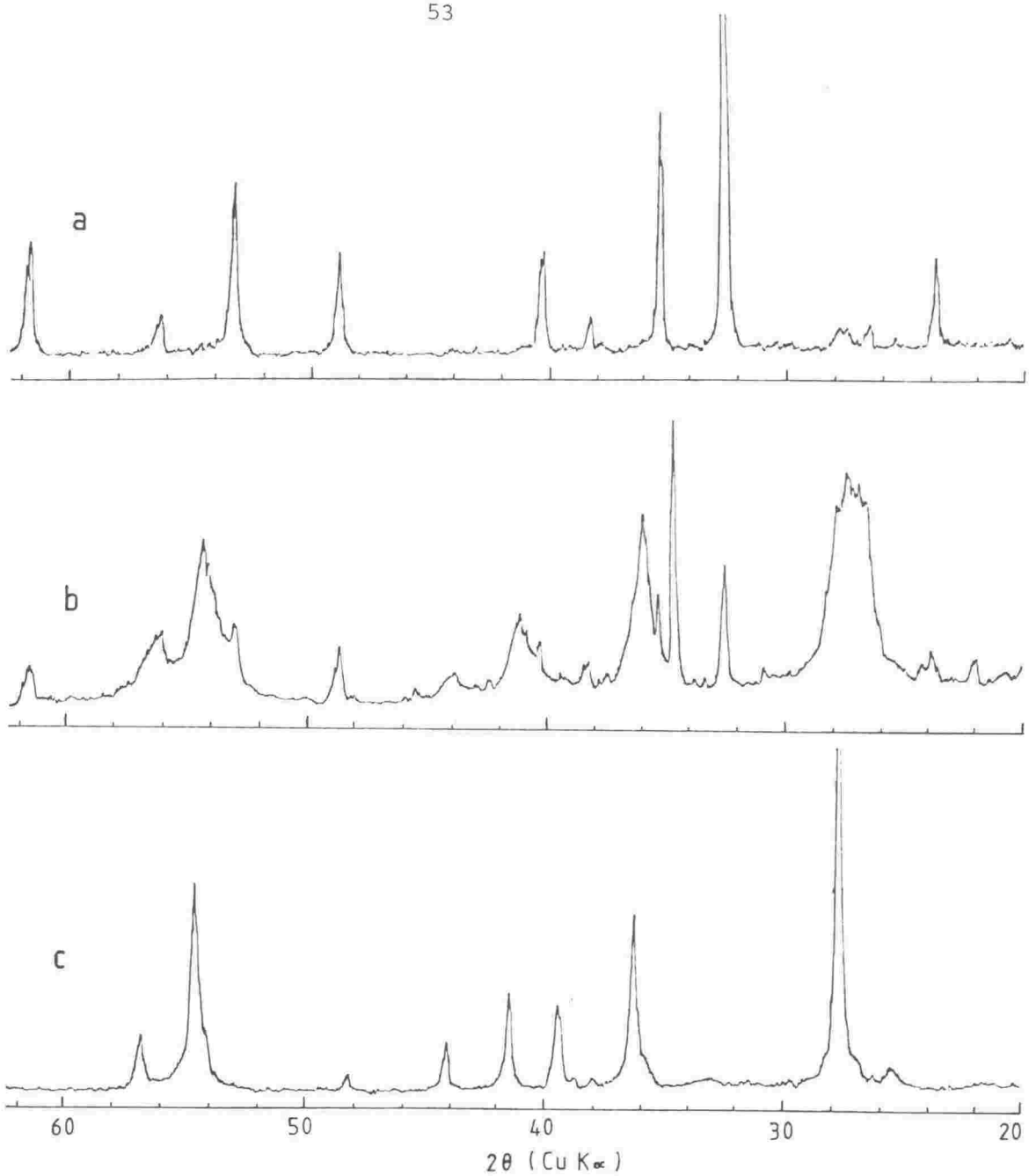

Fig. 4.8 X-ray diffraction traces from (a) Tauranga Bay ilmenite, (b) the residue after 80% dissolution in 10 M HCl, (c) rutile.

rutile possibly containing some pseudorutile. Unfortunately the pseudorutile diffraction pattern is extremely difficult to distinguish from that of rutile if both are present (Grey and Reid 1975).

The dominant quartz peak (3.34 A°) is also enhanced, contributing to the broad reflection centred at 3.27 A°. The diffraction pattern indicates enrichment of the residue in the acid resistant gangue minerals and the precipitation or growth of a poorly crystalline rutile phase.

In all experimental runs involving more than ≈60% dissolution, halting the stirring at the completion of the run allows a thin layer of a grey colloidal sludge to settle above the residual ilmenite. This material can also be extracted by decanting and centrifuging the reaction liquor after the heavier ilmenite residue has been allowed to settle. This colloidal material, after drying in air and over silica gel, gives a diffraction pattern very similar to that of the residue in figure 4.8, corresponding to ilmenite, poorly crystalline rutile and quartz. Examination of the sludge by IR before dehydration (Fig. 4.9) reveals a distinctive peak at ≈890 cm^{-1} which coincides with the 800-920 cm^{-1} range indicative of -Ti-O-Ti-O- chains (Selbin 1964, Barraclough et al 1959, Bragina and Bobyrenko 1972).

Apart from the residual ilmenite, this colloidal material is sparingly soluble in warm concentrated sulphuric acid. The resulting solutions, analysed by atomic absorption spectroscopy showed a variable iron:titanium ratio (Table 4.4) often with enrichment in titanium relative to the bulk solution from the digestion reaction.

TABLE 4.4 Atomic Absorption analyses from the dissolution of colloidal precipitates

Sample	Fe/Ti	Fe/Ti (bulk solution)
6.1 M HCl/H_2SO_4 wash	0.88	1.13
8.3 M HCl/H_2SO_4 wash	0.92	1.02
3.7 M HCl/HCl wash	1.15	1.61

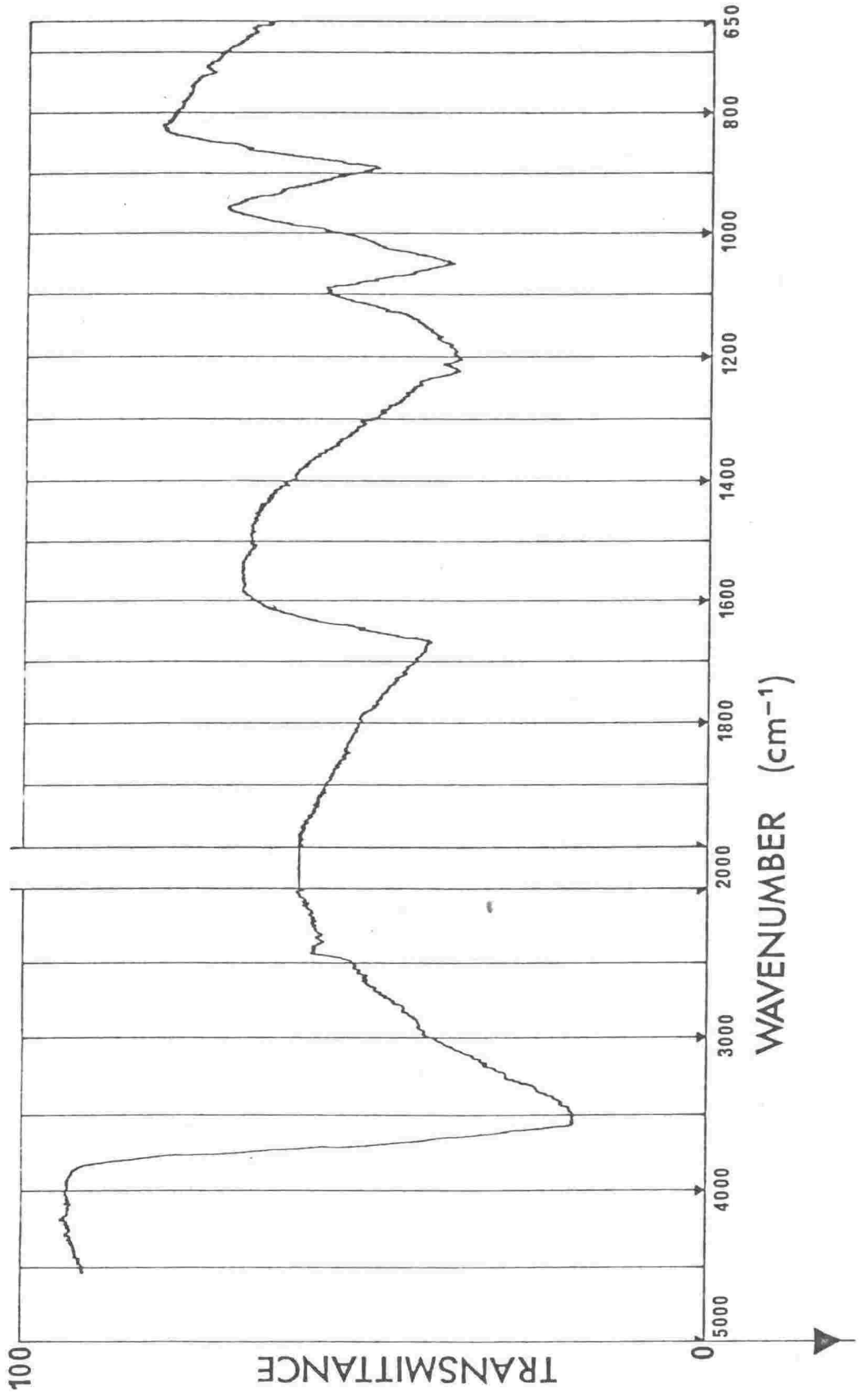

Fig. 4.9 Infrared absorption spectrum of a colloidal precipitate before drying, 6.1 M HCl, 70 °C, 8 hrs.

The precipitate was thus attributed to hydrous titanium dioxide, which settles out with fine grained residual ilmenite. The precipitate was difficult to isolate from the acid without substantial modification of its properties - washing causes partial dissolution and heating causes conversion to the largely insoluble oxide.

When phosphoric acid was added to the solution during reaction, the dissolution was markedly impaired and precipitated material was clearly visible in scanning electron photomicrographs of the grains (Fig. 4.10). This precipitate was also visible in liquid samples extracted from the solution early in the reaction. The material was strongly hygroscopic and not sufficiently crystalline to yield an X-ray diffraction pattern. Its composition was examined by X-ray fluorescence and electron microprobe (Table 4.5). Microprobe analyses, from fragments of the phosphate precipitate yielded poor totals, due to a number of causes:

(a) the softness of the material did not allow a good polishing finish.

(b) fragments are extremely small (rarely more than 5 μm in diameter), making beam location difficult.

(c) the phosphate precipitate tends to nucleate either on ilmenite fragments or on loose gangue minerals, giving mixed analyses.

The water content also causes depressed totals in both methods, however both show a titanium phosphate virtually free of iron and containing phosphate and titanium in an approximately 1:2 ratio. Infrared spectra reveal little about the structure of the precipitate with little evidence of the -Ti-O-Ti-O- bridging structure observed in hydrous oxide precipitates (see Fig. 4.9).

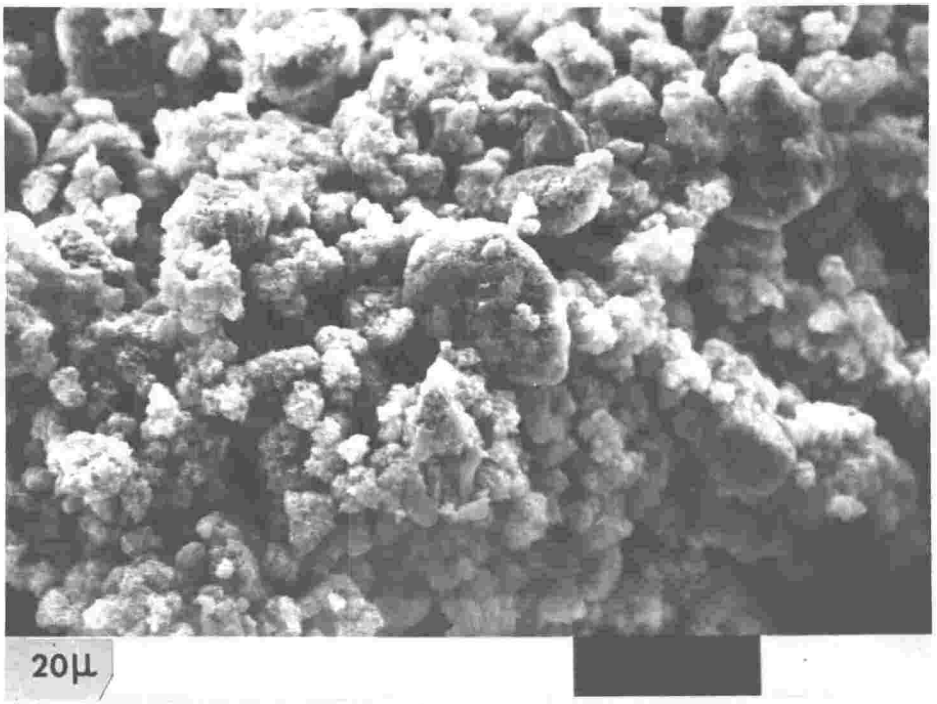

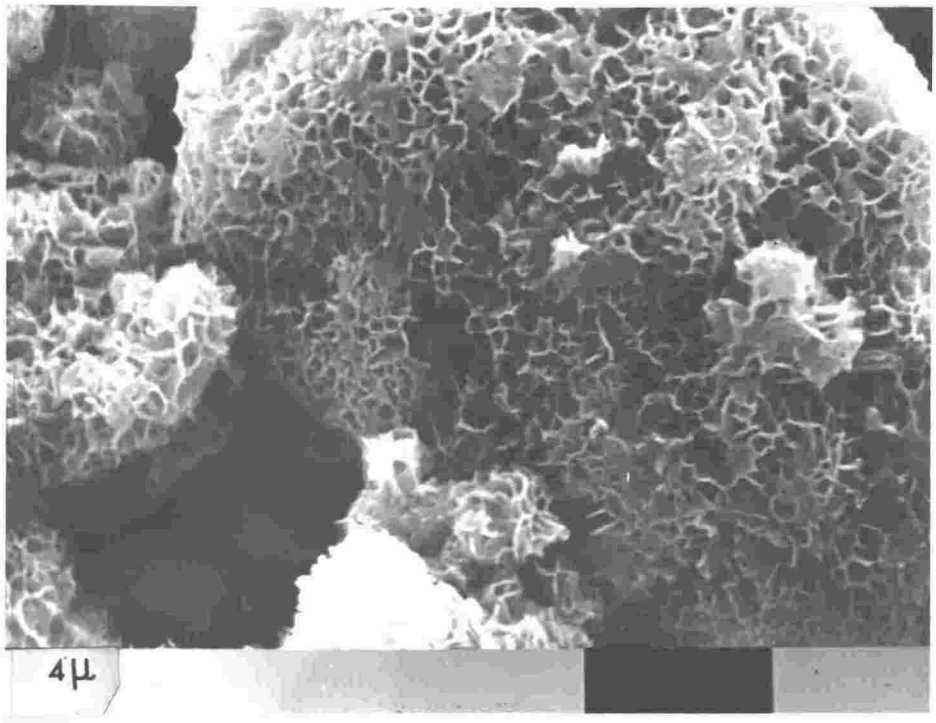

Fig. 4.10 Scanning electron microscopy from grains after partial dissolution, 4 M H_2SO_4 + 0.4 M H_3PO_4.
(Black marker bar = scale in left hand corner).

TABLE 4.5 X-ray fluorescence and Electron micro-probe analyses of residual ilmenites containing phosphate precipitates

	1	2	3	4	5
TiO_2 %	45.47	44.16	38.35	27.12	29.34
FeO	20.30	33.02	2.88	4.14	4.79
MnO	0.94	1.44	0.67	0.08	0.21
MgO	2.55	2.37	0.43	0.73	0.06
Al_2O_3	2.16	1.82	0.30	1.66	0.97
P_2O_5	14.84	7.84	32.60	23.51	24.66
SiO_2*	8.00	3.02	1.45	14.49	4.25
Others	1.44	0.89	0.08	0.04	0.02
	95.70	94.56	76.76	71.77	64.30

1. Residue from dissolution in 4 M H_2SO_4 + 1% H_3PO_4, 12 hrs.

2. 4 M H_2SO_4 + 10% H_3PO_4, 10 hrs.

3. Phosphate precipitate separated by centrifuge from residual ilmenite.

4,5. Microprobe analyses of colloidal fragments surrounding grains after dissolution in 4 M H_2SO_4 + 1% H_3PO_4.

*The significant levels of silica in these analyses suggest that inclusions may serve as nucleating agents for this precipitated phosphate material.

4.1.4 Physical Characteristics of the Dissolving Ilmenite

One of the most significant features of the early stages of dissolution is the formation of a porous structure in many of the grains. This is revealed in electron photomicrographs of polished cross-sections of ilmenite grains (Fig. 4.11). These images show a pattern of attack following preferred planes through the ilmenite grains. This results in internal cavity formation as the reaction progresses, until disintegration of the grains occurs. Two distinct preferred planes of attack can be identified (Fig. 4.11). Single crystal X-ray diffraction was not attempted because of the lack of grains of sufficient crystallite size, so the planes could not be unambiguously identified. However preferential attack has been reported in several studies of ilmenite reactivity (Lynd 1960, McConnel 1978) and the dominant attack always takes place parallel to the basal (0001) plane (refer to Fig. 2.1 for the ilmenite structure). The second plane appears to be the other prominent parting plane of ilmenite ($10\bar{1}1$). The angle between the observed planes of attack when measured over 30 grains shows a maximum of 58→60° which coincides accurately with the 57°59' angle between the two parting planes (Deer, Howie and Zussman 1966). Attack along parting planes is not uncommon in mineral systems for example, in acid attack on pyroxenes and amphiboles (Berner et al 1980).

Also observed in whole grain photomicrographs from the early stages of reaction is evidence for an outer shell on some grains (Fig. 4.12). This appears to be removed relatively rapidly. Well defined holes in ilmenite grains are also visible (Fig. 4.12), consistent with either the

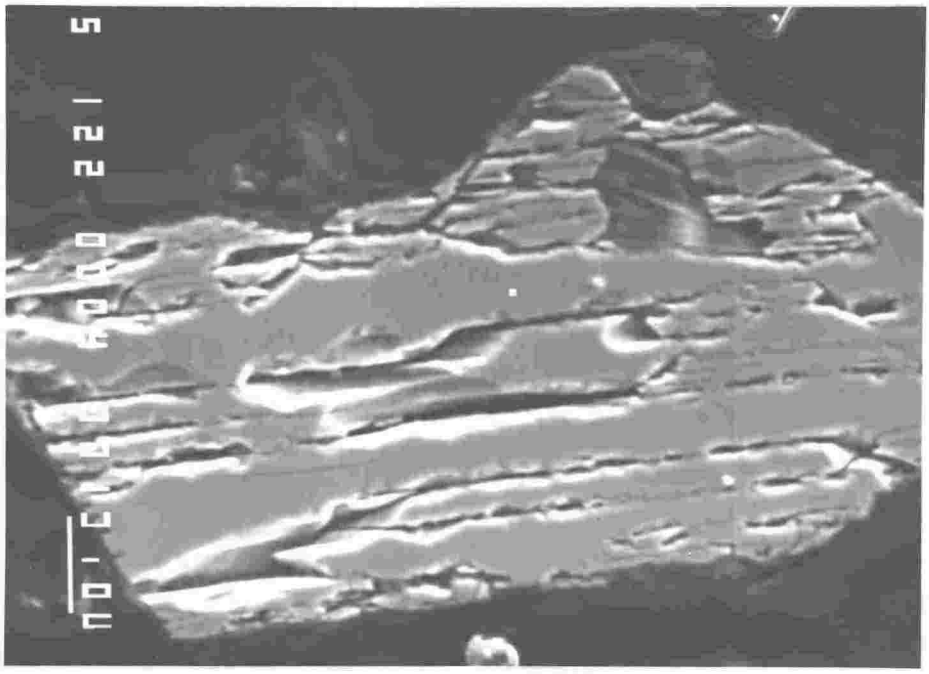

(a) 8 M HCl + 0.5 M Ti^{4+}, 70 °C, 10 hrs. (Marker bar = 10 μm)

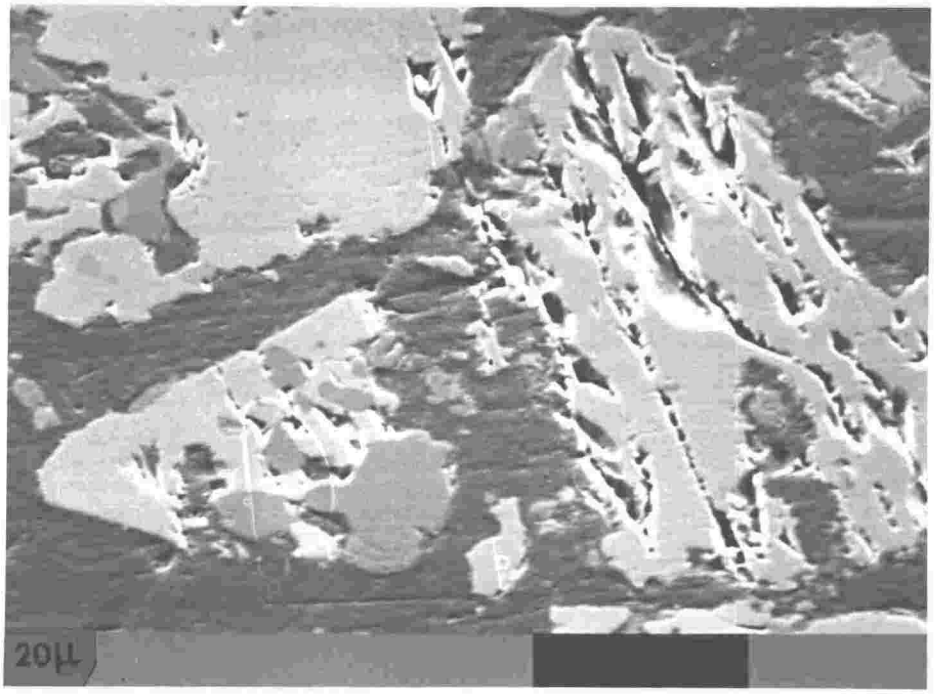

(b) 8.3 M HCl, 70 °C, 12 hrs.

Fig. 4.11 Cross-sections of grains of Tauranga Bay ilmenite after partial dissolution.

cont. over

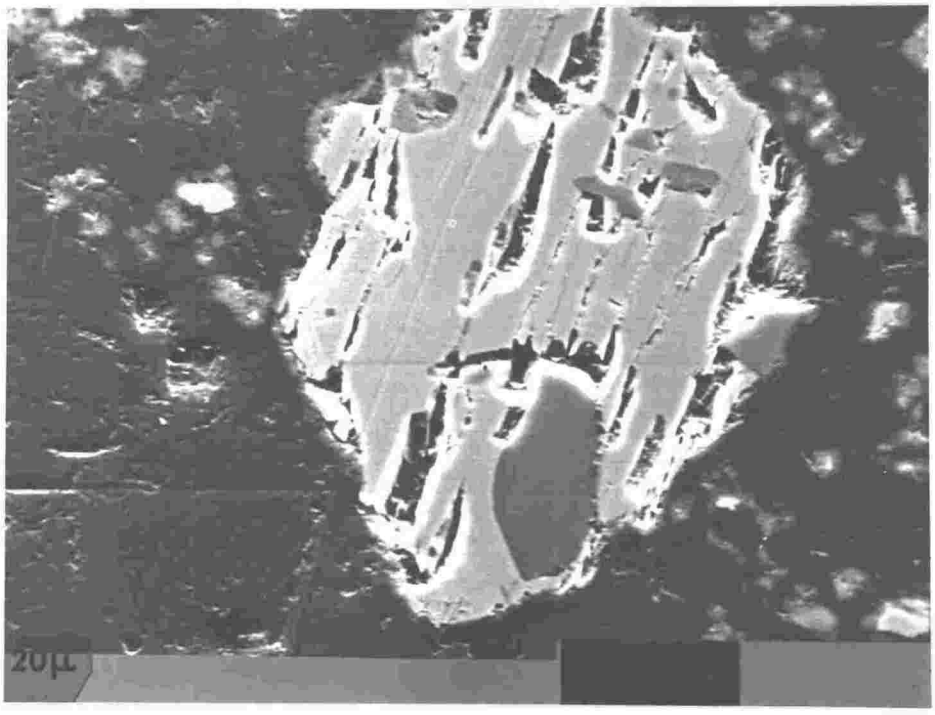

(c) 8.3 M HCl, 70 °C 12 hrs.

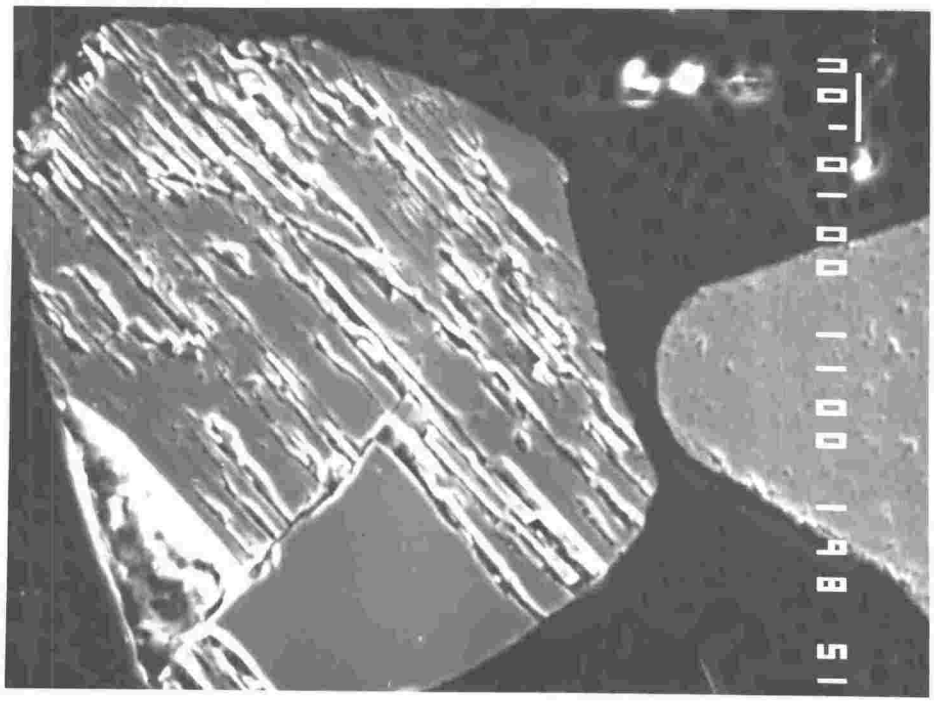

(d) 6.1 M HCl, 70 °C 8 hrs (marker bar = 10 µm)

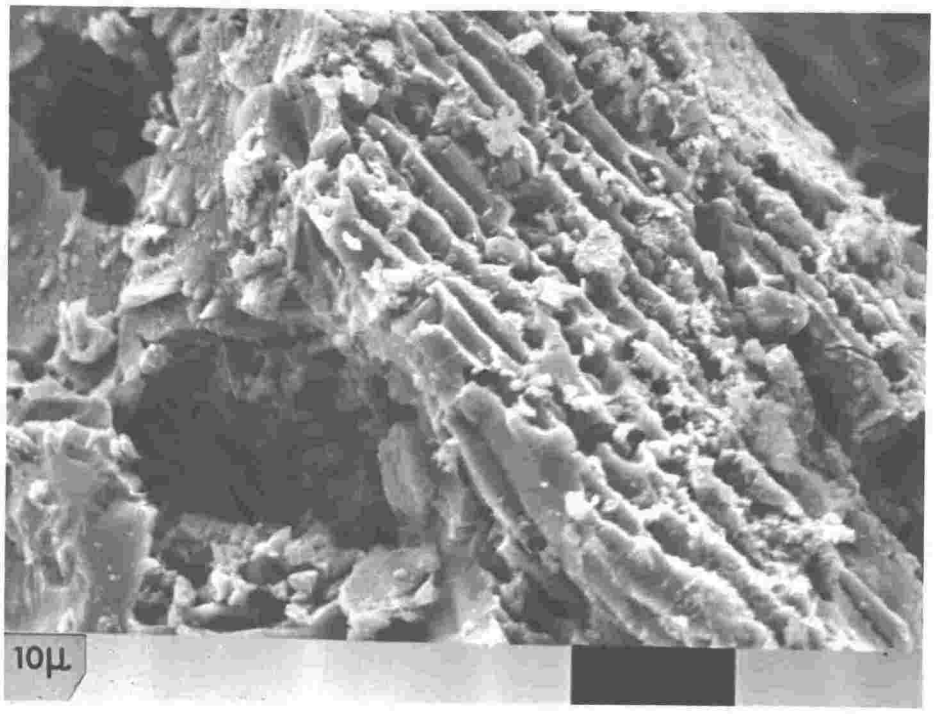

(e) 4 M H_2SO_4 70 °C 2 hrs (whole grain view)

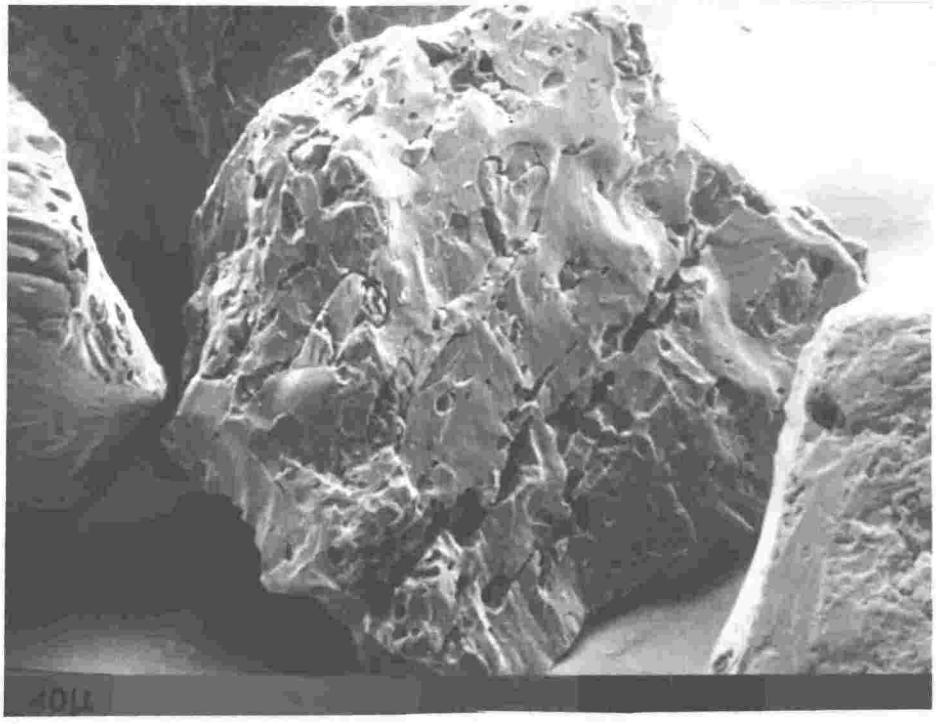

(f) 4 M H_2SO_4 70 °C 30 min. (whole grain view)

Fig. 4.11 (cont.)

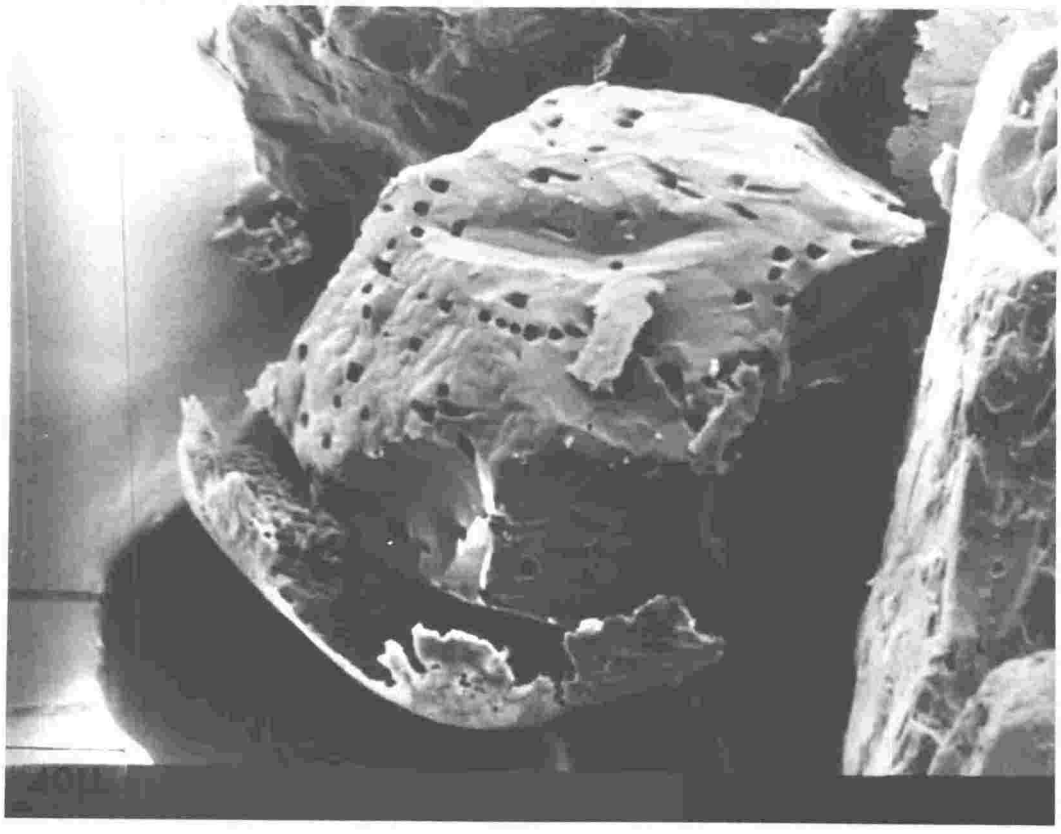

(a) 4 M H_2SO_4, 50 °C, 30 minutes.

(b) 4 M H_2SO_4, 50 °C, 30 minutes.

Fig. 4.12 Evidence of surface layer dissolution after small degrees of reaction - unground Tauranga Bay ilmenite.

dissolution of soluble inclusion material such as apatite (see section 4.1.2), or the start of the pore formation observed in cross-sections later in the reaction. The small number of soluble inclusions, suggests the latter is the more likely explanation.

4.2 The Composition of the Solution

4.2.1 The Form of the Dissolution Curve

Dissolution experiments were carried out as described in section 3.2 and the resulting curves have several features in common. A typical dissolution curve for ilmenite in medium strength (6 M) hydrochloric acid is shown in figure 4.13.

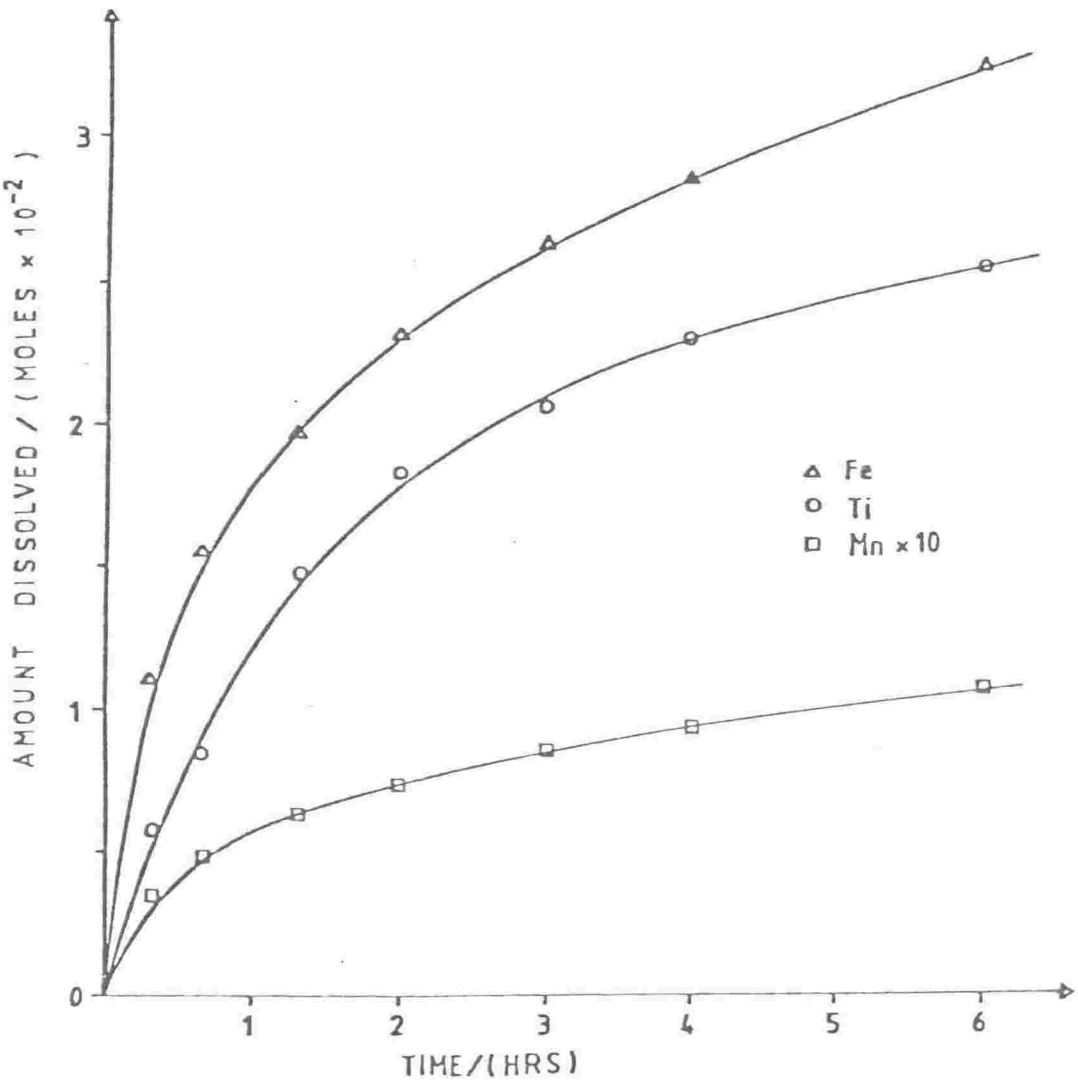

Fig. 4.13 The dissolution of Tauranga Bay ilmenite in 6 M HCl 70 °C.

(a) The basic shape (Fig. 4.13) is the same for all the acid strengths used, provided the acid/ilmenite ratio is constant. Reaction begins rapidly, dissolution rate then declines, reaching a plateau after several hours. This plateau cannot be attributed to either completion of the dissolution (as often only 10% conversion is observed), or acid consumption (as the acid is often in up to 50× excess of the dissolved ilmenite at the plateau). The addition of fresh ilmenite to the reaction vessel (see section 4.2.7) shows solution saturation in the dissolved components is also not responsible, although reduced dissolution of the fresh ilmenite indicates saturation may be a contributing factor.

(b) Above a minimum speed necessary to maintain the circulation of the ilmenite, variation in stirring speed has little effect on reaction rate. Figure 4.14 illustrates the course of reaction in the absence of any stirring.

Through the course of this work some 40 dissolution runs were carried out, 31 of these using hydrochloric acid and the remainder using sulphuric acid. Two distinct acid:ilmenite mole ratios were used, 10:1 and 50:1. The first is more than double the 4:1 stoichiometric requirement for complete dissolution:

$$FeTiO_3 + 4H^+ \rightarrow Fe^{2+} + TiO^{2+} + 2H_2O$$

However this ratio is still close to industrial conditions (see section 3.1). Sufficient acid is present to avoid acid availability in the bulk solution become rate controlling. The second ratio used was 50:1, a very dilute solution by comparison with industrial conditions but chemically convenient in the study of activation energies (see section 4.3) and other features of the dissolution. Figure 4.15 shows the reaction curve of 6 M hydrochloric

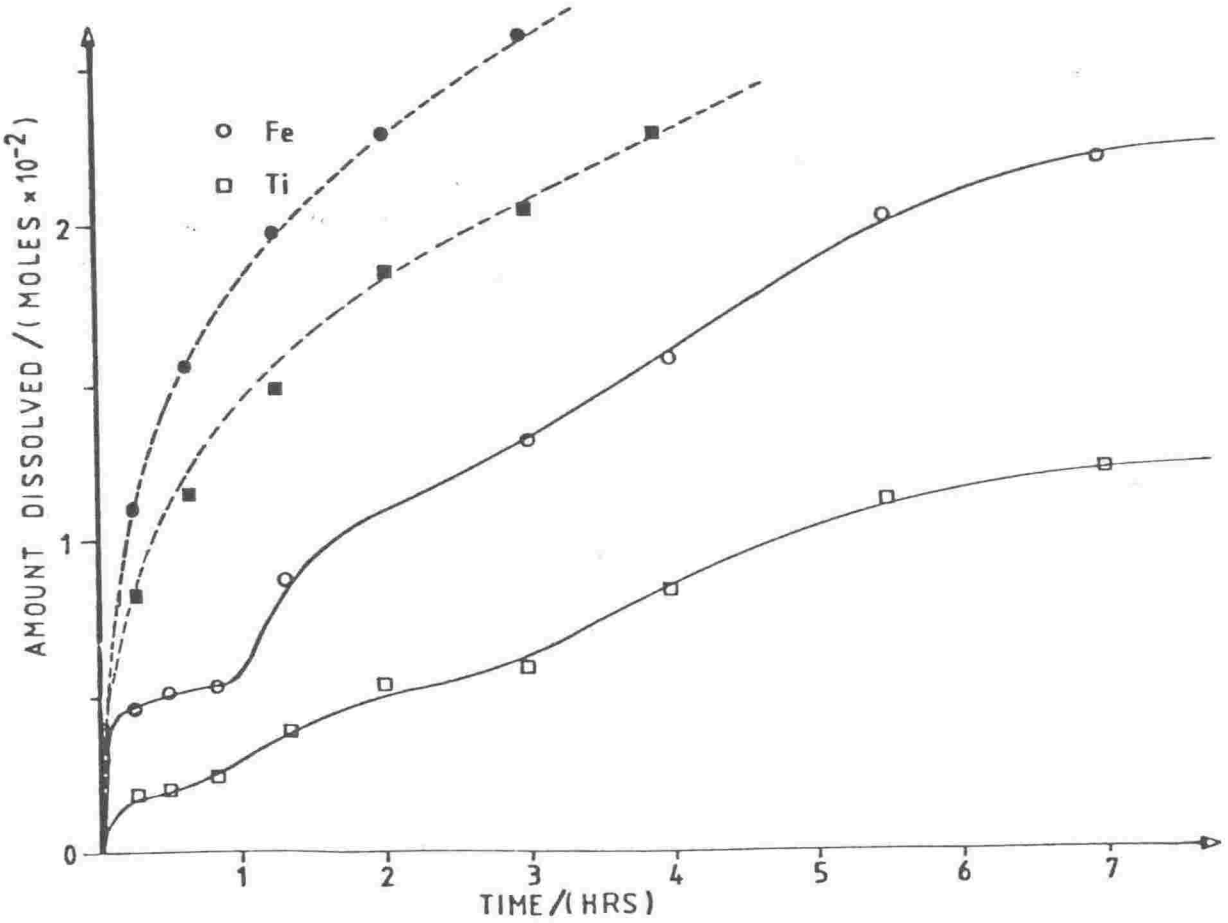

Fig. 4.14 The dissolution of Tauranga Bay ilmenite without (——) and with (----) stirring, 6.1 M HCl, 70 °C.

acid at the two ratios using unground ilmenite.

Considerable similarity in the pattern of the reaction is apparent, particularly in the first hour. In both reactions Ti and Mn display concentration/time linearity with plots passing through the origin. Iron however dissolves considerably more rapidly in the first hour but thereafter shows the same linearity. This is attributed to the dissolution of small amounts of hematite on the ilmenite surface (see section 4.1.2). Conversion in both cases is approximately 5% after 5 hours of reaction.

Significant differences are observed between these reactions using unground samples, and the reaction of a ground sample under the same conditions, at the 10:1 acid:ilmenite ratio (Fig. 4.13). In this reaction,

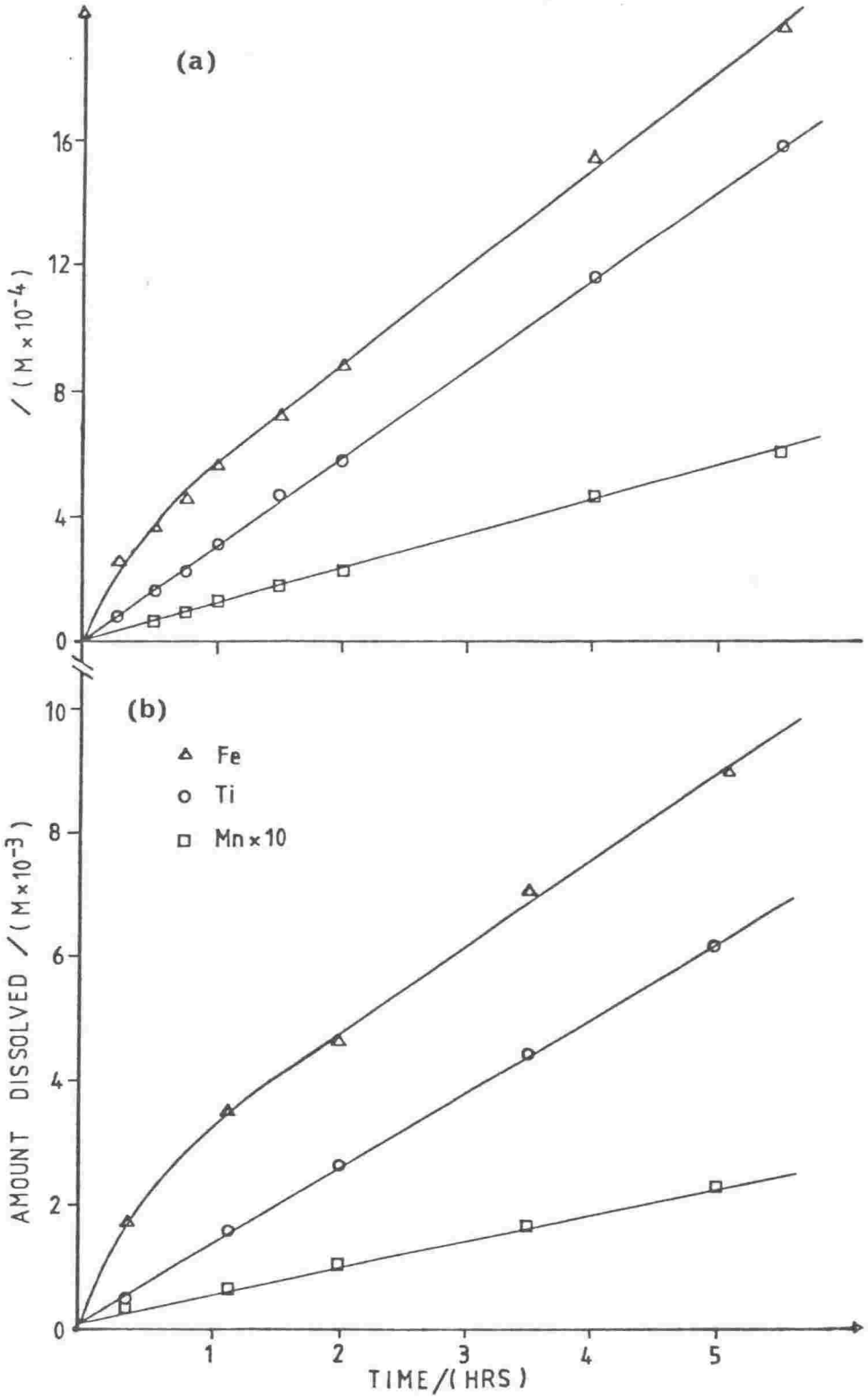

Fig. 4.15 The dissolution of unground Tauranga Bay ilmenite in 6 M HCl, 70 °C, (a) acid:ilmenite = 50:1; (b) acid:ilmenite = 10:1.

conversion of the ilmenite approaches 17% after 5 hours and at this stage reaction rate is still declining. It is also apparent that titanium and manganese follow the same dissolution behaviour as iron from the earliest stages of reaction, but again iron is displaced above titanium.

One feature of the reaction which became apparent in calculating a mass balance, was a small but measurable titanium deficiency. Although the bulk analysis shows slight enrichment in titanium (see Fig. 4.2), there is a distinct deficiency in total titanium calculated after reaction, compared with initial levels. Iron losses were always within experimental error, when before and after totals were compared. For example in the dissolution of Tauranga Bay ilmenite in 3.7 M HCl (see Fig. 4.17)

Fe (remaining solid + dissolving solution + liquid removed during sampling) = $(6.87\pm0.10)\times10^{-2}$ moles

Fe (original ilmenite) = 6.94×10^{-2} moles

Ti (remaining solid + dissolving solution + liquid removed during sampling) = $(6.28\pm0.10)\times10^{-2}$ moles

Ti (original ilmenite) = 6.54×10^{-2} moles

This 4% deficiency was the largest observed in 4 dissolution experiments considered, with other values between 2.5 and 3.5%. There was no reason to suggest interference in Atomic Absorption response was causing this consistent deficiency.

Again the dissolution of an iron rich surface phase could account for the imbalance, provided the amount of iron involved is less than the sensitivity of X-ray fluorescence analysis in detecting changes in the bulk composition. A more likely explanation is that the titanium is either precipitated, or retained in the ilmenite structure by some adsorption mechanism. This feature of reaction is discussed in section 5.3.3.

4.2.2 Hydrolysis of Dissolved Titanium

Thermal hydrolysis is the major step in the formation of titanium dioxide pigments from solutions of dissolved titanium ores such as ilmenite. The mechanism of acid hydrolysis is still the subject of some speculation, however the generally accepted mechanism (Duncan and Richards 1976) is as follows:

1. The unstable hexaquo titanium ion $Ti(H_2O)_6^{4+}$ losses a proton from one of the co-ordinated water molecules.

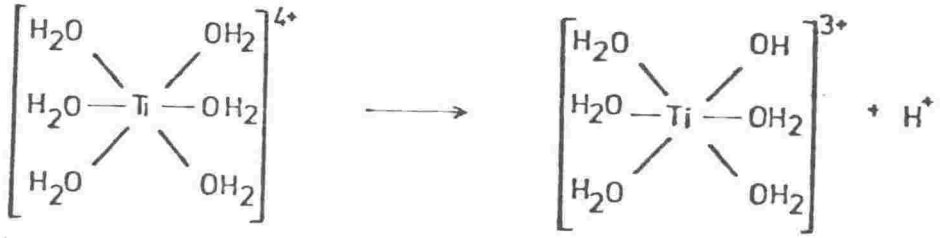

2. Two such hydroxo units then lose two co-ordinating water molecules by forming hydroxy bridges resulting in a binuclear titanium ol-complex.

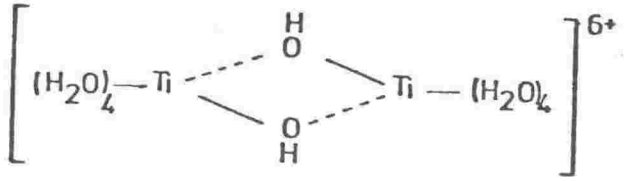

3. This ol-complex then loses two protons from the hydroxo bridges to form an oxo-complex.

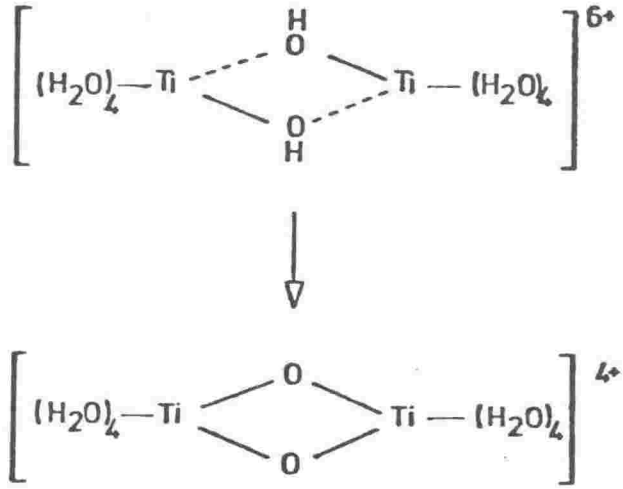

4. Further linkages can then be formed by splitting off further water molecules to form tetra-oxo complexes and the growth of polynuclear titanium compounds follows.

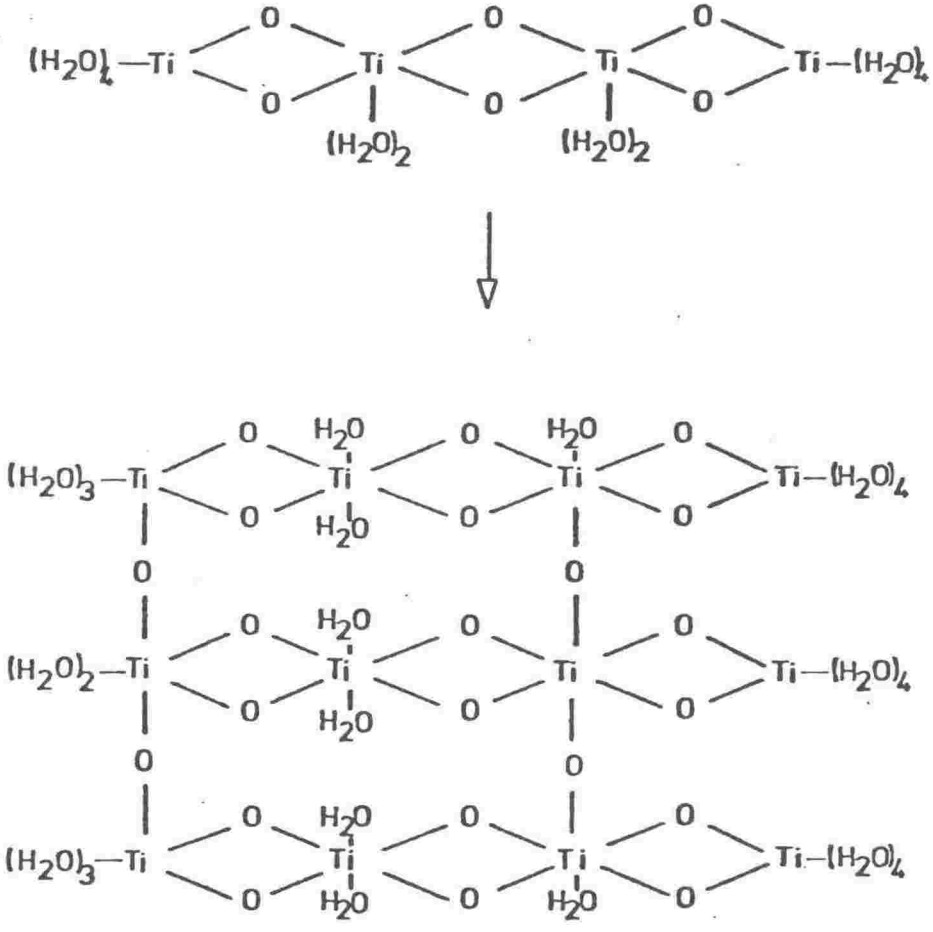

Duncan and Richards (1976) also showed that the anion plays a significant role in the mechanism of hydrolysis, in the case of sulphate solutions, by the formation of a titanium bisulphate complex $Ti(OH)_3(H_2O)_2HSO_4$.

Chloride solutions of titanium are known to hydrolyse more readily than sulphate solutions, in fact sulphate addition can be used to retard the hydrolysis of chloride solutions (Judd 1977). This appears to relate to the mechanism of anion penetration (Richards 1975) which prevents the proliferation of polynuclear complexes. Chloride is a less effective penetrating anion than sulphate, thus allowing hydrolysis to proceed more rapidly. The onset of hydrolysis is determined by titanium concentration, free acid, specific nature of the anion and its concentration and also the presence of suitable nucleating agents to precipitate the polynuclear complexes.

Evidence of the occurrence of hydrolysis during ilmenite dissolution is usually a rapid drop in titanium concentration in the solution, without any corresponding movement in iron concentration. In only one reaction was a clear example of this observed (Fig. 4.16), and this occurred in a reaction extended to 16 hours involving the addition of fresh ilmenite. In dissolution runs using hydrochloric acid, temperatures higher than 80 °C were avoided specifically to minimise hydrolysis.

However the presence of colloidal hydrous titanium dioxide in the residue of a number of dissolution runs (see section 4.1.3) suggested that some hydrolysis was taking place. The presence of -Ti-O-Ti-O- chain vibrations in the IR spectrum of the colloidal material confirms the formation of polynuclear titanium complexes similar to those described above.

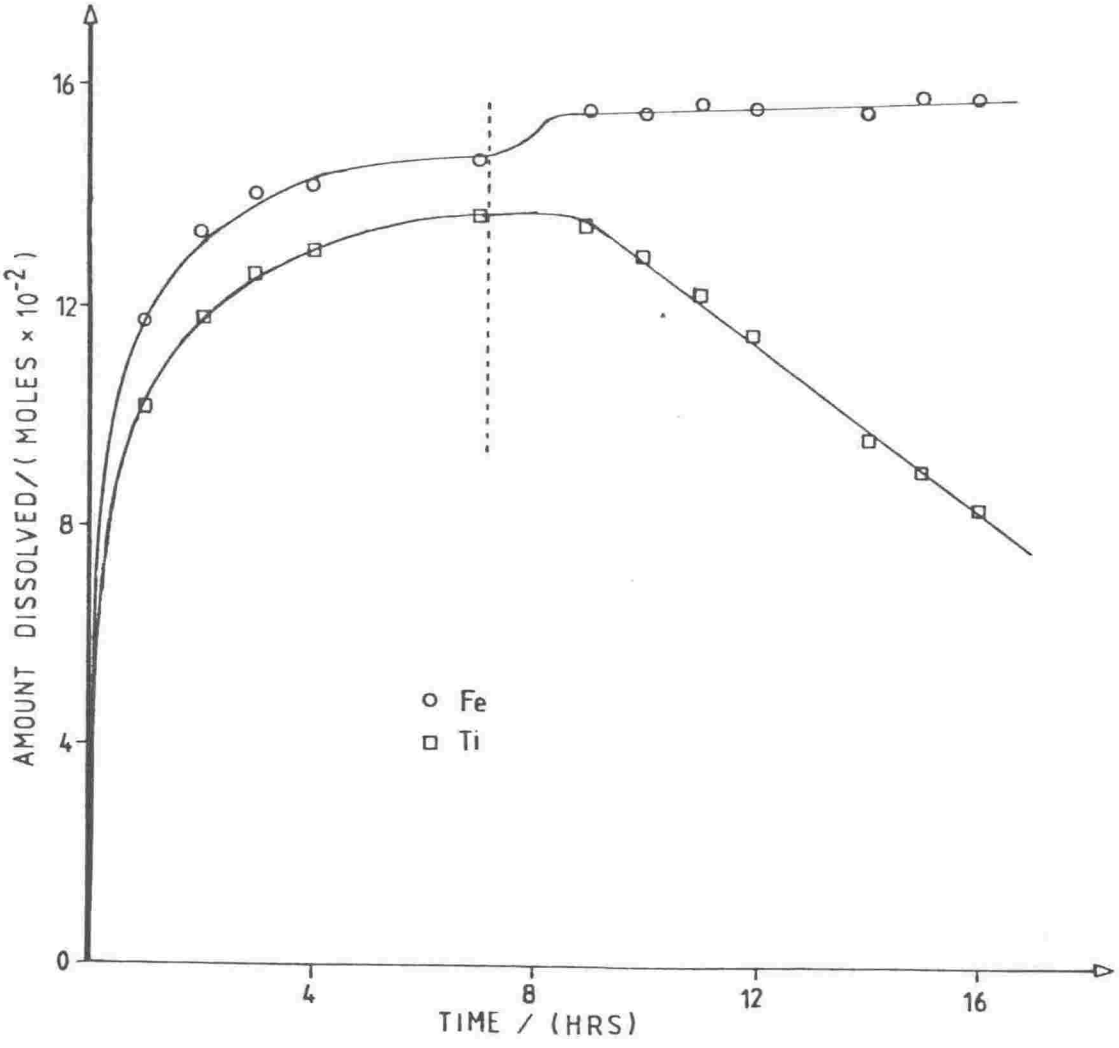

Fig. 4.16 An example of titanium hydrolysis during ilmenite dissolution 10 M HCl, 80 °C. Fresh ilmenite was added at the point indicated by the dotted line.

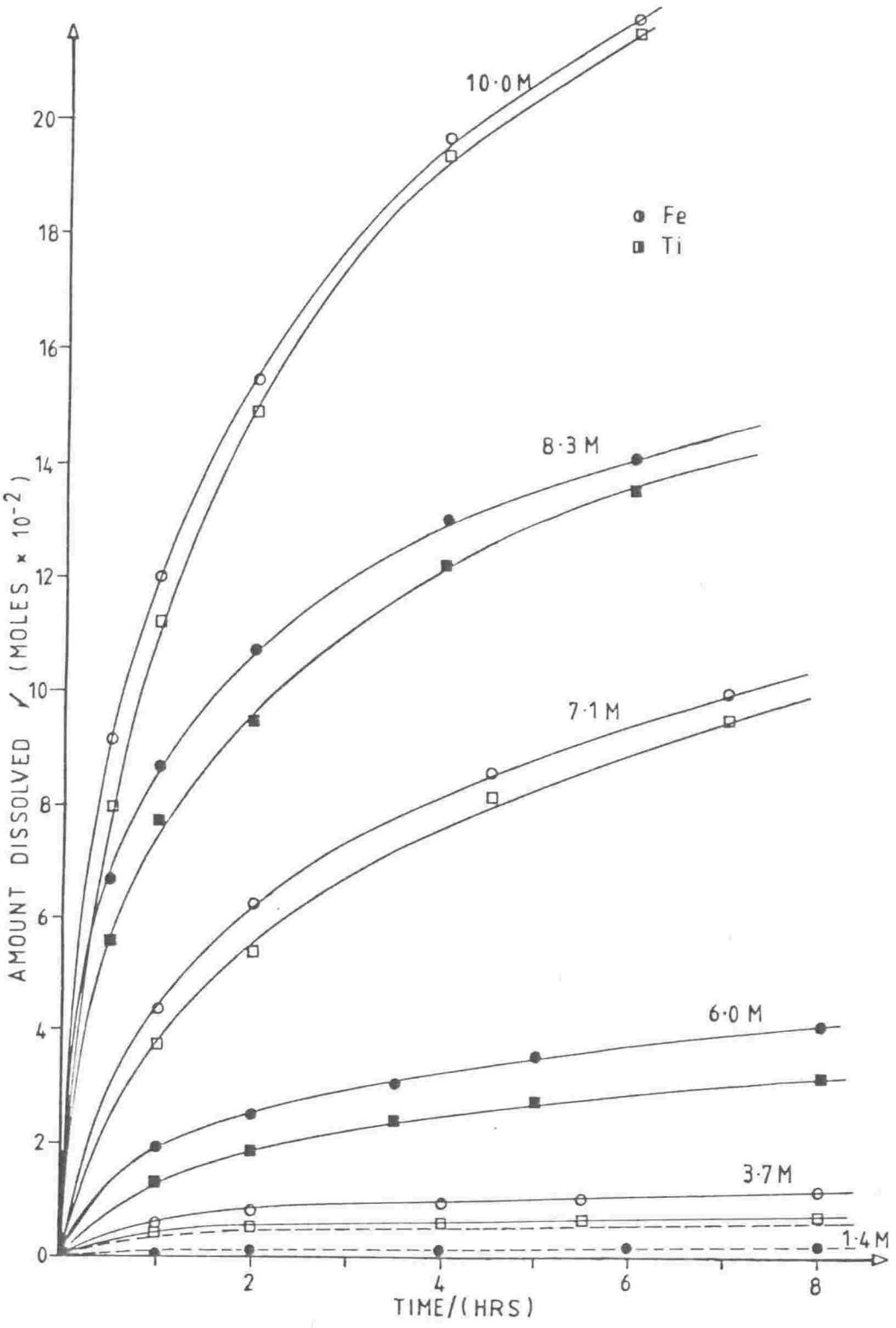

Fig. 4.17 Dissolution of Tauranga Bay ilmenite in 1 → 10 M HCl, 70 °C, acid:ilmenite mole ratio = 10:1.

4.2.3 Effect of Acid Strength

Figure 4.17 shows the comparison of dissolution reactions in 1→10 M hydrochloric acid. The iron:titanium ratio in the solution varies significantly with acid strength, approaching the stoichiometric 1:1 as reaction rate and percent dissolution increase (Fig. 4.18).

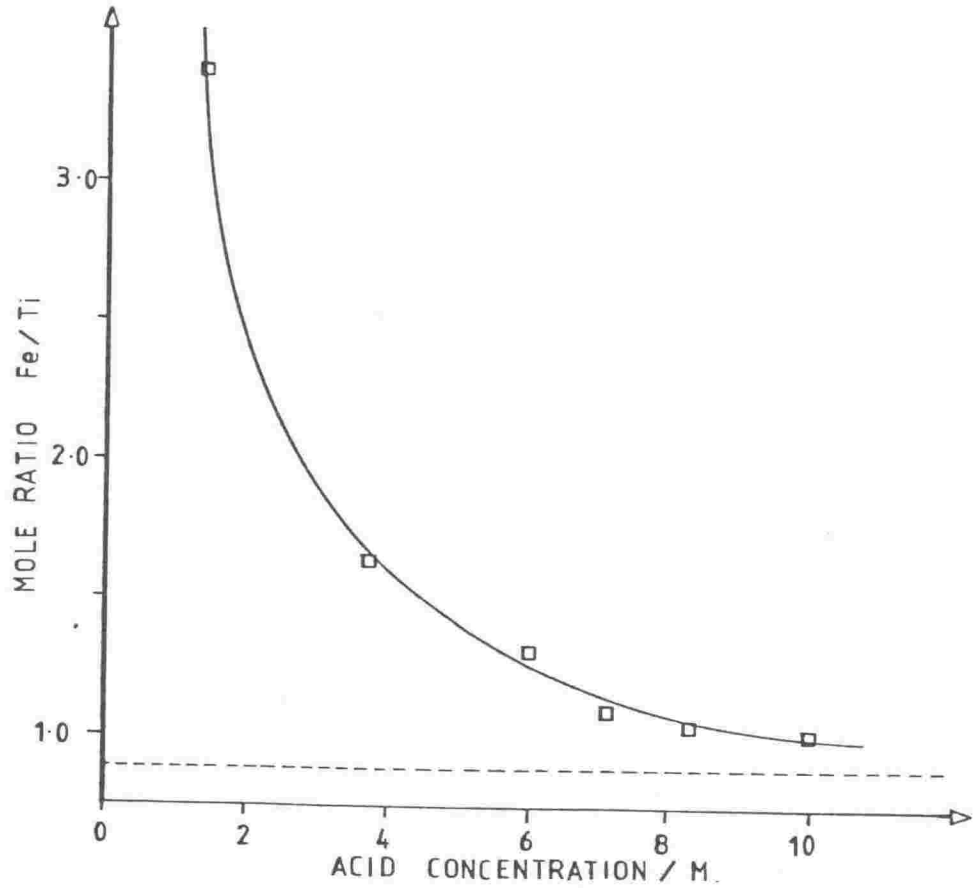

Fig. 4.18 The ratio of dissolved iron to titanium 1→10 M HCl, 70 °C.

Selective leaching of iron is favoured by low acid strength and slow dissolution. This is in agreement with the accepted mechanism of natural alteration of ilmenite (Lynd 1960), which involves progressive oxidation and leaching of the iron, at least until the pseudorutile composition ($Fe_2Ti_3O_9$) is reached (Grey and Reid 1975).

The relationship between reaction rate at zero time and hydrochloric acid concentration in the 1→10 M range is illustrated in figure 4.19(a). If zero time activity of the hydrogen ion in the solution is substituted for molarity the plot approaches linearity (Fig. 4.19(b)). Zero-time activity was calculated from available molal activity coefficient data for 25 °C solutions from Robinson and Stokes (1959), using the relationship:

$a_{H^+} = \nu_{H^+}\, c$ where ν_{H^+} is the molar activity coefficient.

c = molar concentration.

The molal coefficient $\gamma_{\pm}$ was converted to the molar coefficient $\nu_{\pm}$ using the relationship

$$\gamma_{\pm} = \frac{c\nu_{\pm}}{md_o}$$ d_o = density of the pure solvent.

where $$m = \frac{c}{d - 0.001cw_B}$$ w_B = molecular weight of solute

No data for solutions at elevated temperatures were available in this concentration range, apart from studies on sodium chloride solutions (Robinson and Harned 1941), where activity coefficients varied by only 2.5% in the 25→80 °C temperature range.

A plot of percent dissolution of the ilmenite against acid concentration and against hydrogen ion activity (Fig. 4.19) shows that dissolution follows a similar relationship to zero-time rate.

The region of both chemical and commercial interest is around 6 M HCl where there is an apparent point of inflection, best shown in the % conversion vs HCl plot. This coincides with a region noted for difficulty in obtaining reproducible dissolution results (Judd B. pers. comm.). Reference to a plot of activity coefficient ($\nu_{\pm HCl}$) against molarity

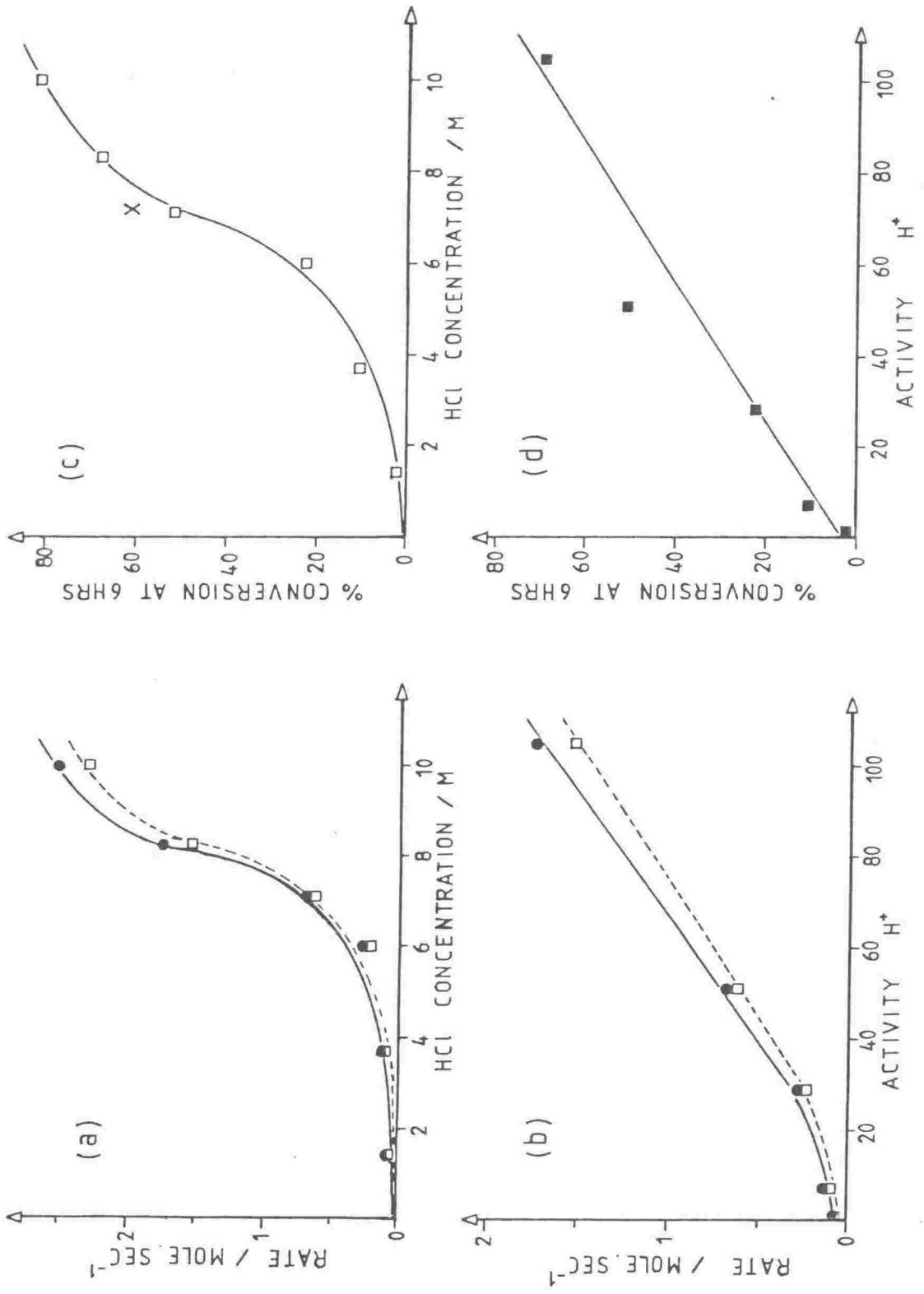

Fig. 4.19 Reaction rate and % conversion vs. hydrogen ion concentration (a), (c), and hydrogen ion activity (b), (d). 1-8 M HCl, 70 °C.

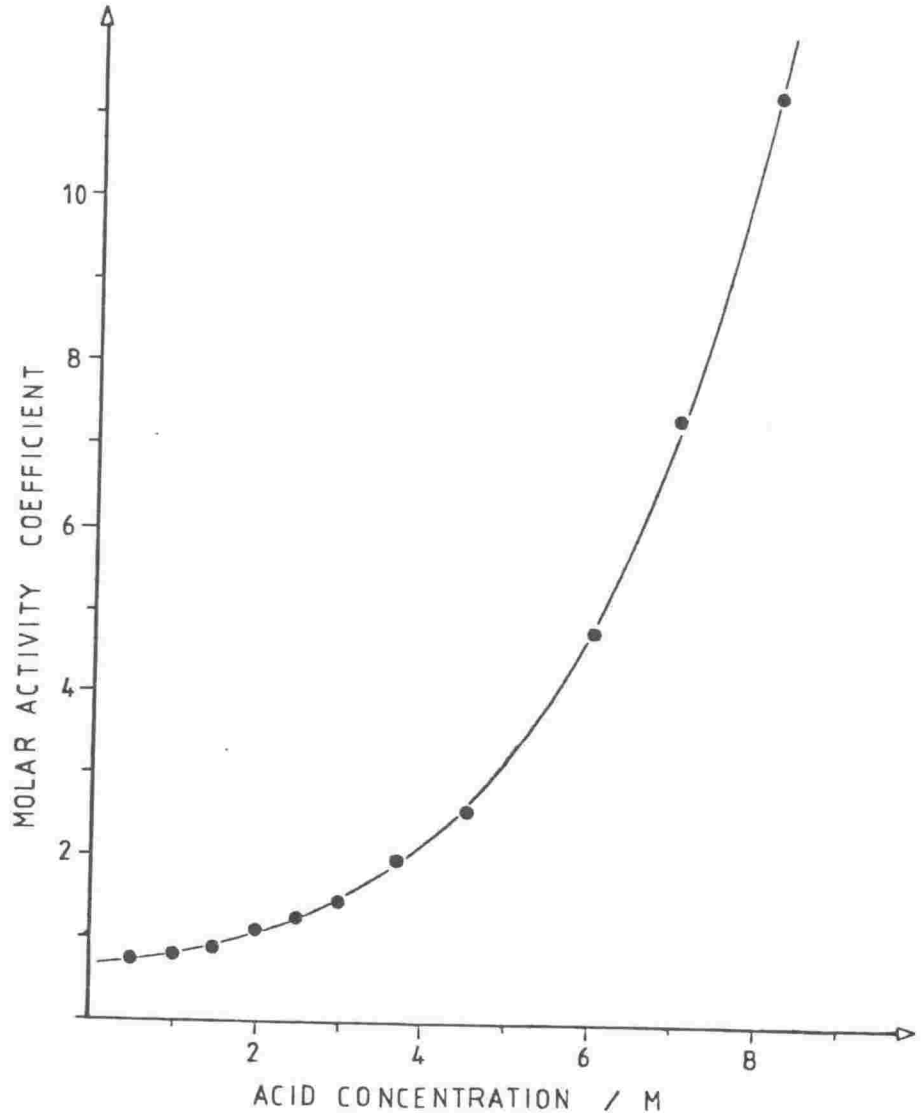

Fig. 4.20 Molar activity coefficient for HCl vs. HCl concentration. (From data in Robinson and Stokes 1959).

(Fig. 4.20) suggests a possible reason, as the activity coefficient increases dramatically in this region.

This concentration range is also significant from a commercial viewpoint as there is a clear region of optimum dissolution against acid strength (region X in figure 4.19(c)). To improve economy of acid use, it would be necessary to avoid the rapid tail-off in acid efficiency below this concentration.

Considerably better acid efficiency on a simple molarity basis is shown by sulphuric acid. A comparison of ilmenite dissolution in ≈4 M solutions of hydrochloric and sulphuric acids is shown in figure 4.21. Conversion at 10 hours differs by a factor of 3.5. Bisulphate addition to a hydrochloric acid solution caused a marked increase in dissolution efficiency (Fig. 4.22). The modest dissociation of the bisulphate ion (pK_a = 1.99) particularly in a solution of $[H^+]$ ≈1.4 M is insufficient to cause the 60% increase in % conversion of Fe and over 100% increase for Ti which were observed. An explanation for this behaviour is seen in the relative ease of hydrolysis of chloride solutions of titanium compared with sulphate solutions (see section 4.2.2). The formation of titanyl sulphate $TiO(SO_4)$ will act as a titanium trap and retard hydrolysis of the titanyl ion TiO^{2+}.

4.2.4 Effect of Temperature

Temperature has considerable influence not only on the rate of the reaction but also on the behaviour of dissolved titanium (see section 5.2). Increasing temperature caused an increase in initial rate (Fig. 4.23), but particularly in reactions involving greater than 50% conversion, had less influence on the position of the eventual concentration

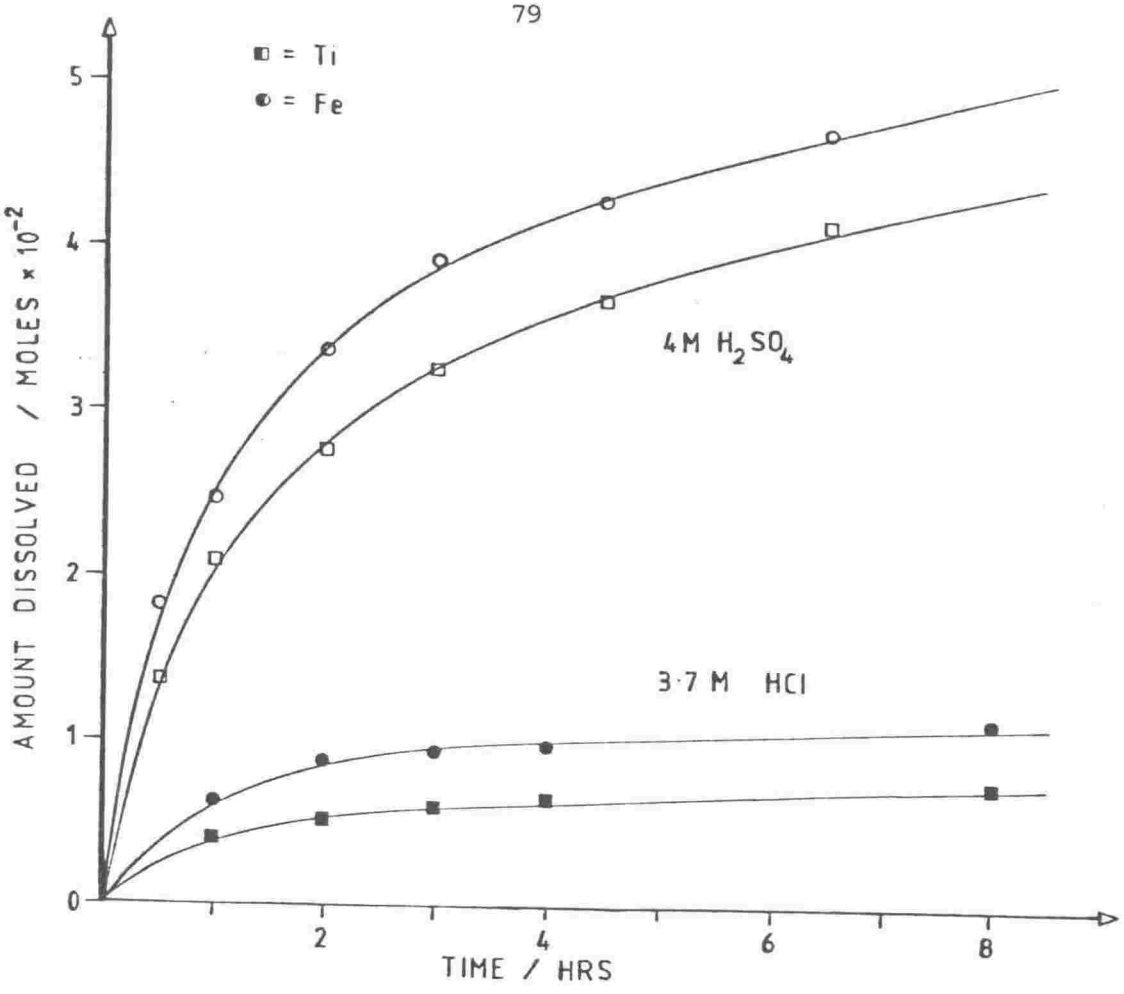

Fig. 4.21 Comparison of dissolution in 3.7 M HCl, 70 °C and 4 M H_2SO_4, 70 °C.

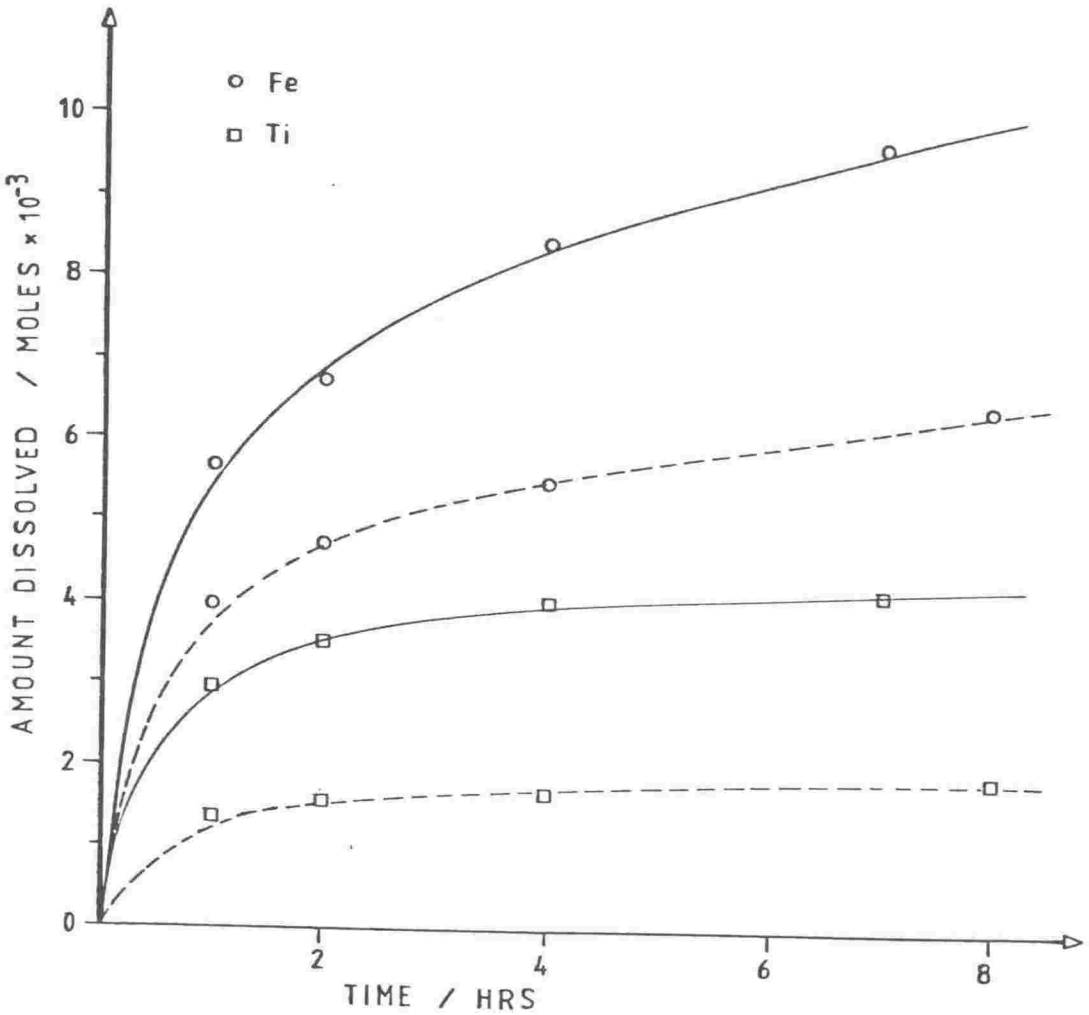

Fig. 4.22 The effect of HSO_4^- addition on the dissolution medium.
----- 4 M HCl, 70 °C ——— 4 M HCl, 1 M HSO_4^-, 70 °C

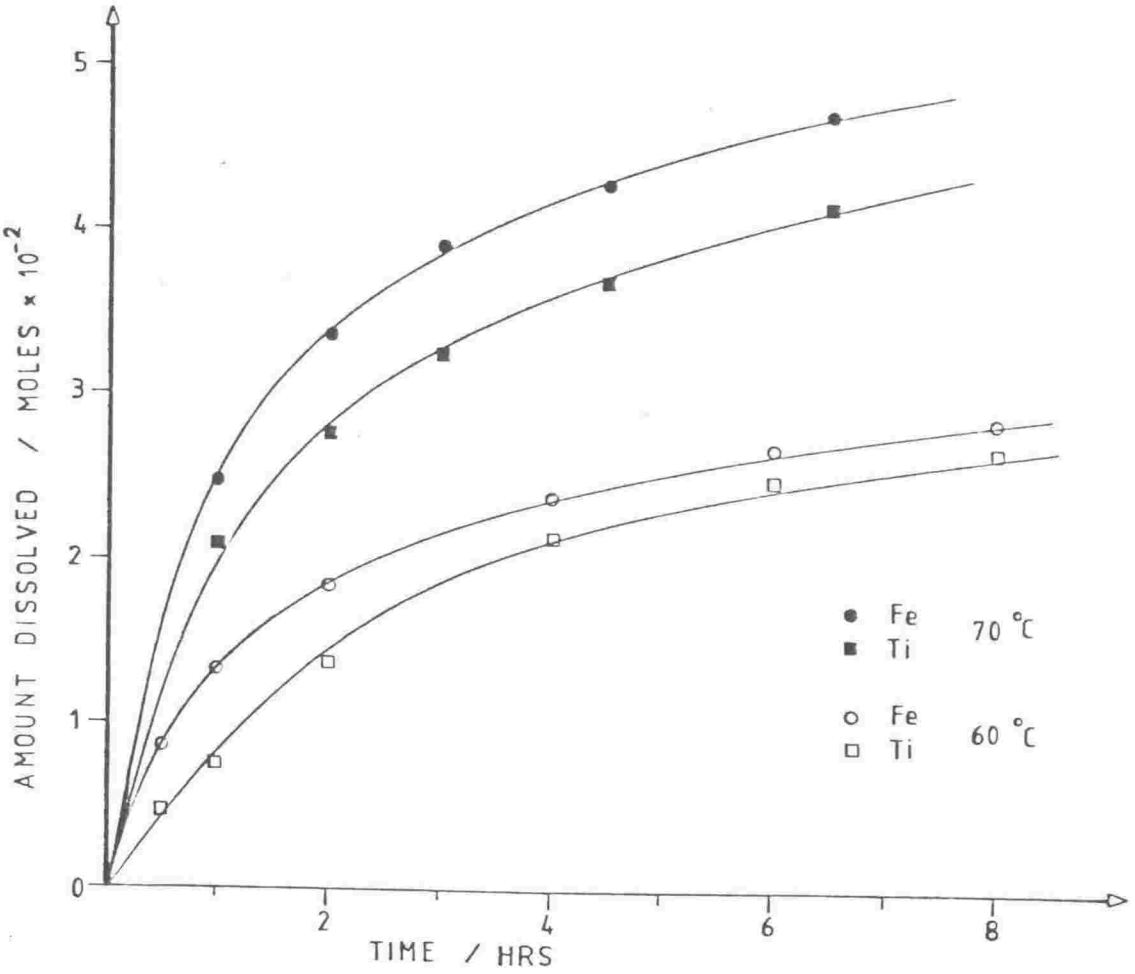

Fig. 4.23 Dissolution in 4 M H_2SO_4 at 60 and 70 °C.

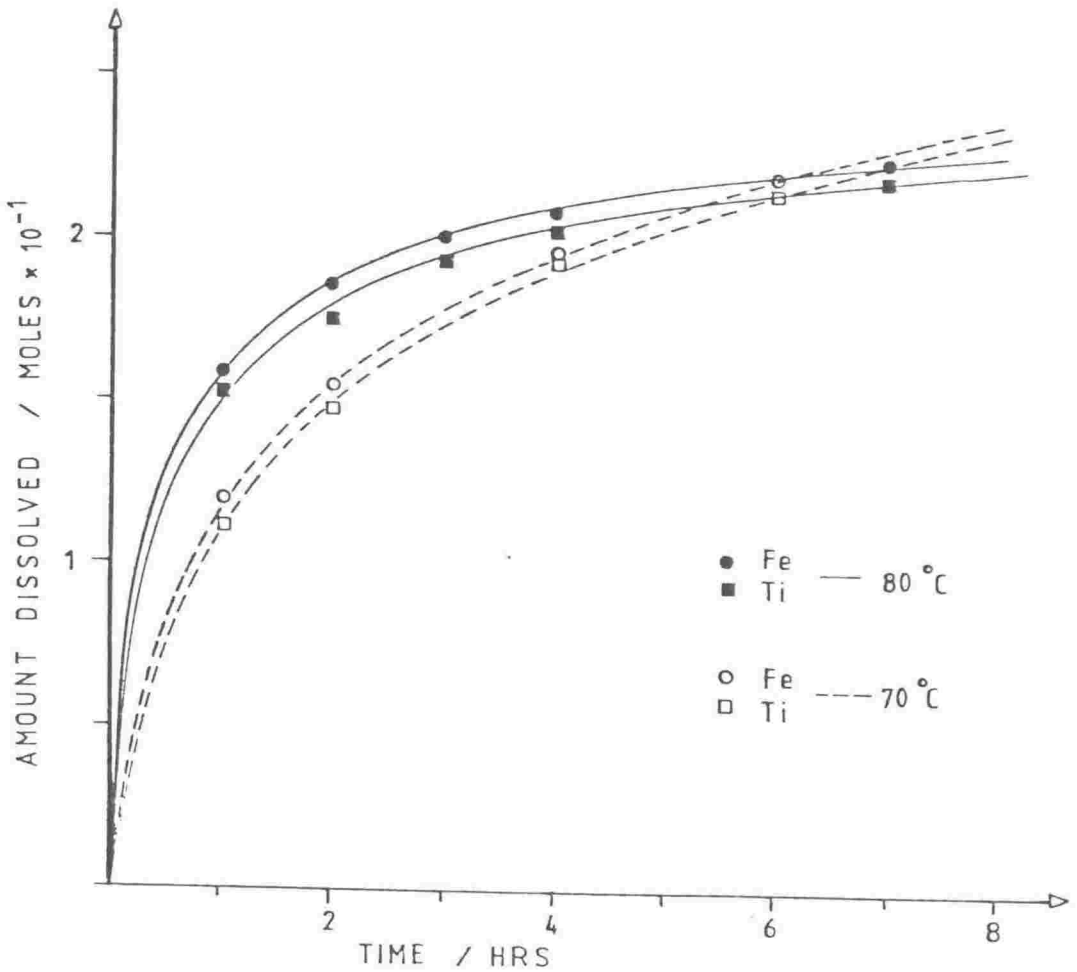

Fig. 4.24 Dissolution in 10 M HCl at 70 and 80 °C.

plateau. Figure 4.24 shows reaction curves at 70 and 80 °C in 10 M hydrochloric acid.

In dissolution experiments using unground ilmenite at a 50:1 mole ratio this behaviour was not observed as a plateau is not reached within the period of the experiment. The temperature dependence of the rate in these reactions was used to calculate an apparent activation energy for the reaction (see section 4.3).

4.2.5 The Effect of Particle Size

Particle sizes were determined by sieving and settling rate, as described in section 3.4.7. In the majority of dissolution runs, a standard ground sample was used. The particle size distribution before and after reaction in 6 M HCl is illustrated in figure 4.25. The particle size distribution does not appear to change markedly, although there is an overall shift to a smaller mean size. In particular the percentage of fines (<20 μm) does not decrease dramatically and in fact appears to increase.

In reactions where a sample of a specific size range was used i.e. the activation energy determinations (see section 4.3) and the iron and titanium additions (see section 4.2.7), the same pattern of behaviour is observed. From a 75-125 μ fraction. approximately 5% of the sample by weight is found below the 75 μm sieve after 10% dissolution in 6 M HCl at 70 °C (Fig. 4.26).

Comparison of experimental curves obtained from dissolutions using similar strength acid and both a broad particle size sample (the standard ground sample - see Fig. 4.25) and a restricted size range (75-125 μm) sample, is shown in figure 4.27. Several significant differences are observed which can be attributed to the effects of particle size. The reaction as anticipated, is considerably more rapid using the broad range

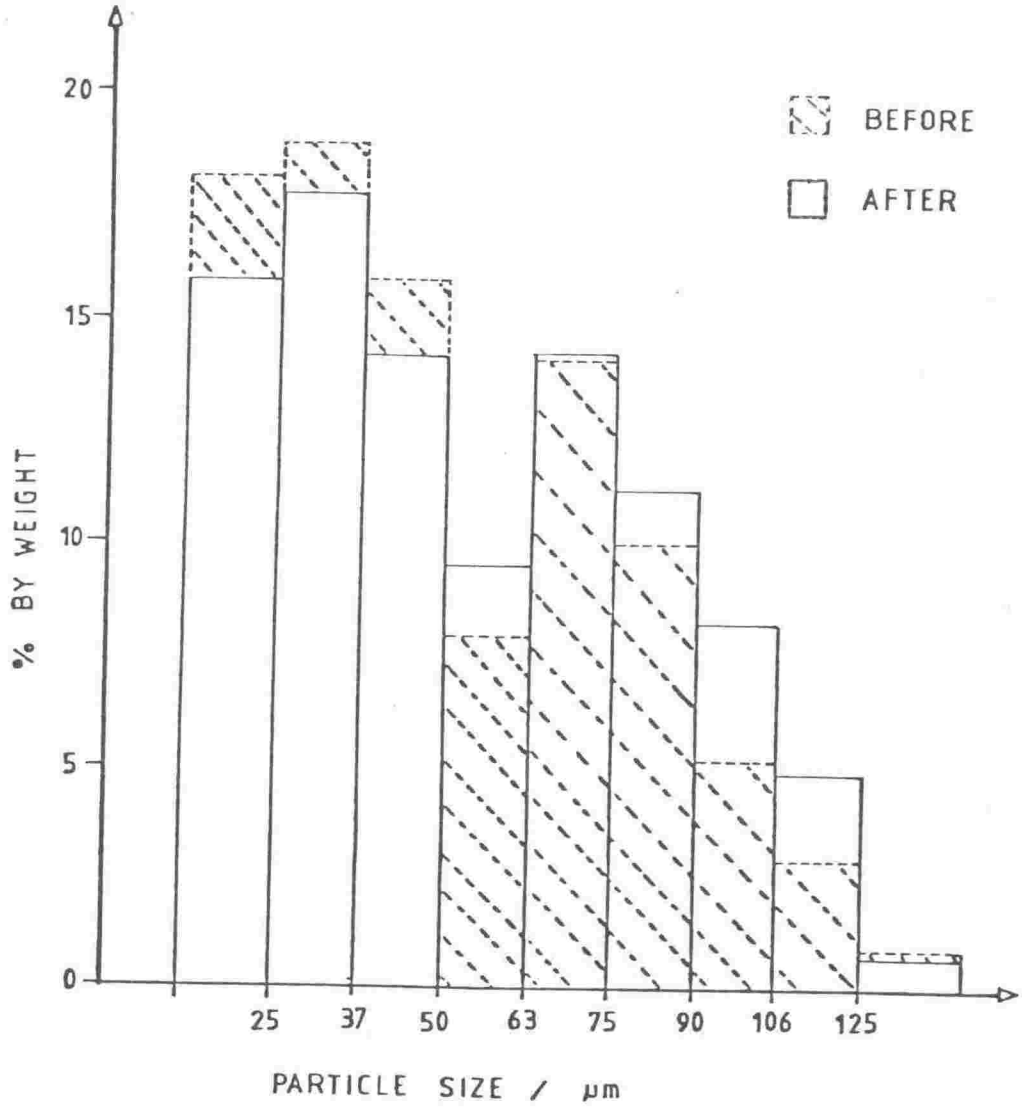

Fig. 4.25 The size distribution of samples taken before and after reaction in 6.1 M HCl, 70 °C, 10 hrs. The 50-63 µm fraction represents the start of 'Sedigraph' analysis and the low values indicate an unresolved calibration difficulty with the instrument.

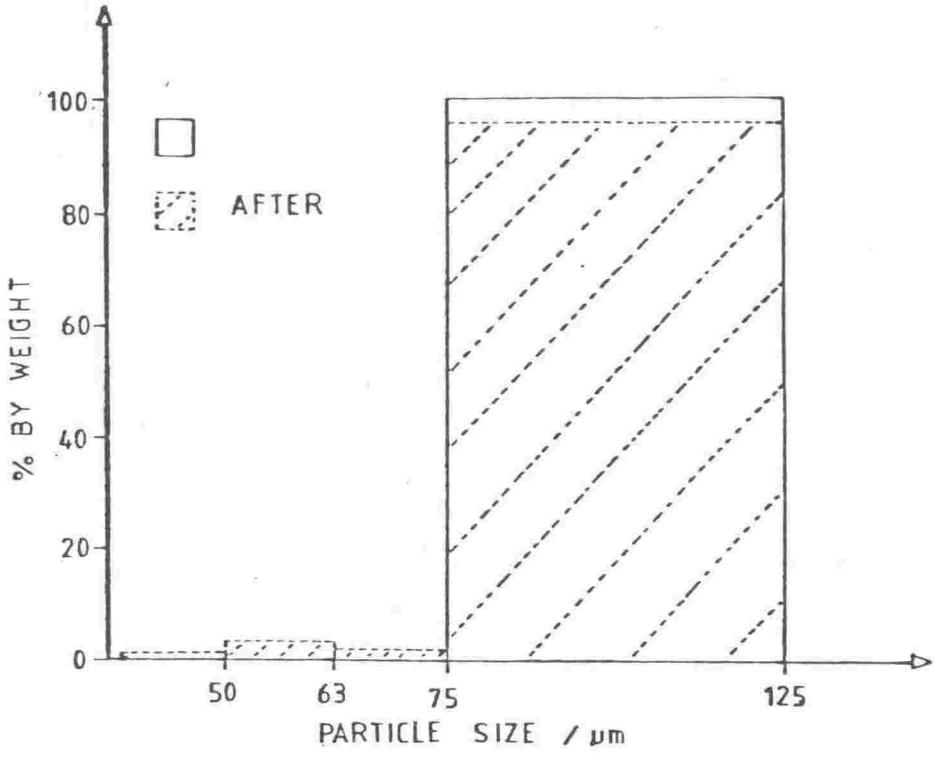

Fig. 4.26 Particle size analysis of a 75-125 m sample before and after 10% dissolution, 6 M HCl, 70 °C.

sample. However a plateau in reaction rate is reached after approximately eight to nine hours of reaction, compared with two hours in the reaction using a 75-125 µm sample. It is also apparent that the two plots are converging. Thus although % conversion is considerably higher for the broad ranged sample, from approximately five hours onward, the dissolution rate is lower, for both iron and titanium, than with the specific size range sample.

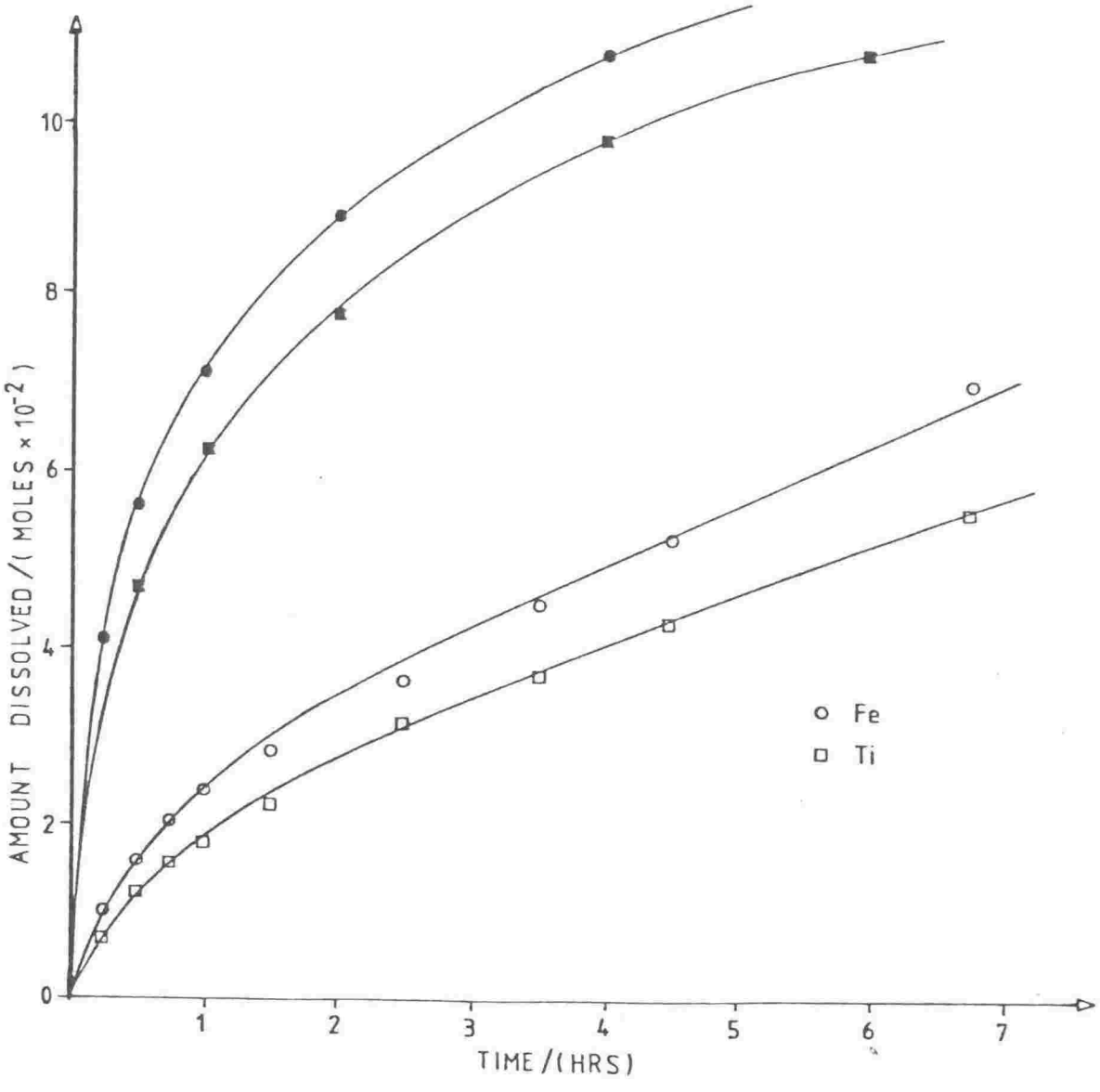

Fig. 4.27 Dissolution of Tauranga Bay ilmenite in 6.1 M HCl, 70 °C.

- broad particle size range - see Table 3.1 **(B)**
- 75-125 µm sample

4.2.6 Interruption and Washing

Attempts were made to alter the physical characteristics of the ilmenite during reaction, by removing the sample and subjecting it to washing, grinding or "in situ" ultrasonic treatment. The purpose of such washing, was to clean the pore structure, which is established early in the reaction (see 4.1.4), of precipitated material such as hydrolysed titanium species (see 4.2.2). Solutions of distilled water, 0.5 M HCl 0.25 M NaOH were used as washing agents, all with negligible effect, unless accompanied by light regrinding (Fig. 4.28).

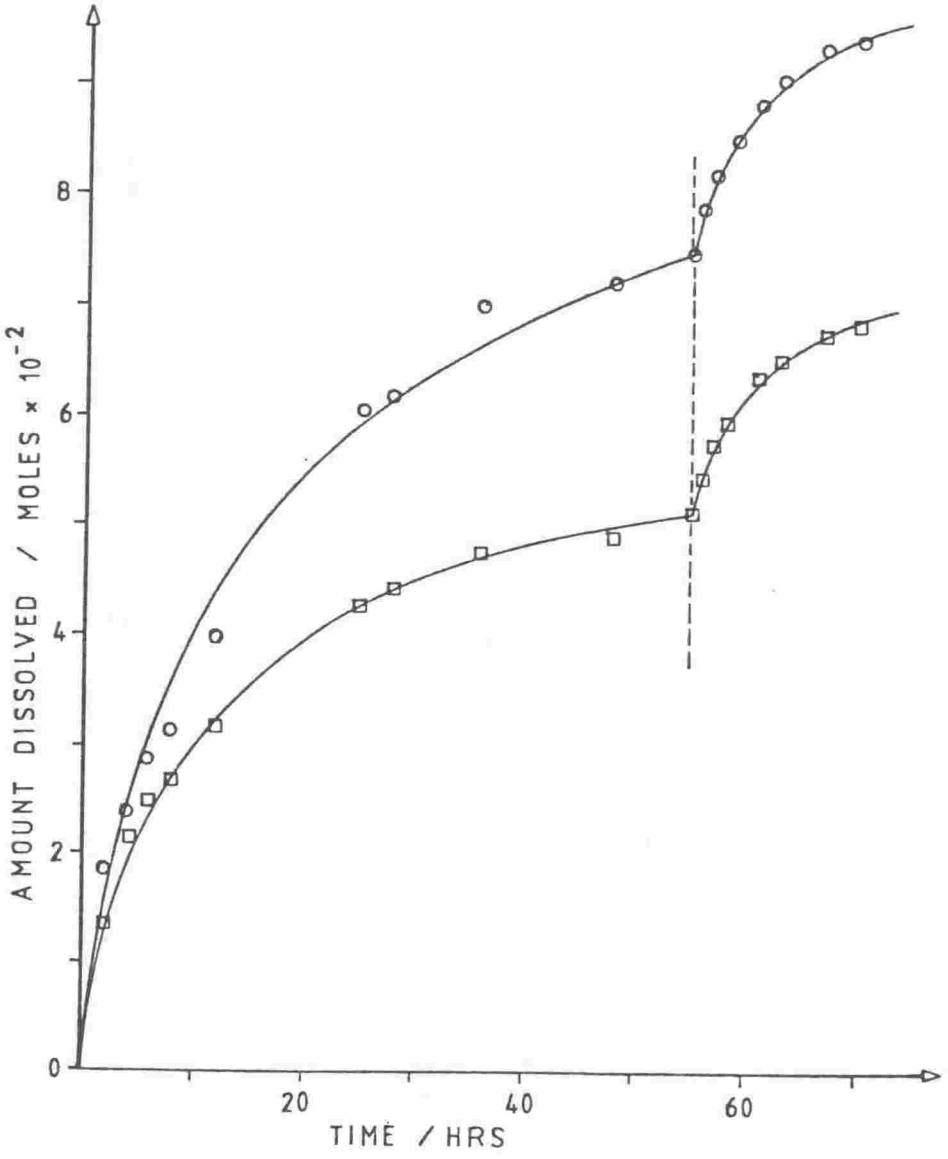

Fig. 4.28 Effect of interrupting reaction, washing and regrinding ilmenite. 4 M H_2SO_4, 70 °C.

Regrinding - consisting of a brief (10 second) milling in a "Tema" ring grinder - has a significant effect on the progress of the reaction. The exposure of fresh ilmenite surface causes an immediate increase in rate, with reaction following the same course as in the previous stage. A second plateau is reached but overall conversion considerably lower than in the first stage of dissolution (Fig. 4.28).

Atomic absorption analysis of water washing solutions generally showed a similar iron:titanium ratio to the bulk reaction solution (Table 4.6), the exceptions being a reaction in which added bisulphate was used and a dilute HCl pre-wash solution.

TABLE 4.6 Iron/titanium ratios from washing solutions

Sample	Washing solution	$\frac{Fe}{Ti}$ (mole ratio)	$\frac{Fe}{Ti}$ (bulk soln)*
Residue from			
/10 M HCl 80 °C	H_2O	1.06	1.02
/8.3 M HCl 70 °C	H_2O	1.03	1.02
/6.0 M HCl 70 °C	H_2O	1.32	1.29
/3.7 M HCl 70 °C	H_2O	1.16	1.61
/1.4 M HCl + 1 M HSO_4^- 70 °C	H_2O	0.599	2.75
Pre-wash before 10 M HCl 80 °C	0.5 M HCl	13.1	1.02

*This refers to the mole ratio Fe/Ti in the acid solution after 8→10 hr of reaction.

In the course of one dissolution run (6 M HCl, 70 °C) ultrasonic treatment was utilized. Treatments for 5 minutes at hourly intervals were carried out by suspending the reaction flask in a Cole-Parmer 50-55 kHz

bath. After 6 and 10 hours of reaction, a 15 minute treatment was applied. The effect was minimal although there were slightly increased concentrations of titanium and iron in solution, particularly immediately after the 15 minute treatments. The conclusion was that ultra-sonic treatment at this frequency had little or no influence on the course of reaction.

4.2.7 The Addition of Interfering Reagents

A number of additives proved to have a marked effect on the course of reaction.

Phosphoric acid: Phosphoric acid addition, had an immediate and dramatic effect on the course of reaction. Even in low concentration (1 mole % of total acid) it completely suppressed the passage of titanium into solution and also restricted the rate of iron appearance. The effect was similar in both hydrochloric and sulphuric acids (Fig. 4.29), so the dominant anion has little influence on this behaviour. The interference in dissolution can be attributed to precipitation of a titanyl phosphate of fairly indeterminate structure (see section 4.1.3). To test the conditions under which precipitation occurs, solutions of potassium titanium oxalate [$K_2TiO(C_2O_4)_2$] and phosphoric acid were mixed in a 4 M sulphuric acid medium to approximate reaction conditions. A concentration range in which precipitation resulted was established, with maximum precipitation at a titanium:phosphate ratio of only 1:50. This reveals why the effect on titanium concentration is so dramatic and occurs early in reaction. The pore forming nature of initial reaction is also significant, as this mode of attack is readily blocked by phosphate precipitation and abrasion in the stirred reaction mixture will not dislodge the precipitate. Interference continues until depletion of the available phosphate in solution, allows reaction to accelerate again.

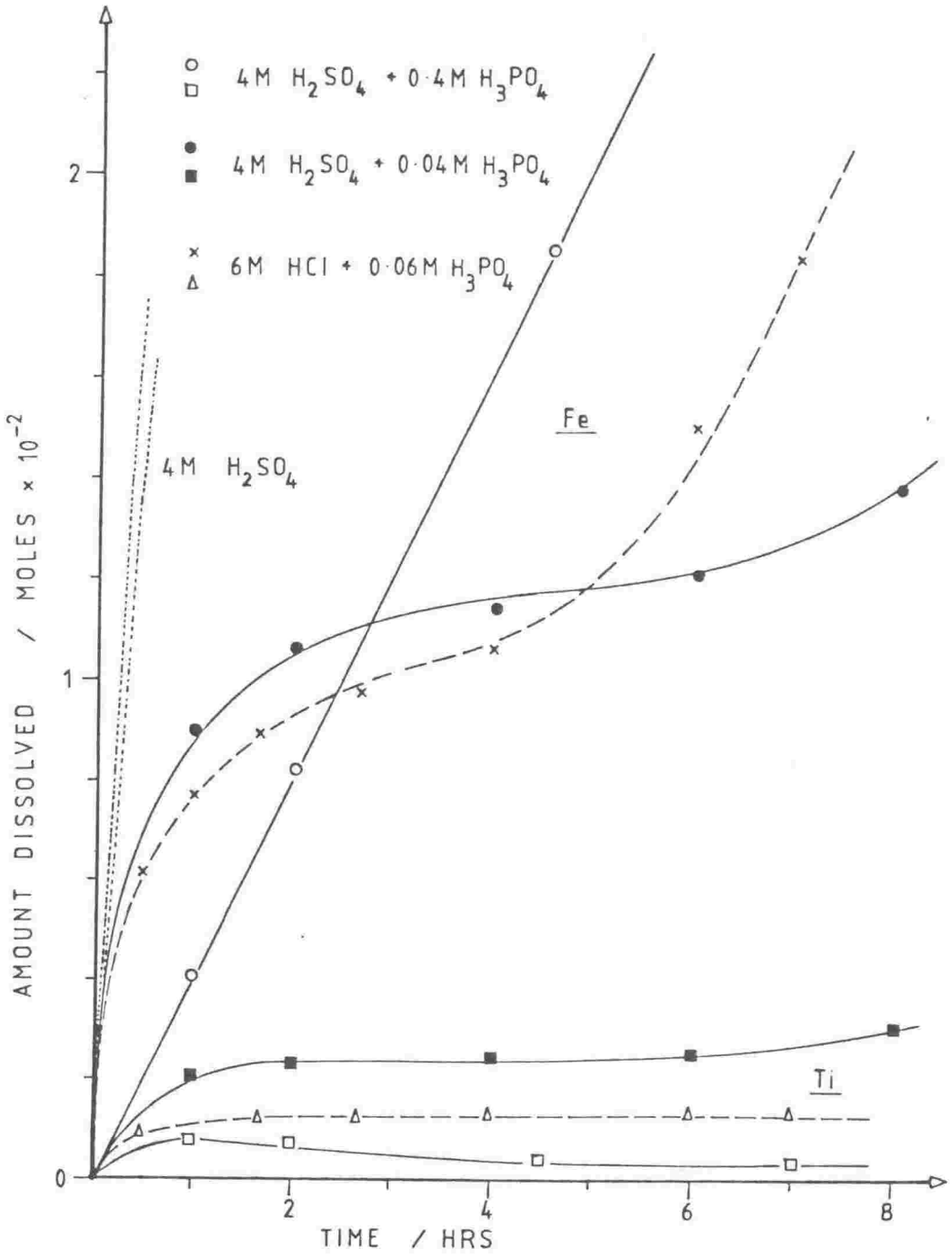

Fig. 4.29 The effect of 1% and 10% H_3PO_4 addition on the dissolution of Tauranga Bay ilmenite in 4 M H_2SO_4 and 1% addition in 6 M HCl.

One seemingly incongruous feature is the effect of using a 10% phosphate solution instead of 1%. Reaction rate is still far below that in the absence of phosphoric acid, but iron dissolution is more rapid in 10% solution than in 1% solution (see Fig. 4.29).

The influence of phosphate from soluble inclusions was considered, but the bulk analysis (Table 4.1) reveals less than 0.5% phosphate (as P_2O_5). Although half this available phosphate is dissolved rapidly (see Fig. 4.2), this quantity is insufficient to cause significant interference in the dissolution, in the absence of added phosphate.

Fluoride: The effect of adding fluoride (as magnesium or sodium fluoride) to the solution was no less dramatic than phosphoric acid, although in the opposite direction. The reaction rate increased dramatically immediately following addition (Fig. 4.30). A plateau was again established later in the dissolution. Titanium was affected to a greater extent than were iron or manganese. Again the effect is independent of the dominant anion in solution.

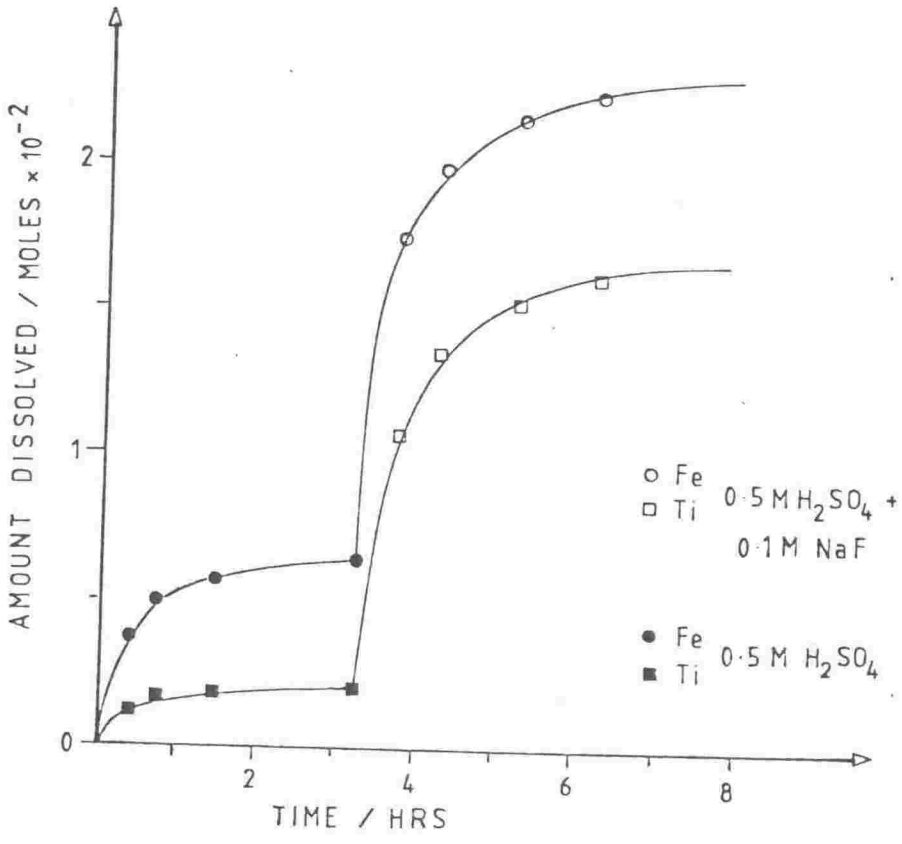

Fig. 4.30 Effect of sodium fluoride addition on the dissolution of Tauranga Bay ilmenite in 0.5 M H_2SO_4, 70 °C.

The improvement in dissolution rate relates to the complexing of titanium in the dissolving solution. The existence of fluoride complexes of the titanyl ion [TiO^{2+}] has long been established and fluoride is known to repress the hydrolysis of TiO^{2+} by complex formation (Cagliotti et al 1960). The chemistry of the Ti^{4+} and TiO^{2+} ions and their influence on the course of dissolution is discussed in section 5.2.

Titanium: Additional titanium (6% of acid concentration, as potassium titanium oxalate) was added to the solution before digestion. Acid concentration was determined by titration and corrected to 8 M, by the addition of a few ml of 33% HCl. The effect of the additional titanium was to restrict dissolution rate to one-third of that observed in an identical run in the absence of added titanium (Fig. 4.31).

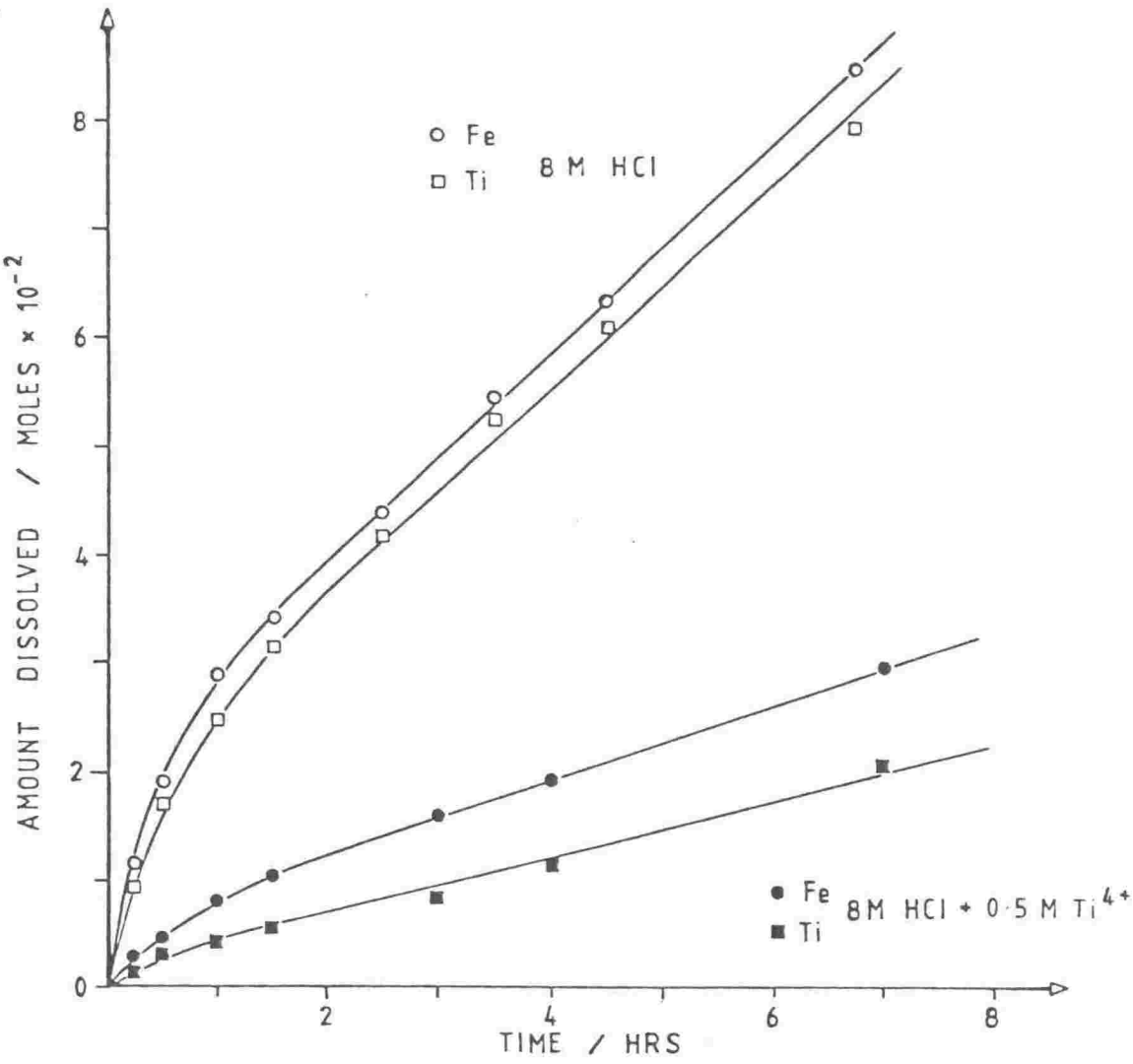

Fig. 4.31 The effect of additional titanium - 8 M HCl, 70 °C.

Optical microscopic examination of the residual solid reveals extensive precipitation of a colloidal white compound (Fig. 4.32) and probe analysis showed clusters of needle-like crystals of approximately 5 μm length (Fig. 4.32). Analyses of these crystal clusters indicate very high titanium levels (Table 4.7) with low totals and extreme softness indicating considerable water content.

X-ray diffraction analysis of the ilmenite residue, the grey sludge extracted after ilmenite removal and the precipitate which appeared in samples on standing for a week, is shown in figure 4.33. This identifies the major components as poorly crystalline titanium dioxide, potassium titanium oxide ($K_2Ti_4O_9$), silica and a variety of silicate gangue minerals.

The liquid samples taken from the reaction flask for analysis were also unstable with regard to titanium concentration. Precipitation was visible in these solutions and duplicate AA samples prepared one week after the experimental run showed a 5→10% reduction in titanium concentration, compared with samples prepared the day following reaction. This indicates further hydrolysis/precipitation of the titanium. Iron levels were invariant in the two sets of samples.

Iron: Additional iron (10% of acid concentration) as iron wire dissolved in 5 ml of conc. HCl was added to the solution before digestion. Acid concentration was again determined by titration (with some difficulty due to the high iron content of the solution - see section 3.3), and corrected to 8 M.

The additional iron had little effect on the dissolution reaction (Fig. 4.34), causing no apparent difference in the rate of iron dissolution and only slight depression of total dissolved titanium after 10 hours. No precipitation of any form was visible, despite iron concentrations approaching 50 g/l in the final solution.

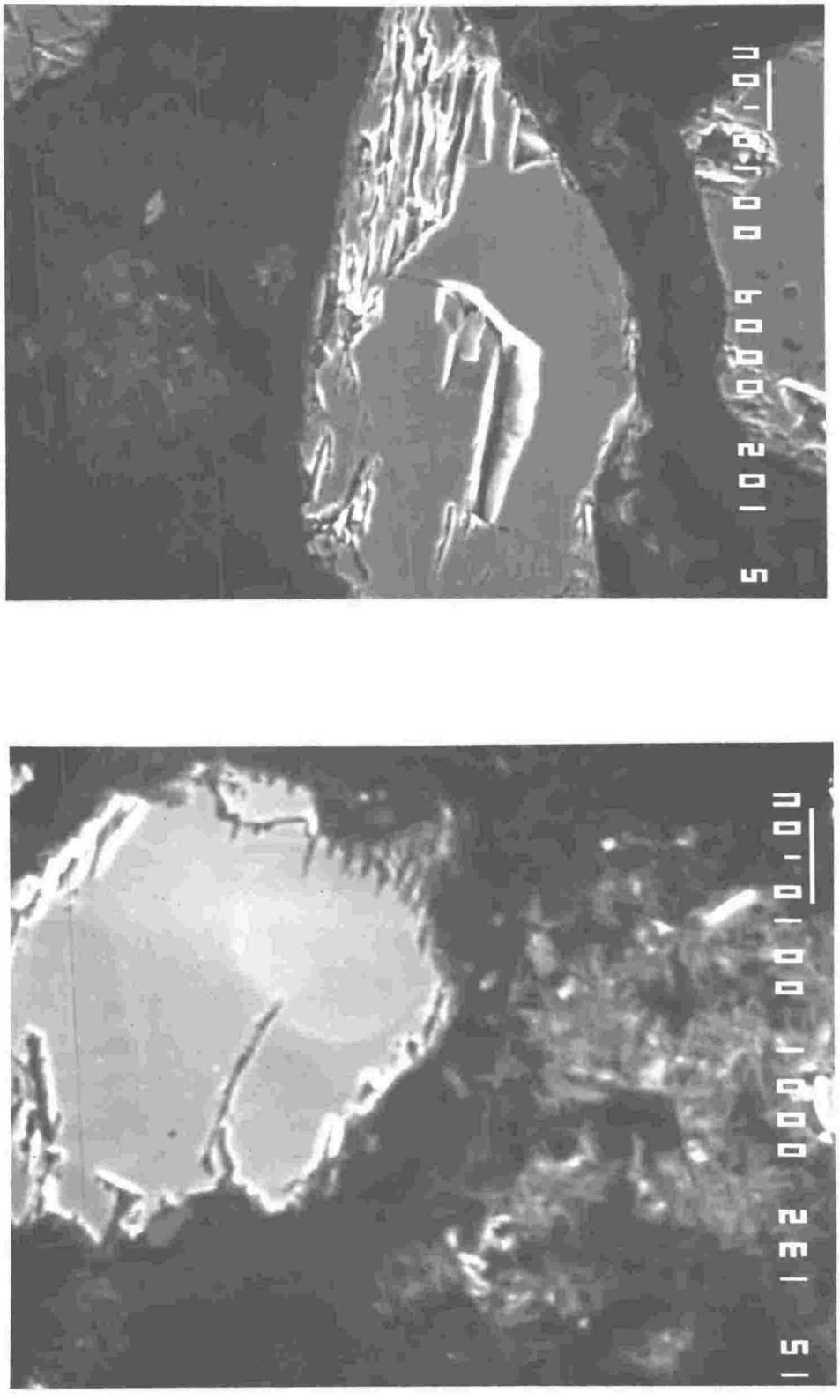

Fig. 4.32 Clusters of needle-like crystals observed in the residue of partial dissolution in 8 M HCl + 0.5 M Ti^{4+}. (Marker bar = 10 µm).

cont. over

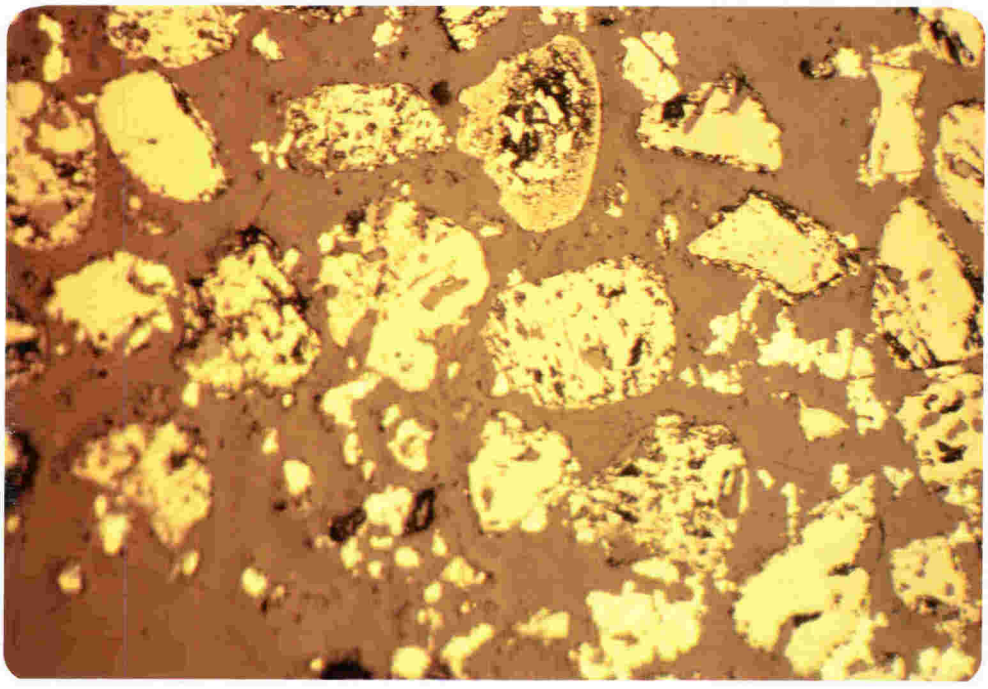

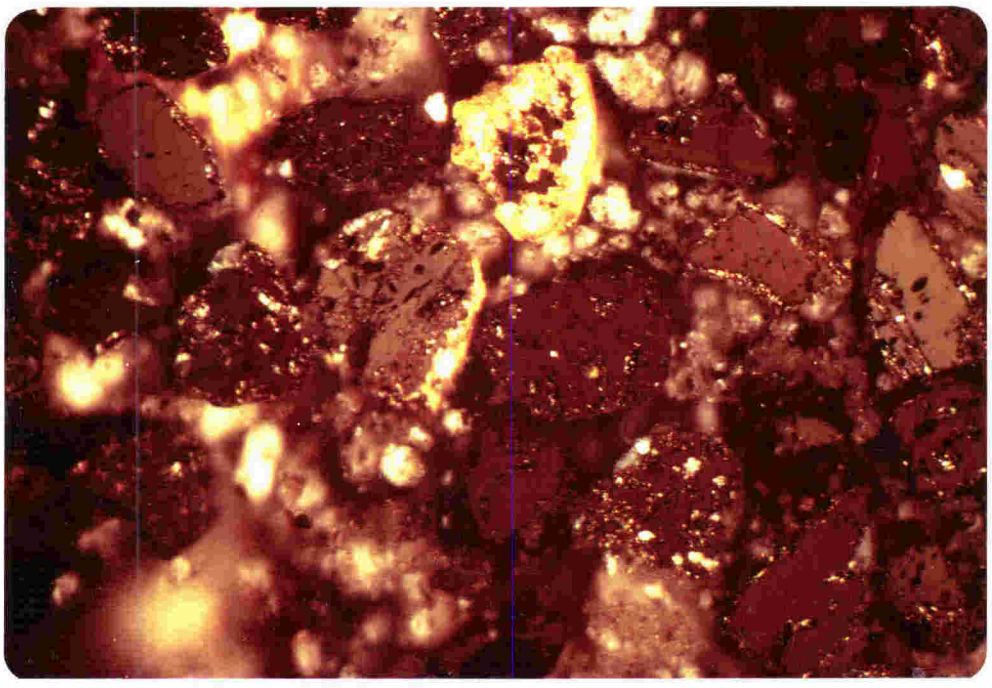

Fig. 4.32 cont. Optical microscope view of titanium rich precipitate.
(a) reflected light
(b) crossed-polarized light
(Field of view 420 μm).

TABLE 4.7 Electron microprobe analyses of titanium rich precipitate surrounding grains - 8 M HCl + 0.5 M Ti^{4+} 70 °C.

	1	2	3	4
TiO_2 %	52.8	60.2	49.4	58.4
FeO	19.4	4.1	2.4	2.1
K_2O*	1.7	4.7	2.6	2.9
SiO_2	1.2	1.3	1.5	1.7
MnO^x	1.4	0.3	0.2	0.1
Total	76.5	70.6	56.1	65.2

* Ti^{4+} was added as $K_2TiO(C_2O_4)_2.2H_2O$, so the K_2O total represents either undissolved or reprecipitated reagent.

x The ilmenite phase is the only significant source of Mn in the ilmenite concentrate, so this indicates the degree of overlap in the excited region (Fig. 3.5), between precipitate and undissolved ilmenite.

$$\text{i.e. } \frac{MnO}{2.1} \times \frac{100}{1} = \% \text{ ilmenite}$$

This indicates that in the above analyses all the iron observed can be attributed to undissolved ilmenite.

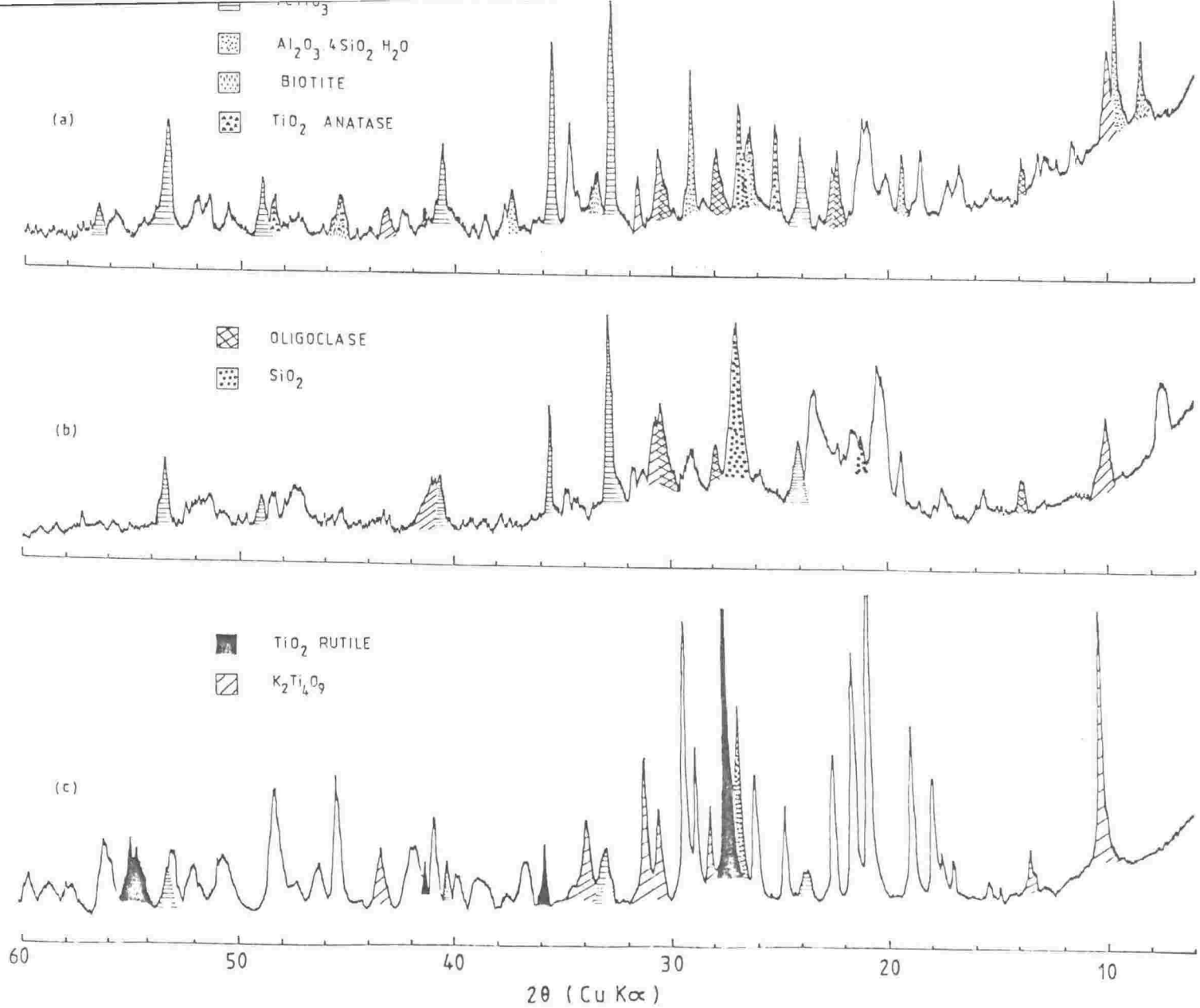

Fig. 4.33 X-ray diffraction traces from (a) solid residue, (b) the grey sludge recovered after centrifuging, (c) the precipitate recovered from liquid samples after standing (≈1 week). 8 M HCl + 0.5 M Ti^{4+}.

Traces are extremely difficult to resolve due to the large number of components.

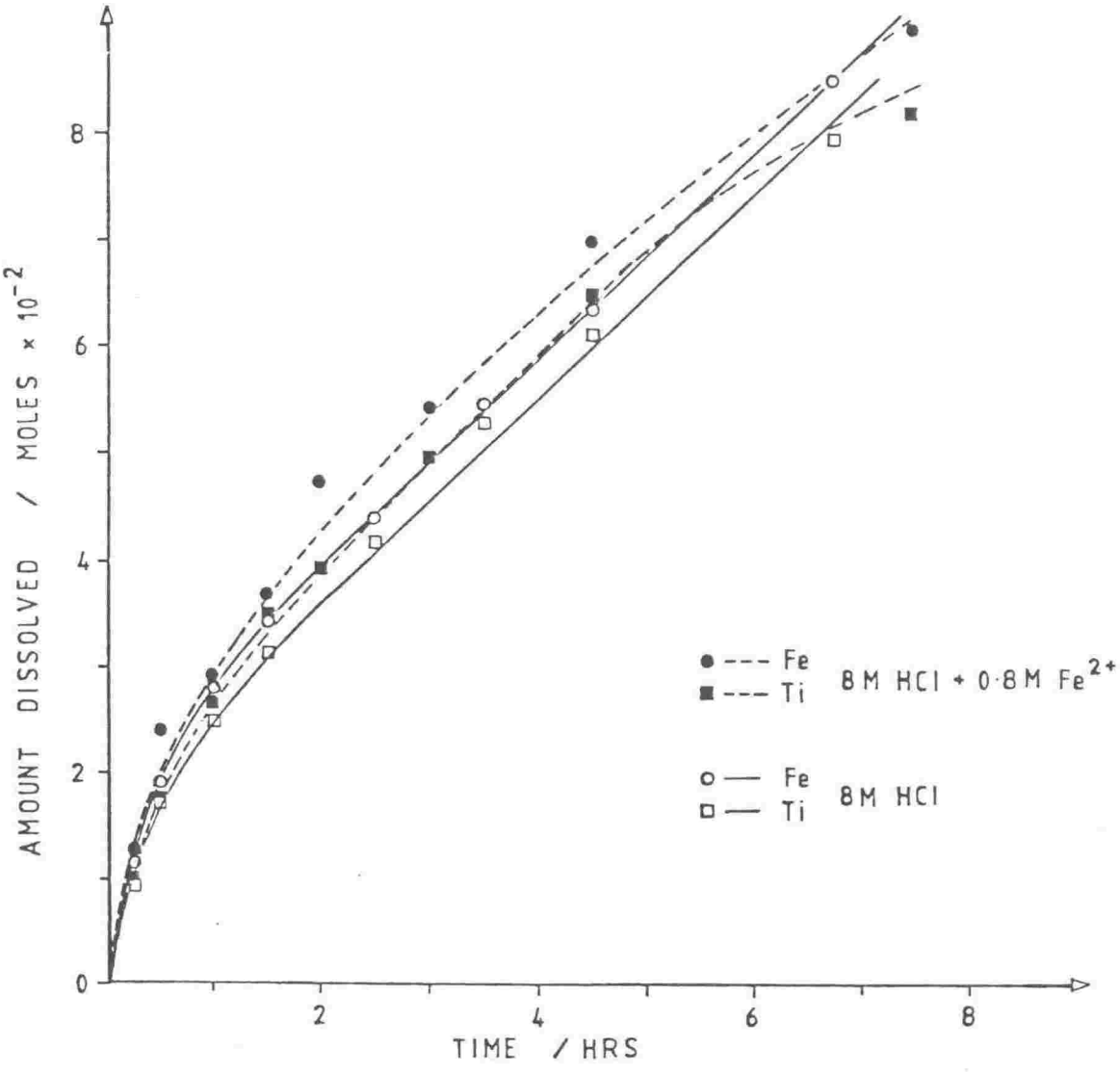

Fig. 4.34 The effect of additional iron on the dissolution of Tauranga Bay ilmenite - 8 M HCl, 70 °C.

The conclusion reached from the titanium and iron addition experiments is that the role of dissolved and dissolving titanium is far more critical than that of iron.

Fresh ilmenite: The addition of fresh, ground ilmenite to the reaction vessel during dissolution causes an immediate increase in the rate of dissolution of both iron and titanium (Fig. 4.35). This would be anticipated from the exposure of fresh surface to the digesting solution and indicates that solution saturation is not the dominant rate controlling influence at the time of addition. The solution used to illustrate this (10 M HCl 70 °C), contained some of the highest levels of iron and titanium encountered in this work (≈40 g/l), all without visible precipitation in the hot solution.

Fresh acid: The addition of fresh acid (up to 30% of the original acid concentration), to the reaction mixture, has a minimal effect on dissolution. If addition takes place once the plateau has been attained, the result is a slight increase in reaction rate. However, if the solution is totally replaced by fresh acid of the same molarity, reaction rate increases sharply and the reaction repeats its initial behaviour (Fig. 4.36).

This suggests that simple availability of ilmenite surface does not cause the observed plateau in reaction and that some solution equilibrium is also involved in the rate decline. The lack of effect of additional acid suggests an irreversible step such as titanium hydrolysis is involved. This effect is discussed further in chapter 5.

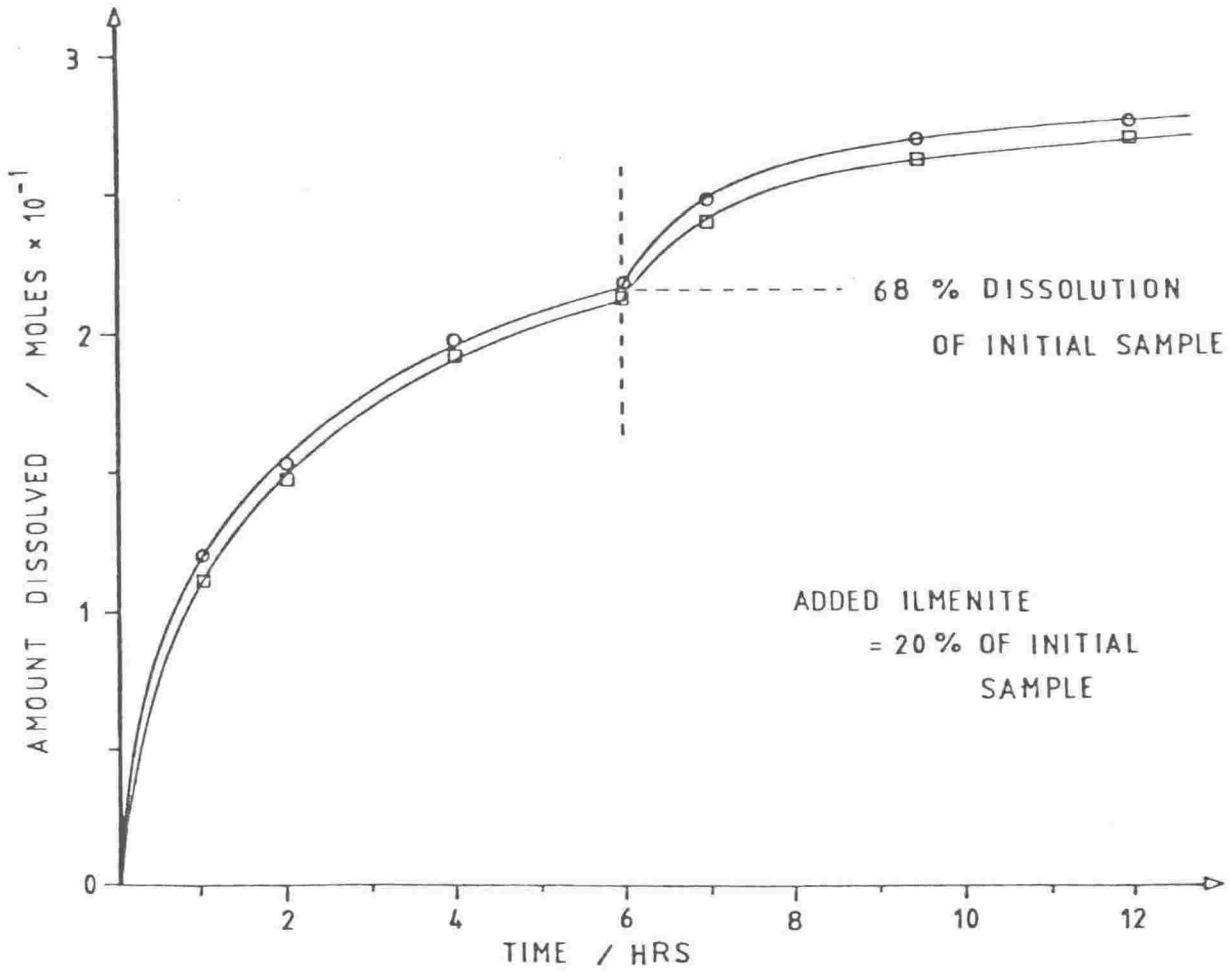

Fig. 4.35 The effect on dissolution of added ilmenite - 10 M HCl, 70 °C.

4.3 Activation Energy of the Reaction

Evidence of the nature of a heterogeneous reaction can be obtained from the temperature dependence of the reaction rate (Bircumshaw and Riddiford 1952). Application of the Arrhenius equation:

$$k = A \exp\left(\frac{-E}{RT}\right)$$

will yield an "apparent activation energy" E which is useful in identifying the nature of the rate determining step in such a reaction. Transport controlled dissolution reactions show apparent activation energies of the

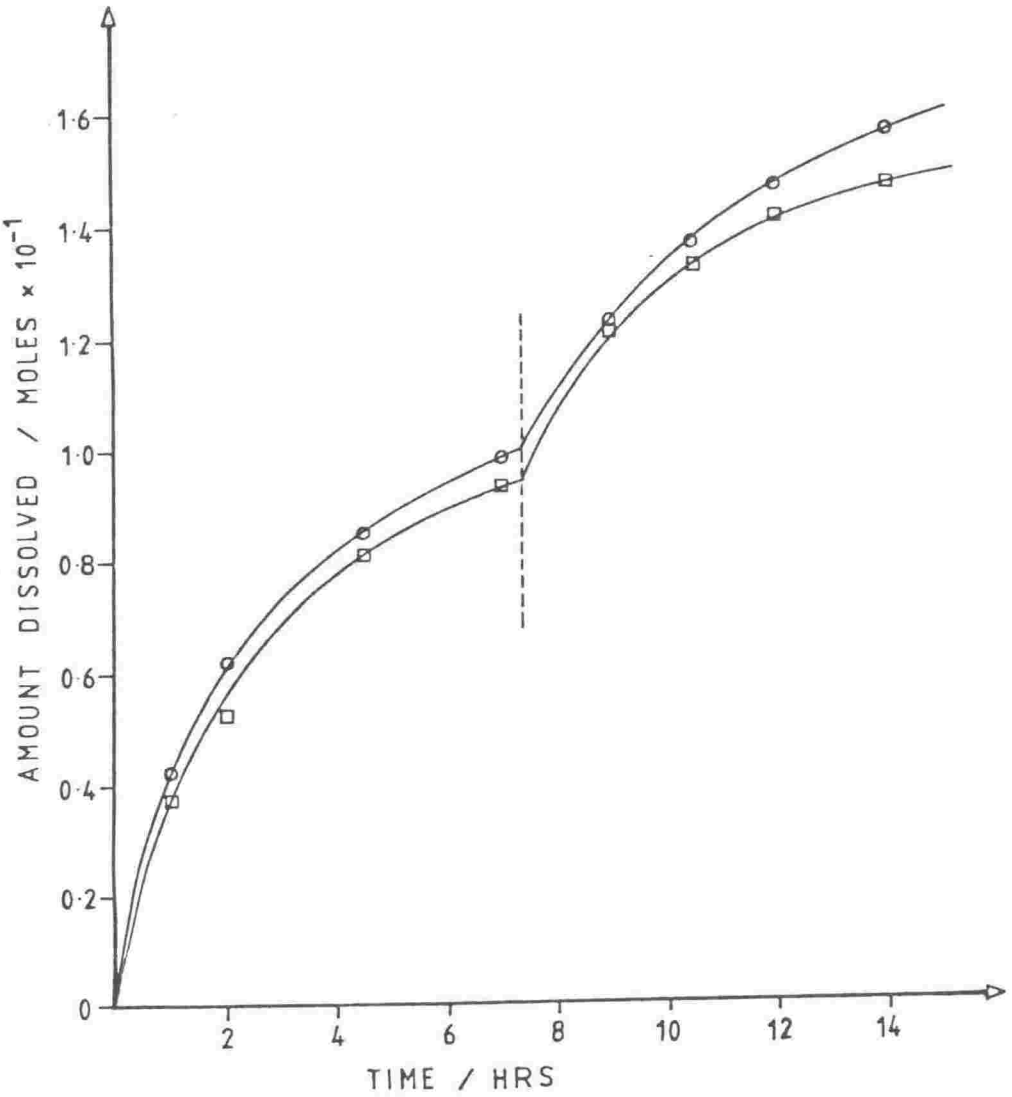

Fig. 4.36 The effect of replacing the acid solution after partial dissolution of ilmenite - 7.1M HCl, 70°C

order of 8 to 25 kJ mol^{-1}, whereas for a chemically controlled reaction the value is considerably higher (Glasstone et al 1941).

To determine this apparent activation energy an experimental run with an identical reaction mixture was repeated at 60, 70 and 80 °C. The

conditions used were quite distinct from earlier digestions, for two reasons:

(1) for comparison with values determined by other workers using high acid:ilmenite ratios.

(2) because only with a controlled particle size, low ilmenite concentrations and thus relatively slow reaction, is it possible to obtain a linear concentration/time plot in the early stages of digestion.

With these considerations in mind, a 50:1 acid:ilmenite ratio was used and a specific size fraction (75-125 μm diameter) of unground ilmenite was used. The resulting concentration/time plots (Fig. 4.37) show remarkable linearity, consistent with the behaviour observed by Barton and McConnel (1979). Both titanium and manganese concentrations plot as straight lines passing through the origin, indicating uniform dissolution from the earliest stages of reaction. The deviation of iron is attributed to the rapid dissolution of a surface phase rich in iron III, as discussed in section 4.1.2. It is also apparent that in the 80 °C reaction the iron and titanium plots are diverging, indicating either non-stoichiometric dissolution or the retention of titanium at the solid/solution interface.

A plot of ln rate vs 1/T (Fig. 4.38) is linear and from the Arrhenius equation above, the slope of this line gives a value for E (the apparent activation energy) of 105±6 kJ mol^{-1}. This compares with 83±7 kJ mol^{-1} for Tauranga Bay, and 101±8 kJ mol^{-1} for synthetic ilmenite in 9 M sulphuric acid, reported by McConnel (1978). Jackson (1974) has reported a value of 92.5 kJ mol^{-1} for Allard Lake ilmenite in 6 M hydrochloric acid. Table 4.8 summarises the reported apparent activation energies for ilmenite dissolution.

TABLE 4.8 Apparent Activation Energies for ilmenite dissolution

Sample	Dissolution medium	ΔE (kJ mol^{-1})	Reference
Allard Lake/ilmenite	HCl	92.5	Jackson (1975)
/hematite	HCl	88.3	
Tauranga Bay	H_2SO_4	83 ± 7	McConnel (1978)
West Coast	H_2SO_4	89 ± 7	
Synthetic	H_2SO_4	101 ± 8	
Tauranga Bay	HCl	105 ± 6	This work

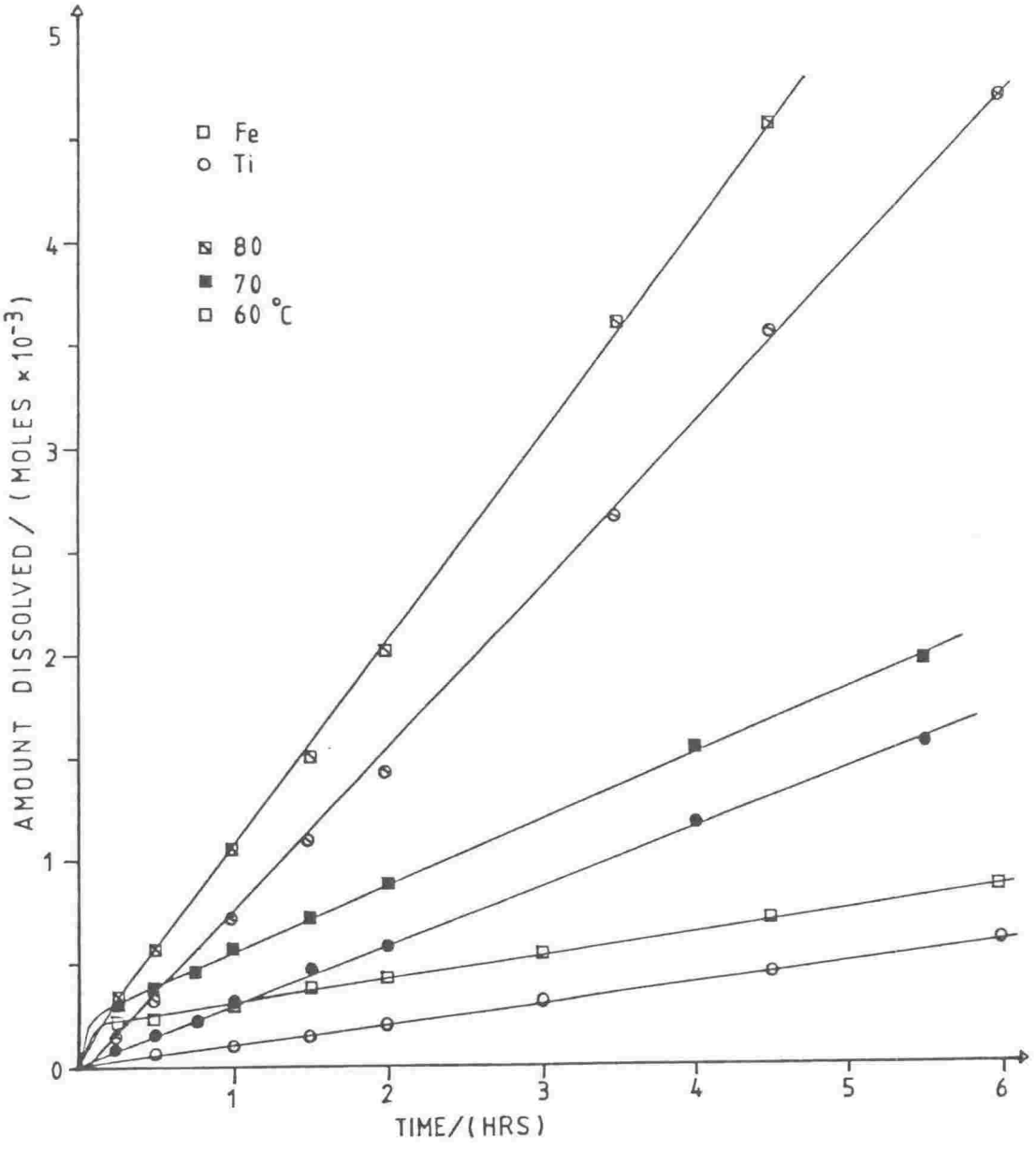

Fig. 4.37 Dissolution reactions used in Activation energy determinations - 6.1 M HCl, 5 g Tauranga Bay ilmenite, 75-125 μm particle size/300 ml acid solution.

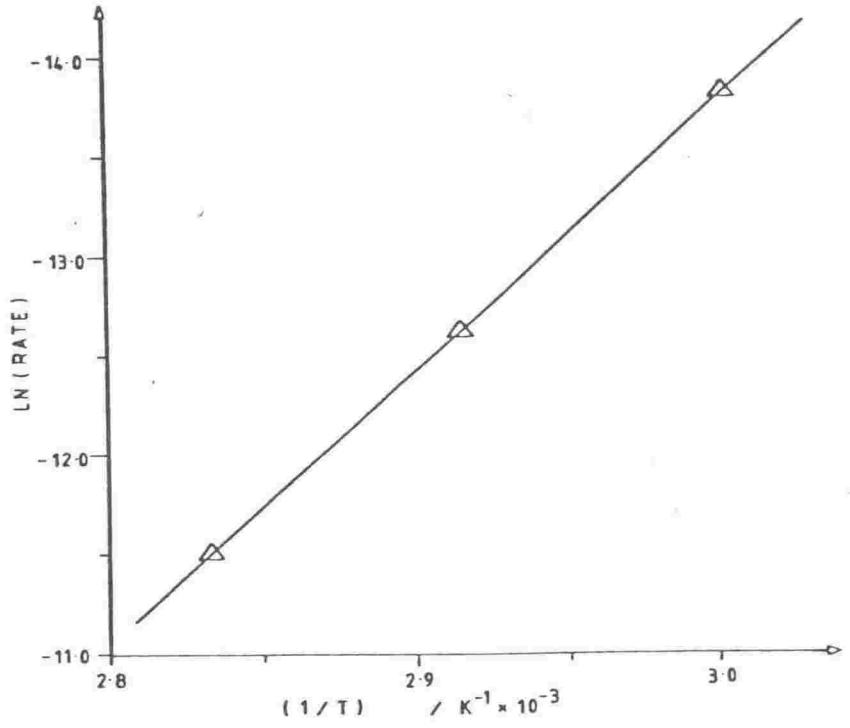

Fig. 4.38 Arrhenius plot for Tauranga Bay ilmenite.

This value was confirmed in the temperature dependence of zero-time rate in the reaction of 10 M hydrochloric acid at 70 and 80 °C, reactions which used a 10:1 acid/ilmenite ratio and ground samples, and did not show concentration/time linearity (see Fig. 4.24).

These values indicate chemical control of the rate determining step under these conditions, rather than any transport process at the ilmenite surface. The independence of rate from stirring speed in rotating disk experiments (McConnel 1978) confirms chemical control of the reaction at the ilmenite exterior. However neither the activation energies, nor the stirring speed independence eliminate the possibility of a significant contribution from reaction at the internal surfaces of the grains. This is discussed in chapter 5.

4.4 Mössbauer Spectroscopy

Samples of Tauranga Bay ilmenite, taken before and after partial dissolution, were examined using Mössbauer spectroscopy. Ground samples were mounted in a sellotape walled perspex holder, with an iron density of approximately 10 mg/cm^2. Spectra were recorded as described in section 3.4.6.

Before reaction, the spectrum (Fig. 4.39) can be resolved into a typical high-spin ferrous doublet, using the computer fitting procedure described earlier (section 3.4.6). Parameters are in agreement with reported values for the ilmenite ferrous resonance (Table 4.9).

However the χ^2 value for the computer fitted doublet is unacceptably high (χ^2 = 610.6, 1 and 99% points are 402.9 and 281.4 respectively). The low velocity peak of the experimental curve shows distinct asymmetry and a residual deviations plot from the computer-fit (Fig. 4.40), reveals the presence of at least one additional peak. Further computer-fitting confirms the presence of a second doublet, resolved with some difficulty due to its proximity to the ilmenite resonance, and broadening of the lower velocity peak, due probably to a small ferric resonance (Fig. 4.41). The χ^2 value is now excellent (= 356.0) and the residual deviations plot is apparently random (Fig. 4.42). The isomer shift δ = 0.81 mm s^{-1} is slightly below that of ilmenite (see Table 4.9), but still consistent with ferrous iron. The small quadrupole splitting Δ = 0.95 mm s^{-1}, excludes almost all Fe^{2+} containing primary minerals, which show Δ values between 1.7 and 2.9 mm s^{-1} (Bancroft 1973) and any of the ferrous iron-titanium oxides (see Table 5.4). This suggests a second ferrous site within the ilmenite itself.

TABLE 4.9 Mössbauer parameters for ilmenite samples

Sample	Isomer shift* (δ mm s^{-1})	Quadrupole splitting (Δ mm s^{-1})	Reference
Finnish ilmenite	0.857	0.71	Gibb et al (1969)
Kishengarh ilmenite	0.86	0.73	Singhvi et al (1974)
Synthetic ilmenite	0.86	0.65	Avrahami and Golding (1969)
Synthetic ilmenite	0.75	0.71	Singhvi et al (1974)
Synthetic ilmenite (4 peak)	1. 0.88 2. 0.93	0.62 1.30	Ruby and Shirane (1961)
Tauranga Bay (2 peak)	0.865±0.008	0.687±0.006	This work (Fig. 4.39)
Tauranga Bay (4 peak)	1. 0.863±0.010 2. 0.81 ±0.05	0.673±0.008 0.95 ±0.03	(Fig. 4.41)
Tauranga Bay (8 M HCl)	1. 0.845±0.010 2. 0.77 ±0.07	0.635±0.008 1.01 ±0.05	
Tauranga Bay (4 M H_2SO_4)	1. 0.852±0.008 2. 0.75 ±0.03	0.653±0.006 1.10 ±0.02	

* Relative to Cu.

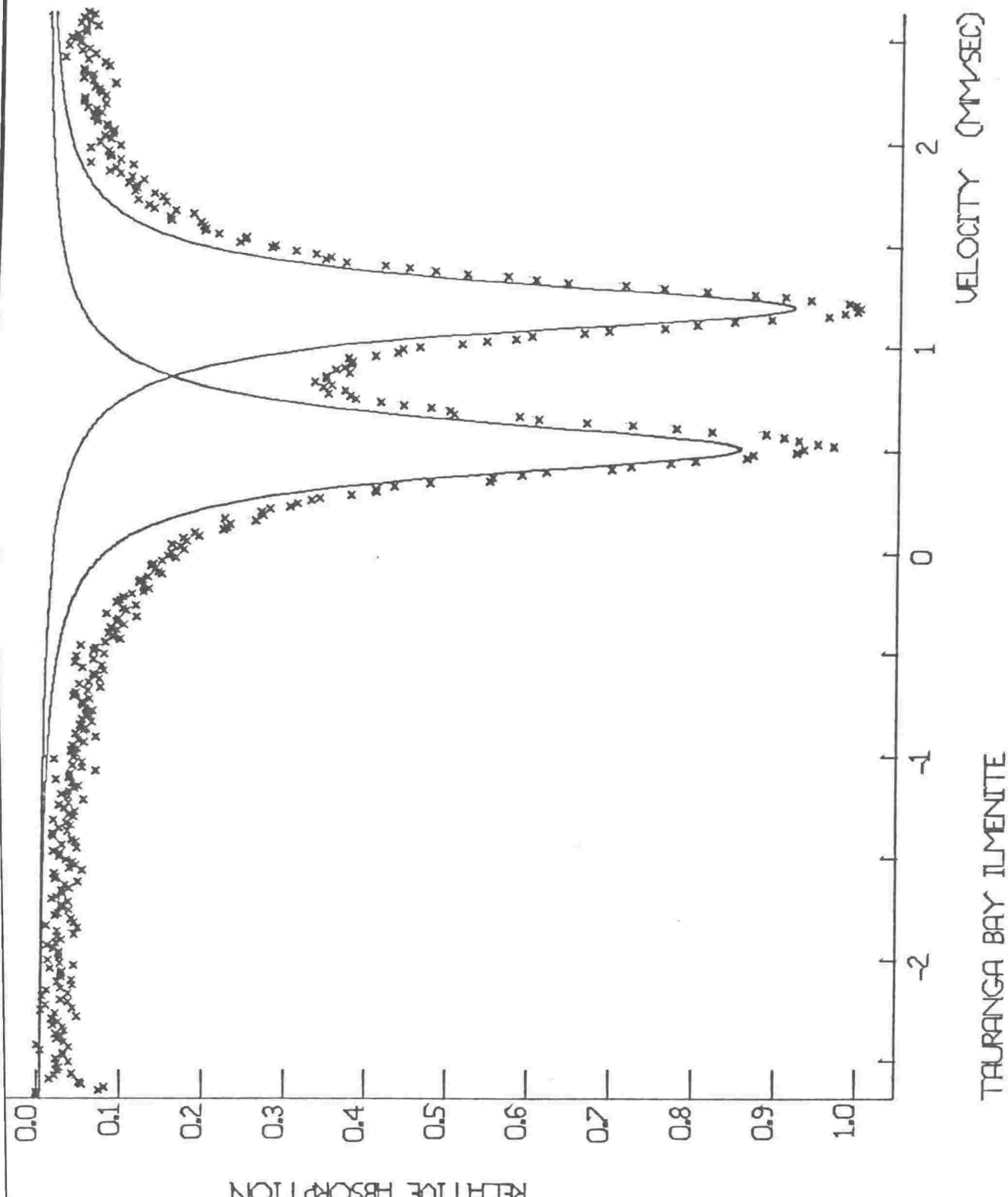

Fig. 4.39 Mössbauer spectrum of Tauranga Bay ilmenite, showing the two peaks of the initial computer fit.

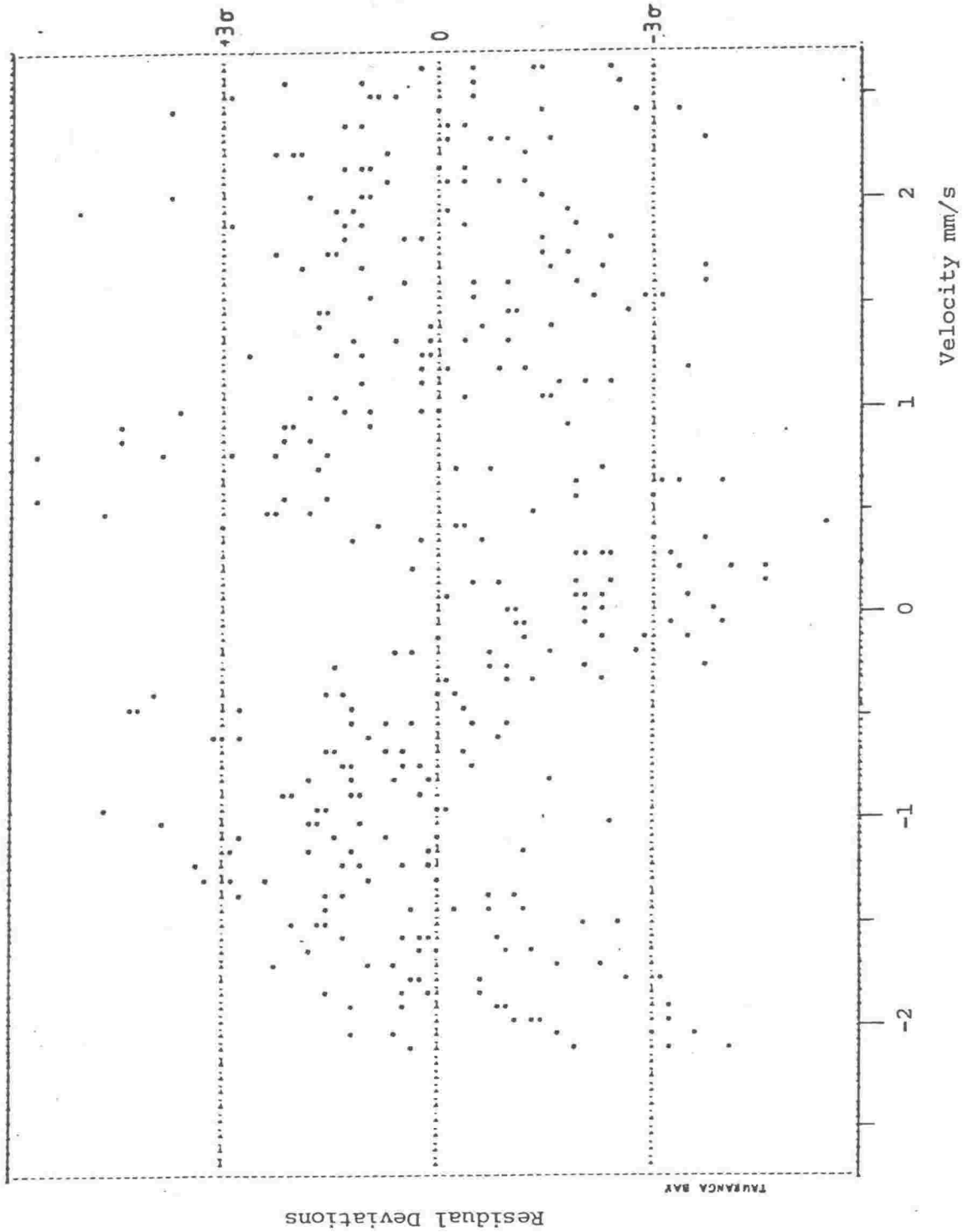

Fig. 4.40 Residual deviations plot for the initial computer fit.

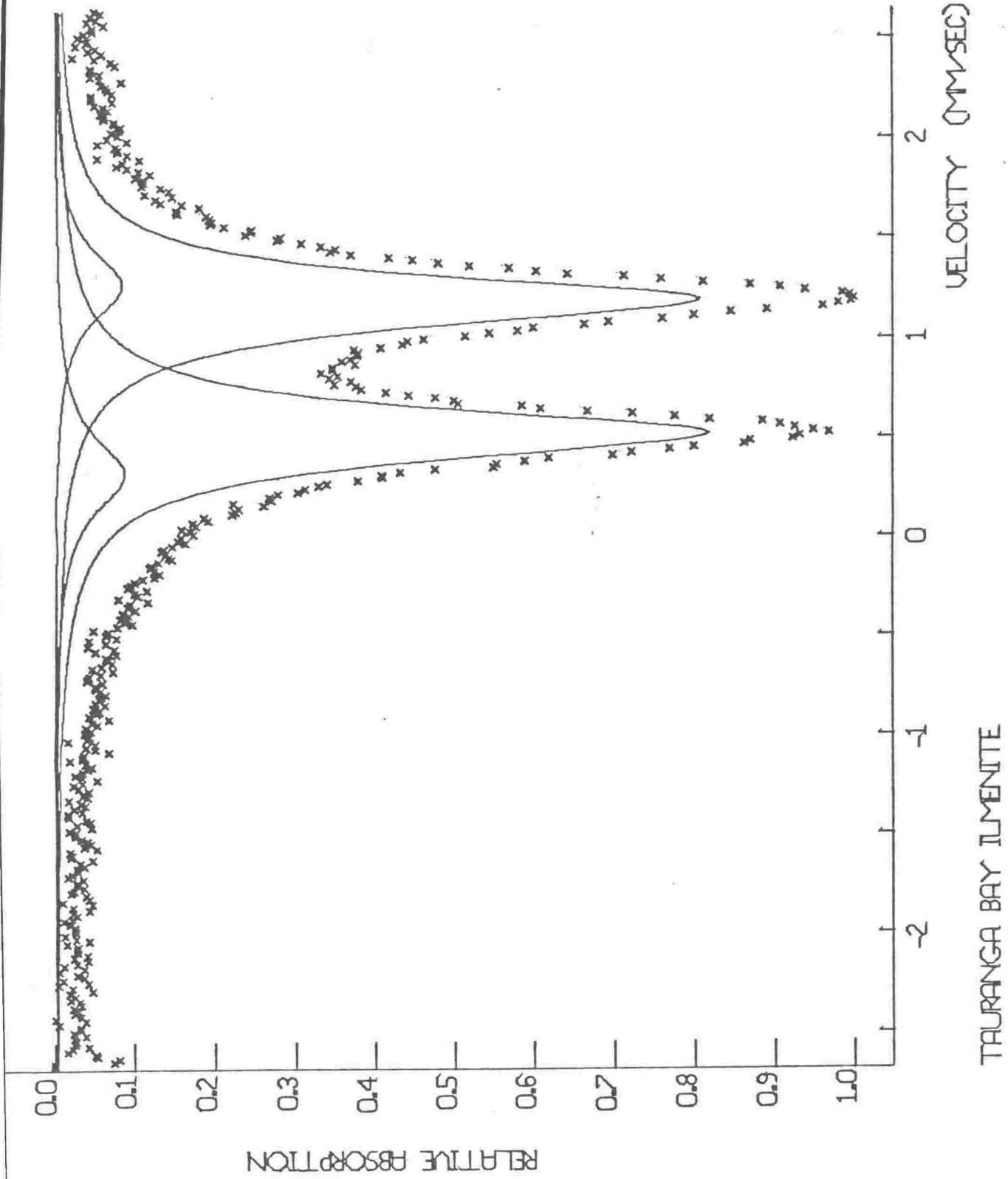

Fig. 4.41 The Mössbauer spectrum of Tauranga Bay ilmenite, showing the two doublets of the successful four peak fit.

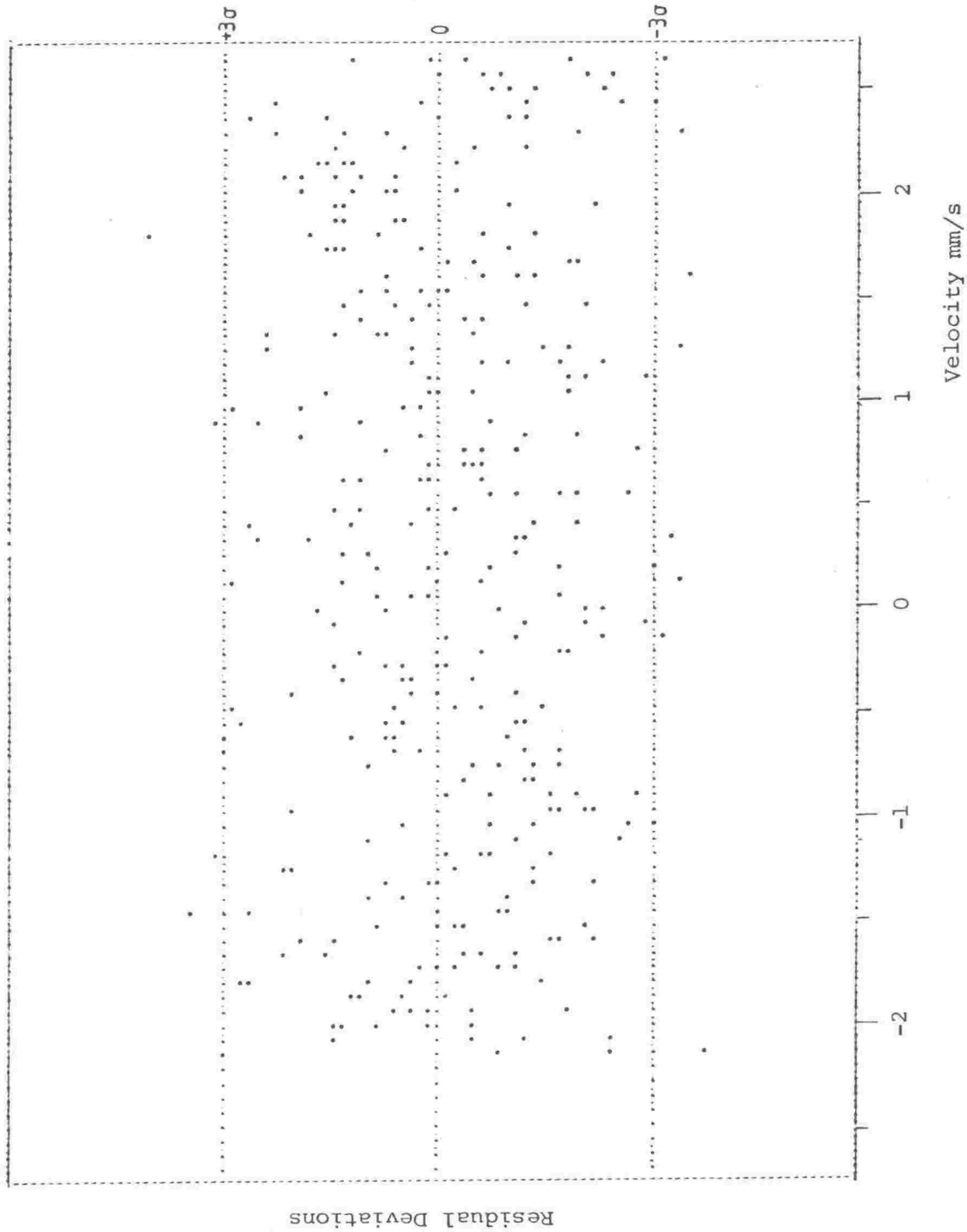

Fig. 4.42 Residual deviations plot from the successful four peak fit.

Ruby and Shirane (1961) showed by neutron diffraction study that Fe^{2+} is found in the Ti^{4+} site of ilmenite, approximately 5% of the total Fe^{2+} in the sample they considered. In a poorly resolved Mössbauer spectrum of the material, they also observed two satellite peaks on the outer shoulders of the ferrous doublet (see Table 4.9). Thus, the second doublet is attributed to Fe^{2+} in the ilmenite Ti^{4+} site. The difference in quadrupole splitting of the two doublets can be readily explained by the different chemical environments between octahedral sites on the Ti^{4+} and Fe^{2+} layers of mineral ilmenite (Shirane et al 1959).

To confirm the presence of hematite in the ilmenite concentrate, a spectrum was recorded using a velocity range of ± 9 mm s^{-1} (Fig. 4.43). However the six peak magnetic hyperfine split resonance characteristic of hematite, and observed in the spectra of North Island concentrates (see Fig. 5.13) was absent. This indicates only a small level of hematite in the Tauranga Bay sample, as concentrations of 2-4% (of the total iron) would be detectable.

In two samples considered after partial dissolution the same peak structure was fitted to the experimental envelope (Table 4.9). Comparison of peak areas can be used to give a measure of the relative populations of the two sites (Bancroft 1973). Unfortunately in this case, the uncertainty in resolving peak areas in the minor doublet is of similar magnitude to the apparent difference in relative populations between the three samples:

(Before reaction)	$Fe^{2+}(Ti^{4+}$ site$)/Fe^{2+}(Fe^{2+}$ site)	= 7.3/100
(8 M HCl, 70 °C, 10 hr)		= 6.5/100
(4 M H_2SO_4 70 °C, 36 hr)		= 5.8/100

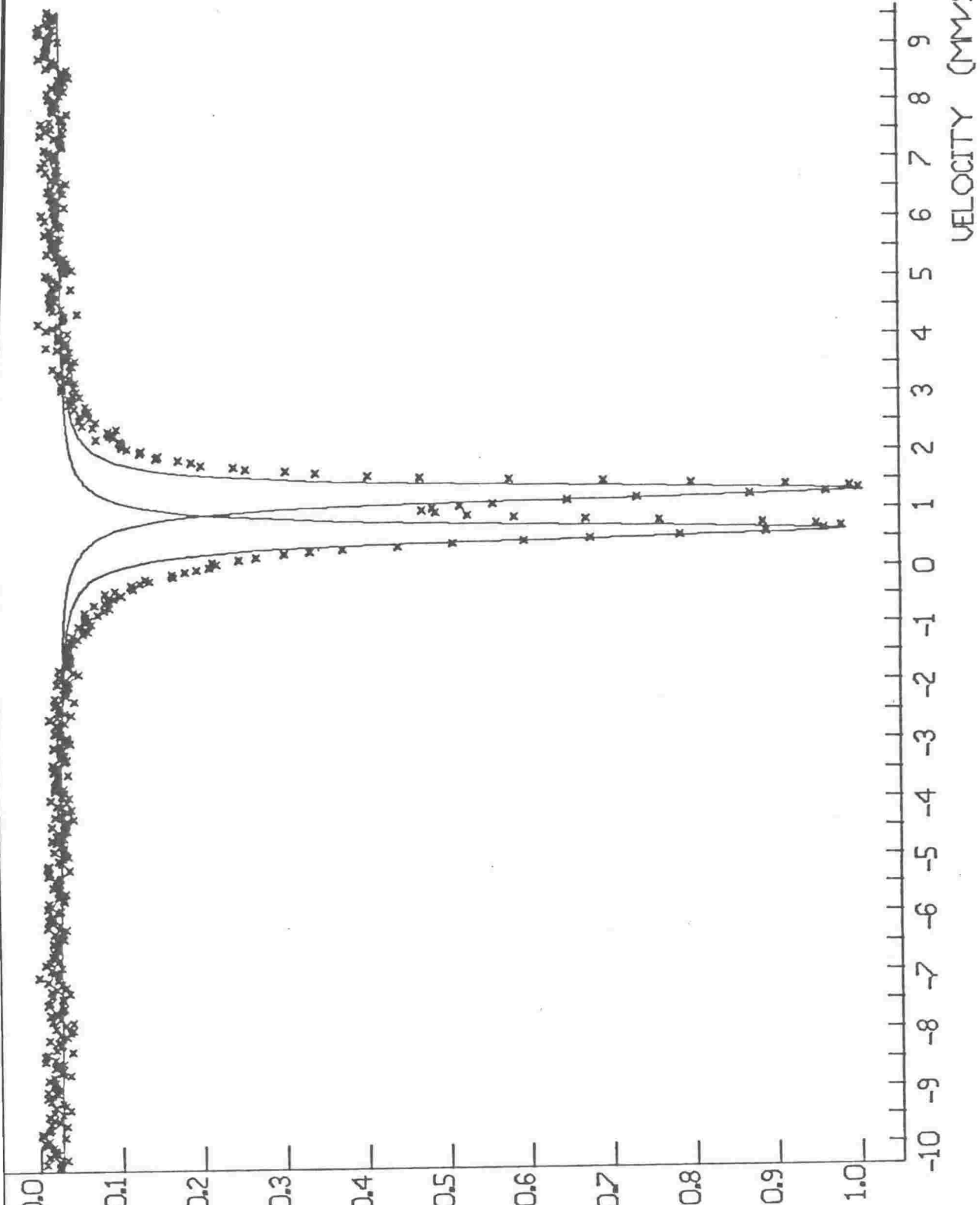

Fig. 4.43 The Mössbauer spectrum of Tauranga Bay ilmenite using an expanded velocity scale.

It is therefore not possible to reach any conclusion with regard to the relative reactivity of the two sites or possible localization near the grain surface.

From this study and the investigation of the nature of weathering in other ilmenites (see section 5.5.3) it is apparent that there is considerable scope for a detailed investigation of ilmenite structure and weathering utilizing Mössbauer spectroscopy. Such an exercise is however beyond the scope of this study.

Chapter 5

THE NATURE OF ACID ATTACK ON MINERAL ILMENITE

5.1 Introduction

Control of a heterogeneous reaction such as mineral dissolution will depend on one (or more) of the following processes (Bircumshaw and Riddiford 1952):

(a) Transport of the reactants to the solid/solution interface - including diffusion in the bulk solution and through any stationary layer. This also includes any diffusion process through a porous layer at the solid surface.

(b) Chemical processes at the solid/solution interface - including adsorption of reactants, reaction and desorption of products.

(c) Transport of products away from the interface - the reverse of the processes listed in (a).

Reaction is controlled by the slowest of these processes but complications may arise in real systems from a wide variety of sources, such as formation of insoluble layers on the solid surface or further reaction of the product in the bulk solution. Control may also be shared by different processes either simultaneously or at different stages of the reaction.

The dissolution of ilmenite in acid solution at commercially used concentrations of acid and ilmenite is one such complicated reaction. Firstly attack in the early stages of reaction is selective (see section 4.1.4) and results in the formation of a pore structure deep into many of the grains.

This introduces considerable complexity into the relationship between surface area of the remaining ilmenite and time.

Secondly, one of the product species Ti(IV) is unstable in solution (see section 5.2) and probably exists as a polymeric form of the titanyl ion TiO^{2+}. The titanyl ion however undergoes rapid hydrolysis and precipitation if fairly rigid free acid requirements are not maintained (Walker et al 1975, Judd 1977). This suggests that the rate controlling step in ilmenite dissolution, will also be a function of the titanium concentration in the dissolving solution.

Many previous investigations of ilmenite reactivity (see section 2.3) have either avoided discussion of the mechanism or proposed a variety of controlling influences. However McConnel (1978) argues strongly in support of chemically controlled reaction (i.e. step (b) above is the slowest step). This argument is supported by high apparent activation energies, rate independence of rotation speed (in rotating disk studies) and the comparison of calculated and experimentally derived rate constants. Imahashi and Takamatsu (1976) observed two regions of reactivity with respect to temperature and acid concentration, with chemical control in one and diffusion control (of iron through an insoluble residual titanium rich layer) in the other.

Both studies work in near infinite dilution (McConnel 2 g/300 ml acid solution), Imahashi and Takamatsu 1 g/250 ml), so there is a considerable gap in the understanding of ilmenite dissolution at concentrations approaching commercial levels ($\approx$30→50 g ilmenite/250 ml acid solution).

In the following sections the results of dissolution studies in concentrated solutions will be discussed. They suggest that ilmenite dissolution is controlled in the early stages of reaction, by the selective nature of attack at the ilmenite surface. A porous structure is established

and the diffusion of polymeric and/or partially hydrolysed titanium species through this structure becomes rate controlling. After approximately 1→2 hr of reaction, the increasing titanium concentration in the bulk solution causes extensive polymerisation, preventing product transport through the pore structure and thus blocking the pore reaction. Reaction rate declines, and the chemically controlled reaction at the exterior ilmenite surface dominates. Before discussing the nature of attack on ilmenite, it is appropriate to consider the behaviour of dissolved titanium, which has considerable influence on the mechanism of dissolution.

5.2 The Aqueous Chemistry of Titanium (IV)

The Ti^{4+} ion, because of its extremely high charge to radius ratio does not exist as a simple aquated ion in solution (Cotton and Wilkinson 1966). What it does exist as, is still the subject of considerable debate. Richards (1975) discusses much of the relevant literature with the overall conclusion that a variety of hydrous species such as $Ti(OH)_3^+$ and $Ti(OH)_2^{2+}$ predominate at pH >1 with the species depending on the solution composition e.g. $Ti(OH)_3HSO_4$ and $Ti(OH)_2HSO_4^+$ exist in sulphuric acid solutions (Beukemkamp and Herrington 1960). There is strong support for polymeric species above titanium concentrations of 10^{-2} M (Zhukov and Nazarov 1964, Nabivanets and Kudritskaya 1967, Sinibaldi 1973, Bragina and Bobyrenko 1972, Selbin 1964).

Nabivanets and Kudritskaya (1967) studied the polymerisation of titanium(IV) in hydrochloric acid solutions, a study particularly relevant to this work. They established by electromigration, comparative dialysis and ion exchange chromatography, that at titanium concentrations of 10^{-3} M

and below and $[H^+] > 0.1$ M monomeric TiO^{2+} ions predominate in solution. Above this acid concentration, chloro-complexes of titanyl are formed and in higher titanium concentrations polymerisation results. The extent of polymer formation was determined in HCl and HCl/LiCl mixtures. These results are shown in figure 5.1. The similarities of these curves with the plot of conversion efficiency versus acid concentration (Fig. 4.19) are readily apparent.

The results of these dialysis studies also suggest the concentration of Cl^- ions and not the acidity of the medium largely determines the production of polymeric forms. Polymerisation is more or less independent of acidity in the range $[H^+]$ = 10.5-0.5 M. However below 0.5 M colloidal forms are produced and, depending on titanium concentration, titanium dioxide may be precipitated.

With reference to the solutions encountered during this study, the proposed titanium concentration for the onset of polymerisation (10^{-3} M) is passed within the first few minutes of reaction in all cases except those in which the 50:1 acid/ilmenite mole ratio was used. These are also the only reactions in which titanium shows concentration/time linearity from the earliest stages of dissolution (see section 4.3). In the other hydrochloric acid solutions, the degree of titanium polymerisation will thus be a function of chloride ion concentration.

The effect of polymerisation will be to slow the transport of dissolved titanium out of the porous solid. The evidence for such a transport process becoming rate controlling is discussed in section 5.4.

The dramatic result of fluoride addition in the dissolution reaction is now considered. Cagliotti et al (1960) studied complex formation between titanium(IV) and the fluoride ion in aqueous solution. They concluded that titanium(IV) is strongly complexed by fluoride, and that all

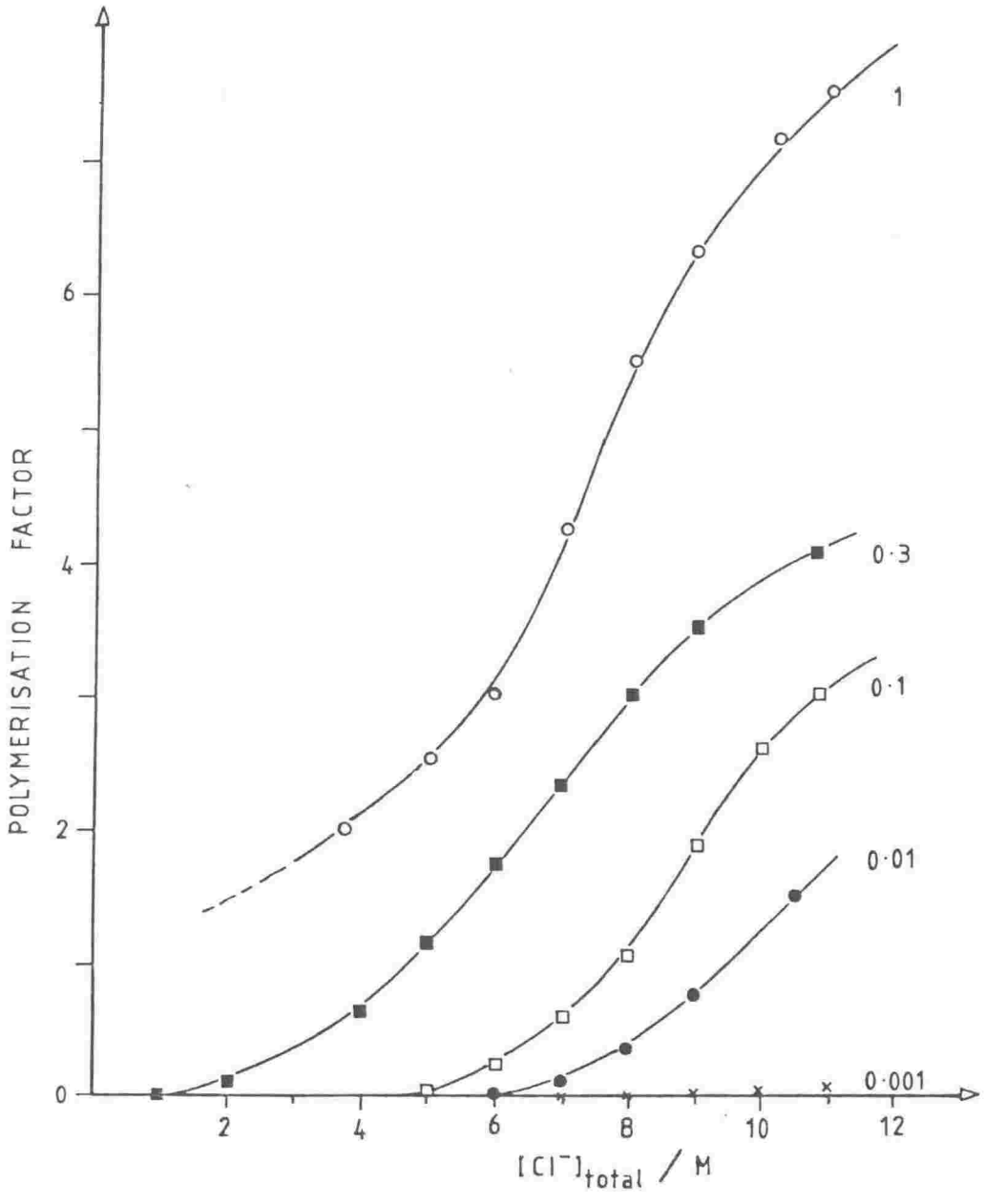

Fig. 5.1 Dependence of polymerisation factor P on the HCl concentration. Numbers against the curves indicate titanium concentration (M). - From Nabivanents and Kudritskaya (1967).

complexes formed were mononuclear. The highest number of coordinated fluorides was found to be four, in $TiOF_4^{2-}$. Table 5.1 shows equilibrium constants for the three complexes studies.

TABLE 5.1 Equilibrium constants for titanium fluoride complexes (from Cagliotti et al 1960)

$TiOF^+ + F^-$	$TiOF$	$\log \beta_1 = 4.35\ M^{-1}$
$TiOF^+ + 2F^-$	$TiOF_3^-$	$\log \beta_2 = 8.31\ M^{-1}$
$TiOF^+ + 3F^-$	$TiOF_4^=$	$\log \beta_3 = 12.03\ M^{-1}$

Thus titanium polymerisation can be prevented by the presence of fluoride during dissolution. Nabivanets and Kudritskaya (1967) found the addition of HF to titanium containing hydrochloric acid solutions decomposed the polymeric forms of titanium with the formation of stable fluoro-complexes, so addition at any stage of reaction will provide a similar effect.

The same mechanism will apply in the prevention of hydrolysis of dissolved titanium (see section 4.2.2). In dissolution reactions observed in this work hydrolysis does not appear to be significant, in the bulk solution at least, with no visible precipitation or irregularity in plots of dissolved titanium with respect to time. The exceptions are reactions which are either extended beyond the usual duration (see Fig. 4.16), or the

percent conversion of the ilmenite is very high (see section 4.1.3).

The reaction of titanium(IV) with phosphoric acid is considerably more complex. Phosphates precipitated from aqueous solutions of titanium are of variable composition (Barksdale 1949) and the formation of titanic phosphates by this method is generally avoided. Phosphoric acid added to chloride solutions of titanium(IV) yields a precipitate of basic titanium phosphate corresponding to the formula $3TiO_2.P_2O_5.6H_2O$ under carefully controlled conditions of concentration, free acidity and temperature (Llewellyn and Crundell 1933). The use of titanium phosphate precipitation has even been considered as a commercial route for titanium extraction from chloride solutions (Whitehead et al 1972).

Thus in dissolution runs in which phosphoric acid was introduced into the solution such titanium phosphates were precipitated. Average Ti:P ratios of the products were approximately 2:1. This precipitated material appears to block both surface and pore dissolution, causing a major depression of reaction rate and a large deficiency in titanium concentration in the solution. This precipitate is shown in electron and optical photomicrographs (Fig. 4.10) and the solution composition is shown in figure 4.29.

5.3 Mechanism of the Dissolution Reaction

5.3.1 Nature of Selective Attack

The dominant feature in the early stages of the dissolution of Tauranga Bay ilmenite in acid solution is the selective attack of grains along channels lying parallel to the basal (0001) plane. This type of attack is observed on a majority of the grains (see section 4.1.4) and has been noted in previous studies of ilmenite reactivity (Lynd 1960, McConnel 1978). A second, less dominant plane of attack is also observed. This appears to be the second parting plane of ilmenite, the $(10\bar{1}1)$ plane

(the basal plane is the other parting plane - see section 4.1.4). This type of attack is not unexpected as the prominent parting planes should be sites of high numbers of dislocations due to structural mismatch. In augite for example, parting dislocations appear to constitute the major sites of attack by acid solutions (Berner et al 1980). Twinning is also often associated with the ilmenite basal and $(10\bar{1}1)$ planes (Deer, Howie and Zussman 1962).

Reference to figure 2.1 illustrates a peculiarity in the ilmenite crystal structure whereby the Fe^{2+} and Ti^{4+} ions lie in discrete layers parallel to the basal plane. Thus if attack is favoured at one metal ion site rather than the other, it will occur more rapidly parallel to these layers than at right angles to them. Selective removal of one component on a large scale would not be anticipated because of the major problem of access to the sites of attack. However if only a small degree of reaction is followed, or attack is extremely slow, then selective leaching might be expected (see section 5.3.3). Anfinger et al (1973) followed very small degrees of dissolution ($\approx$0.02%) of ilmenite in weak (<0.01 M) sulphuric acid and observed only iron in solution.

This relates closely to the observed behaviour of ilmenite in natural weathering, where attack is often selective and stringers of altered, titanium rich material are found lying in the basal plane (Lynd 1960, Temple 1966, Bailey et al 1956). Berner et al (1980) showed that natural selective weathering and etch patterns observed in pyroxenes and amphiboles, could be reproduced in the laboratory by etching mineral samples with HCl/HF mixtures. Photomicrographs of these etched grains bear a striking resemblance to those in figure 4.11, taken after partial dissolution of ilmenite samples.

The close structural relationship between ilmenite and the intermediate weathering product pseudorutile (Grey and Reid 1975) also provides an explanation for the slight unit cell shrinkage observed in the course of

the dissolution reaction (see section 4.1.2). The partial leaching of ferrous iron and minor oxidation of the remaining iron causes a small readjustment in the anion lattice to accommodate the cation vacancies, and thus unit cell size will decrease.

The large cavities formed within grains (see Fig. 4.11) indicate greater reactivity in the grain interior. Thus titanium polymerising or precipitating within the grain interior will:

(a) restrict a preferred avenue of attack, and

(b) cause a titanium deficiency relative to iron concentration in the bulk solution.

These effects are discussed in the following sections.

5.3.2 The Effect on the Observed Reaction Rate

Bircumshaw and Riddiford (1952) derive an expression for the observed unit rate constant k for a heterogeneous reaction, based on a general intermediate type reaction:

$$k = k_c k_T / [k_c + k_T(A/\sigma A_c)]$$

where k_c = chemically controlled rate constant

k_T = transport controlled rate constant

A = the apparent surface area

σA_c = the true area available for reaction.

The limiting cases are

(i) $k_c \sigma A_c >> k_T A$ for transport control, and

(ii) $k_c \sigma A_c << k_T A$ for chemical control.

Factors affecting k_c and k_T during the course of reaction are:

(a) If there is a significant change in the true surface area A_c of the dissolving solid, the overall chemical rate constant will change in the same direction.

(b) The preferential development of particular crystal faces during dissolution may cause an increase in k_c, whereas k_T is independent of the face attacked.

(c) Increasing the size of the solute species by, for example, addition of a complexing agent will result in a decreased diffusion coefficient, and a shift toward transport control.

(d) The adsorption of a product species will affect σ, the proportion of available surface, and cause a shift toward chemical control.

(e) The accumulation of a product species as an insoluble layer on the grain surface may cause diffusion of reactants or products through this layer to become rate controlling.

(f) If reaction is diffusion controlled, then a rise in the bulk concentration of the solute c_∞, such that it is no longer negligible compared with the saturation concentration c_s, will cause an apparent change in order of the reaction.

In the case of ilmenite dissolution, the effect of pore and cavity formation is to markedly increase the exposed ilmenite surface. If chemical control of reaction rate were dominant we would anticipate a corresponding increase in dissolution rate. However dissolution rate is observed to decline rapidly in all reactions using high ilmenite/acid ratios (see section 4.2.1). In relation to the factors considered above, this discounts (a) as the controlling mechanism. However the nature of dissolved titanium (see section 5.2), makes (c), (d) and (f) possible options, even in low concentration dissolutions, where low free acidity makes titanium unstable in solution (Walker et al 1975).

McConnel (1978) calculates a transport controlled rate constant k_T for a rotating disk of ilmenite, dissolving in sulphuric acid and shows this value gives a dissolution rate far greater than the observed rate.

Transport $\frac{dn}{dt} = 3\times10^{-5}$ mol s^{-1} for synthetic ilmenite,

observed $\frac{dn}{dt} = 1\times10^{-8}$ mol s^{-1}

The transport rate constant was calculated from the Levich (1962) theory, where

$$k_T = 0.620\ D^{-2/3}\ \nu^{-1/6}\ \omega^{1/2}$$

D = diffusion coefficient of the diffusing species

ν = kinematic viscosity

ω = rotational velocity

$$\frac{dn}{dt} = k_T.A'c$$

A' = projected surface area

c = hydrogen ion concentration

McConnel uses the diffusion coefficient of the hydrogen ion in strong sulphuric acid ($\simeq 1\times10^{-5} cm^2\ s^{-1}$), however as is shown in sections 5.2 and 5.4, the diffusion of the hydrogen ion will be several orders of magnitude faster than the diffusion of polymeric titanium units through the unstirred solution, within the porous structure. Thus if the calculated transported controlled rate is based on a polymeric titanium species, it moves considerably closer to the observed reaction rate, particularly in the relatively concentrated solutions used in this work,where polymerisation will be significant (see section 5.2). The evidence for diffusion becoming rate controlling is discussed further in section 5.4, but first it is necessary to discuss the iron-titanium balance between the dissolving solid and solution, a feature which must be considered in any proposed mechanism.

5.3.3 The Iron:Titanium Imbalance

The lower bond strength of the Fe^{2+}-O bond compared with Ti^{4+}-O (Pogorelov and Boitenev 1974) together with the observed predominance of iron over titanium in all the reaction solutions in this study is consistent with the ferrous site being more readily attacked in mineral ilmenite. Also slower reaction favours the selective dissolution of iron, or at least the selective appearance of iron in solution (see figure 4.18). Simple surface reaction cannot account for this imbalance unless:

(a) an extensive iron-rich surface layer is preferentially dissolved or

(b) a titanium-rich lattice is left at the grain surface.

Microprobe and optical mineralogical studies support neither. There is evidence for the isolated occurrence of surface hematite (see section 4.1.2) but this phase is not in sufficient quantity to account for the observed imbalance.

The conclusion is that although iron is attacked more readily under these conditions, the dissolution reaction requires corresponding removal of titanium unless reaction is extremely slow, e.g. natural weathering.

The titanium deficiency in the dissolving solution (see section 4.2.1) indicates that titanium is either precipitated in the bulk solution, or adsorbed on the surface of the ilmenite grains, and is removed during preparation of the ilmenite for X-ray fluorescent or microprobe analysis. The lack of evidence for precipitation, except in reactions involving greater than 50% conversion (see section 4.1.3) and the lack of effect of ultrasonic treatment, suggest a simple precipitate of hydrous titanium dioxide is not responsible.

The tendency for the Ti^{4+} ion to polymerise in strong hydrochloric acid (see section 5.2) provides an explanation for both the iron:titanium imbalance observed in dissolutions at lower acid strengths and the titanium deficiency in the mass balance. A large polymeric titanium species formed in an unstirred pore solution may diffuse to the ilmenite surface sufficiently slowly to cause a titanium accumulation within the pore structure and a decline in reaction rate. Some precipitation may result when titanium concentration exceeds its stability with regard to free acid concentration. This is also consistent with the observed effect of additional titanium in the dissolving solution (see section 4.2.7). Additional titanium severely inhibits dissolution, whereas additional iron has little effect. Evidence for this diffusion process is discussed in the following section.

5.4 Diffusion Control

5.4.1 Theoretical Treatment

The theory associated with liquid phase transport control of heterogeneous reactions has been developed around the existence of a stationary "Nernst layer" at the solid/solution interface (Bircumshaw and Riddiford 1952). The implications of this theory and its application to the case of ilmenite dissolution will now be considered.

Provided the bulk solution is well stirred, concentrations will be uniform and reactants and products reach or leave the surface by diffusing through a thin solution layer. Ficks law can then be expressed:

$$-\frac{dc}{dt} = (DA/V)\frac{dc}{dy} \qquad \ldots(1)$$

where $\frac{dc}{dy}$ is the concentration gradient normal to the surface,

D is the diffusion coefficient of the solute,

A is the apparent surface area of the solid,

V is the solution volume.

The simplest treatment of transport controlled dissolution rate, assumes a linear concentration gradient dc/dy normal to the surface and

$$\frac{dc}{dy} = (c_\infty - c_o)/\delta \qquad \ldots(2)$$

where c_∞ = the concentration of solute in the bulk solution,

c_o = solute concentration at the interface,

δ = thickness of the stationary layer.

Barton and McConnel (1979) consider solid dissolution reactions in terms of the pseudo zero order rate constant k_o for a transport controlled dissolution reaction:

$$k_o = (\frac{V}{A})\frac{dc}{dt} = A^{-1}\frac{dn}{dt} \qquad \ldots(3)$$

combining equations (1), (2) and (3),

$$k_o = (\frac{D}{\delta})(c_o - c_\infty) \qquad \ldots(4)$$

For a fully transport-controlled reaction $c_o = c_s$ (the solubility of the solute). k_o and the transport controlled rate constant k_T are related by:

$$k_o = k_T(c_o - c_\infty) = k_T(c_s - c_\infty) \qquad \ldots(5)$$

Where the solution volume is large compared with the concentration of the solute, $c_\infty << c_s$ and thus

$$k_c = k_T c_s \qquad \ldots(6)$$

For a chemically controlled reaction $c_o = c_\infty$ and $k_o = 0$, implying no transport contribution to the control of the reaction rate.

These are the extreme cases and most reactions fall into an intermediate category with some contribution to rate control from both transport and chemical processes (Bircumshaw and Riddiford 1952). For example, the concentration c_o of the solute at the interface may be neither the same as that in the bulk solution (chemical control), nor equal to the saturation concentration c_s (as will occur if transport of solute from the interface is rate controlling - Barton and McConnel 1979). The observed rate will then be a function of both the rate of chemical reaction at the interface, and the rate of the slowest transport process.

5.4.2 Application to Ilmenite Dissolution

To consider the specific case of ilmenite dissolution in concentrated acid solutions:

(a) $c_\infty \ll c_s$ (see equation 1) will only apply in the very early stages of most reactions i.e. small amounts of dissolution, particularly for dissolved titanium.

(b) the diffusion layer thickness δ, will be replaced by the depth of the pores, as the pore sizes are sufficiently small to leave the solution within them at rest relative to the bulk solution. Thus δ (and the pore forming reaction rate) will be independent of stirring speed.

(c) the nature of the solute species will change depending on concentration in the bulk and in the pore solution. This applies specifically to dissolved titanium which will polymerise and/or hydrolyse, depending on titanium concentration, chloride concentration and free acidity (see section 5.2). The increase

in size of the solute species, due to polymerisation will progressively lower D, the diffusion coefficient of this species away from the interface.

If at the stage of reaction where pore formation is dominant, the reaction rate is controlled by diffusion within the porous solid, we would expect the parabolic law (Mott and Gurney 1948) to be followed. As attack in one direction is dominant (in this case along holes parallel to the basal plane), then the surface area under attack (the "end wall" of the pore) can be assumed to be constant. The change in concentration (dc) will then be proportional to the pore depth (ds).

$$dc = K\,ds \qquad \ldots(7)$$

where K = a constant

From equations (1), (2) and (7)

$$\frac{dc}{dt} = K\frac{ds}{dt} = \left(\frac{DA}{V_s}\right)(c_s - c_\infty) \qquad \ldots(8)$$

Integrating (8) yields

$$s^2 \propto Dt \qquad \ldots(9)$$

and as $s \propto D^{\frac{1}{2}}t^{\frac{1}{2}}$ then $\frac{dc}{dt} = D^{\frac{1}{2}}/t^{\frac{1}{2}}$

$$\therefore \quad c \propto D^{\frac{1}{2}}t^{\frac{1}{2}} \quad \text{and} \quad c^2 = kDt \qquad \ldots(10)$$

Thus we would expect a plot of concentration against $t^{\frac{1}{2}}$ to be linear with a slope proportional to the square root of the diffusion coefficient of the diffusing species. This relationship, the parabolic law, holds with some accuracy for the first few hours of reaction, over a wide range of acid strengths (Fig. 5.2) and for both titanium and iron.

The point of breakdown of the $t^{\frac{1}{2}}$ relationship varies considerably over the range of 3.7 → 10 M HCl (Fig. 5.3), with the longest span of

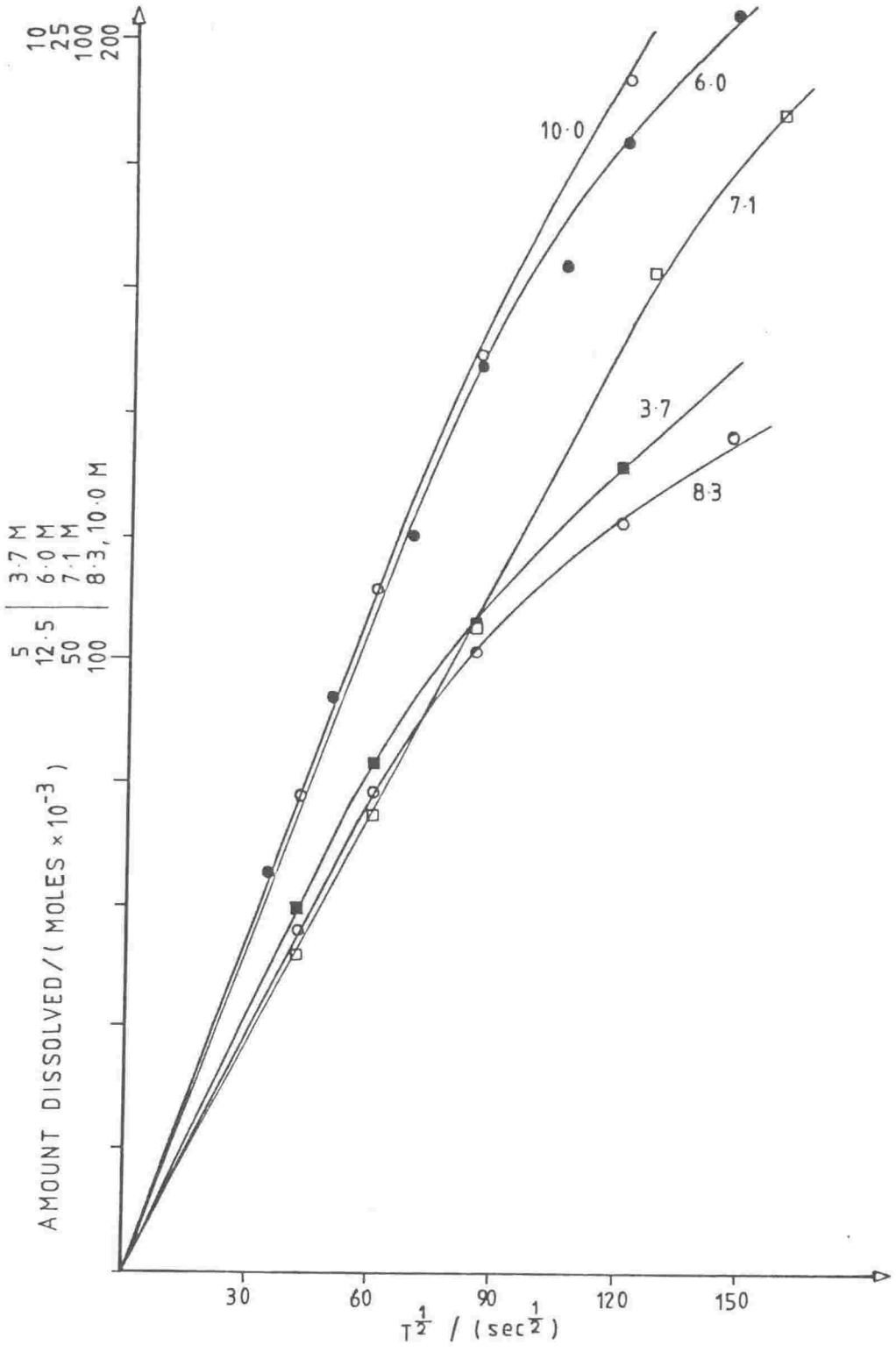

Fig. 5.2 (a) Plot of concentration vs $t^{\frac{1}{2}}$ for titanium dissolution in 3.7→10 M HCl, 70 °C.

cont. over

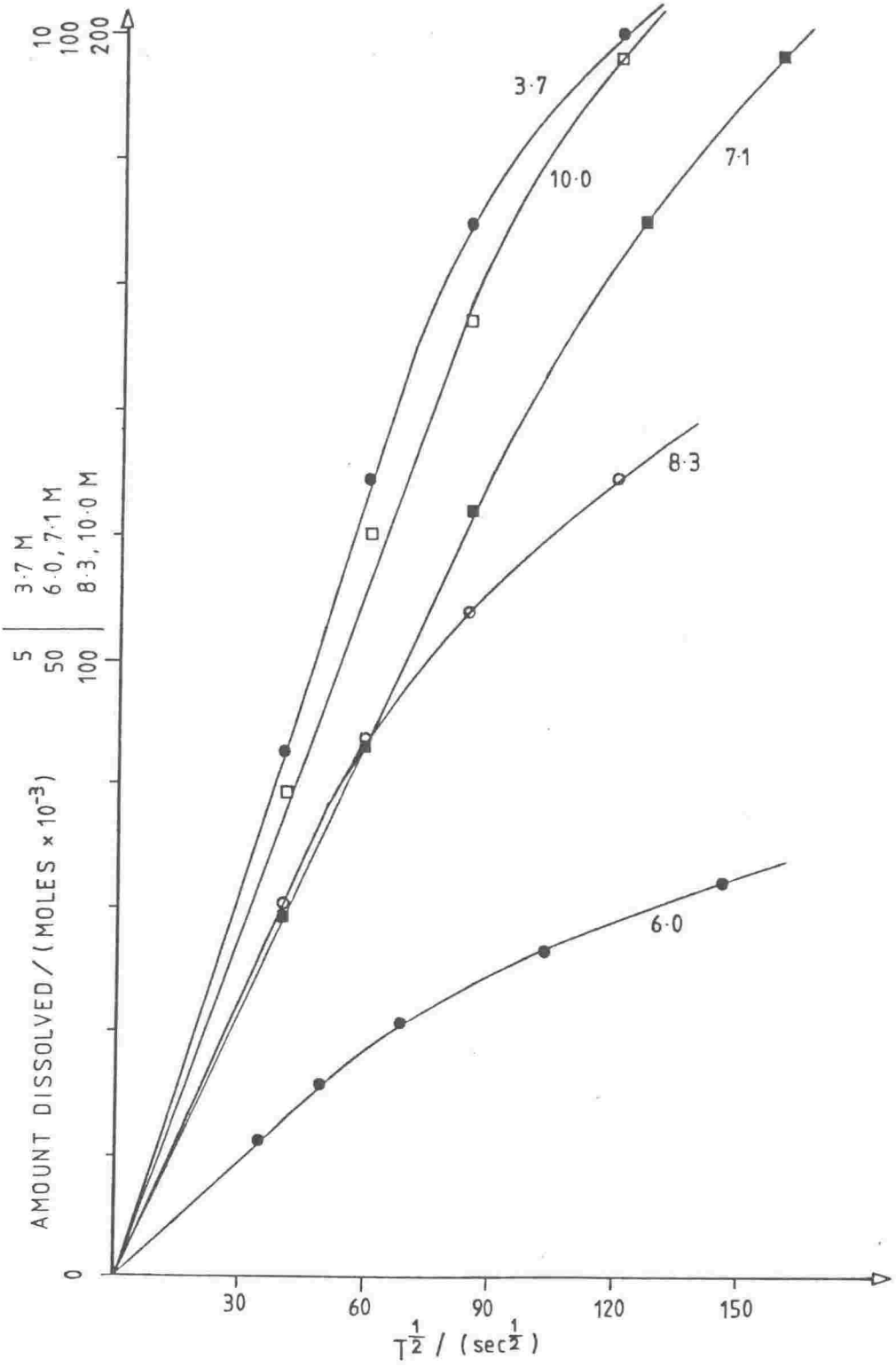

Fig. 5.2 (b) Plot of concentration vs $t^{\frac{1}{2}}$ for iron dissolution in 3.7→10 M HCl, 70 °C.

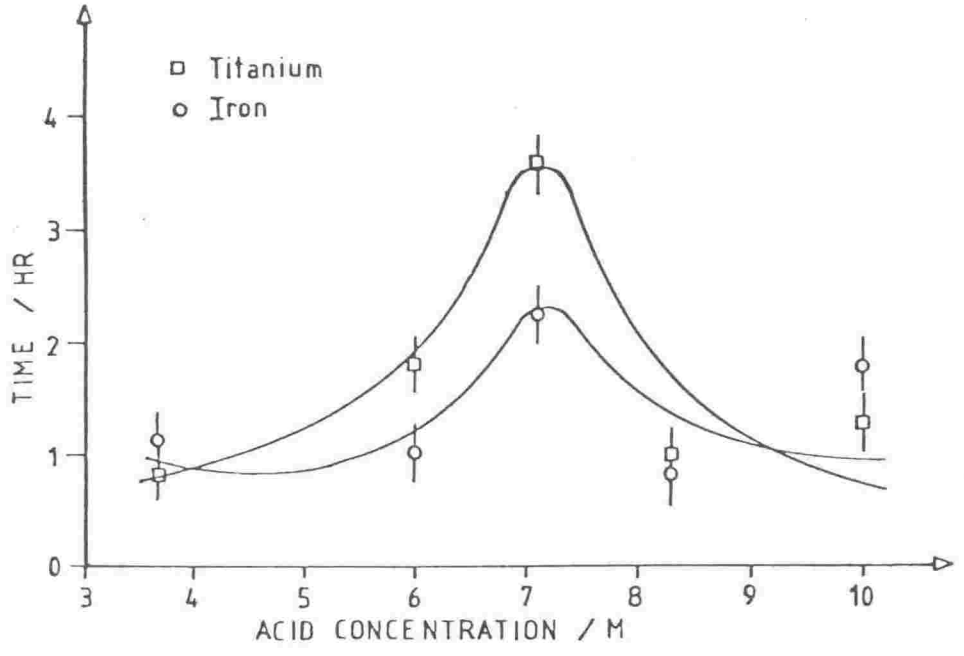

Fig. 5.3 The point of breakdown of the concentration/$t^{\frac{1}{2}}$ relationship 3.7→10 M HCl, 70 °C.

diffusion control observed for reaction around 7 M HCl. This region is of some interest in the study of other features of the reaction (see figure 4.19 - effect of acid strength - and figure 5.1 - polymerisation factor vs [HCl]).

Further support for titanium diffusion out of the porous solid being rate determining in the early stages of reaction comes from experiments in which phosphate, fluoride or additional titanium were introduced. The influence of additional titanium (see section 4.2.7) in particular demonstrates a significant rate dependence on the concentration of dissolved titanium. A similar dependence on the concentration of iron is not observed. Richards (1975) has shown that varying iron concentration from Fe:Ti = 0 to 1, had a negligible effect on the hydrolysis of titanium in sulphate solutions, so iron concentration appears to have little influence on either the polymerisation or hydrolysis of titanium(IV).

Phosphate and fluoride provide excellent means for trapping or accelerating transport respectively, of dissolved titanium (see section 5.2), showing that the transport of titanium is readily interferred with by small concentrations of additives.

Support for this type of mechanism is found in the so called 'selective leaching' of ilmenite considered by Jain and Jena (1977), and used in a number of commercial processes based on ilmenites modified by oxidation/reduction (see for example Sinha 1973). Jackson (1975) showed this selective leaching was actually due to titanium dioxide insolubility and reprecipitation. Experiments undertaken by CSIRO suggested that although in the early stages of leaching both iron and titanium dissolved in the leachant, as penetration into the grain proceeded and diffusion rates deteriorated, a point was reached where titanium dioxide reprecipitated at or near the reaction sites. X-ray examination of wet leach residues identified a largely rutile structure (Minerals Research in CSIRO 1976).

Rutile residues were identified in experiments in this work where large degrees of ilmenite conversion (>60%) were achieved (see section 4.1.3). This rutile precipitation occurs despite using relatively low temperatures (70→80 °C), so as polymerisation and hydrolysis are involved, the precipitation process would be expected to be rapid when using temperatures close to the boil and pore blocking would occur very rapidly. At lower temperatures, slower dissolution rates are thus compensated for by increased pore formation and the associated increase in surface area. Sulphuric acid or added bisulphate can also be used to retard the polymerisation/ precipitation process (see section 4.2.3).

5.5 Other Features of Reaction

5.5.1 The Role of Inclusions

West Coast, New Zealand ilmenites display in cross-sections, a large number of inclusions, mainly feldspars and quartz (see section 4.1.1). These inclusions appear to play little part in the dissolution process although the pattern of selective attack is sometimes initiated at the inclusion/ilmenite boundary. They do however act as nuclei in the precipitation of titanium phosphates and other titanium species, as do fragments of undissolved ilmenite. This is shown in the mixed analyses obtained from precipitated materials by electron-microprobe (see section 4.1.3).

So despite contributing to the relatively low grade classification of the West Coast ilmenites (based on the low TiO_2 content), the major silicate inclusions do not interfere in the dissolution process. They do however interfere later in processing when titanium hydrolysis is carried out. "In situ" hydrolysis, which is readily achieved in hydrochloric acid solutions (Judd 1977), must be avoided or these acid resistant gangue minerals will report in the crude TiO_2 product. Removal from the solution before hydrolysis requires a careful filtration step as many inclusions are extremely small ($\approx$5 μm diameter).

Inclusions which do dissolve rapidly in acid solutions such as apatite (see section 4.1.2), are not in sufficient quantity to influence the course of reaction by phosphate blocking or other mechanisms.

5.5.2 The Effect of Natural Weathering

Natural alteration of ilmenite involves progressive oxidation and leaching of iron, with corresponding enrichment in titanium (see section 2.2). Alteration becomes visible in photomicrographs of weathered ilmenites as titanium rich zones around the grain exterior and stringers lying parallel to the basal plane (see 5.5.3 and McConnel 1978, Lynd 1960).

This suggests that a similar mechanism applies to both natural weathering and to initial acid attack, in this selectivity of reaction. Lynd (1960) has shown the effectiveness of naturally occurring acids in rainwaters as weathering agents for ilmenite. However the time scale and conditions involved differ considerably in the two processes, with natural weathering expected to be close to an equilibrium process. It was noted in section 5.2.3 that the slower the reaction, the higher the ratio of Fe:Ti leached from the ilmenite. Natural weathering is the extreme example of this, iron alone being selectively removed, at least until the pseudo-rutile composition ($Fe_2Ti_3O_9$) is reached. After this the titanium must be taken into solution and reprecipitated to allow the formation of a high titanium "leucoxene" product (see section 2.2), approaching rutile in composition (Grey and Reid 1975).

The result of this selective leaching and reprecipitation even producing a slightly titanium enriched phase

in acid dissolution of these altered ilmenites, the preferred zones of initial attack are blocked. On these grounds we would expect weathered ilmenites to show markedly less reactivity toward acid dissolution, despite the presence of large zones of essentially unaltered material (see section 5.5.3). McConnel (1978) in a study of the reactivity of ilmenites of widely varying compositions showed this to be the case.

This behaviour is also consistent with the observed formation of large cavities in the grain interior once pore formation has been initiated. The largest concentration of altered material lies near the grain surface leaving the more reactive unweathered ilmenite in the grain interior. This weathering pattern is discussed in the following section.

5.5.3 Other Ilmenites

Studies on ilmenites other than Tauranga Bay, were limited to structural and compositional studies using X-ray diffraction and fluorescence, electron microprobe and Mössbauer spectroscopy. The samples considered represented a broad compositional range, from a relatively low grade concentrate (Manukau ilmenite), to high grade Australian concentrates. The source and bulk composition of the samples are listed in Table 5.2.

From microprobe analyses, these concentrates show marked inhomogeneity by comparison with Tauranga Bay ilmenite. A material such as HYTI 68 shows widely differing Fe:Ti ratios both within and between grains. Analyses range from near stoichiometric ilmenite to near pure rutile (Fig. 5.4).

Table 5.2 Composition of ilmenite concentrates

Sample	Manukau ilmenite concentrate	Bowentown ilmenite	Western Titanium ilmenite concentrate	Westralian Sands ilmenite concentrate	Westralian Sands HYTI 68	Westralian Sands HYTI 75
Location	West Coast North Island NZ	Coromandel Peninsular North Island NZ	Western Australia	Western Australia		
TiO_2 %	40.2	35.1	51.5	54.9	67.2	72.8
FeO	33.2	35.4	23.8	20.6	6.3	3.1
Fe_2O_3	20.6	21.3	20.8	19.6	18.9	11.4
MnO	1.1	1.0	1.5	1.6	0.6	0.2
MgO	3.0	3.4	1.6	1.7	1.6	2.5
CaO	0.4	-	-	-	-	-
Al_2O_3	1.1	1.0	0.9	1.0	2.2	3.1
P_2O_5	0.2	0.1	0.1	-	0.4	0.2
SiO_2	1.1	0.7	0.4	0.9	0.9	4.3
Total	100.9	98.0	100.6	100.3	98.1	97.6

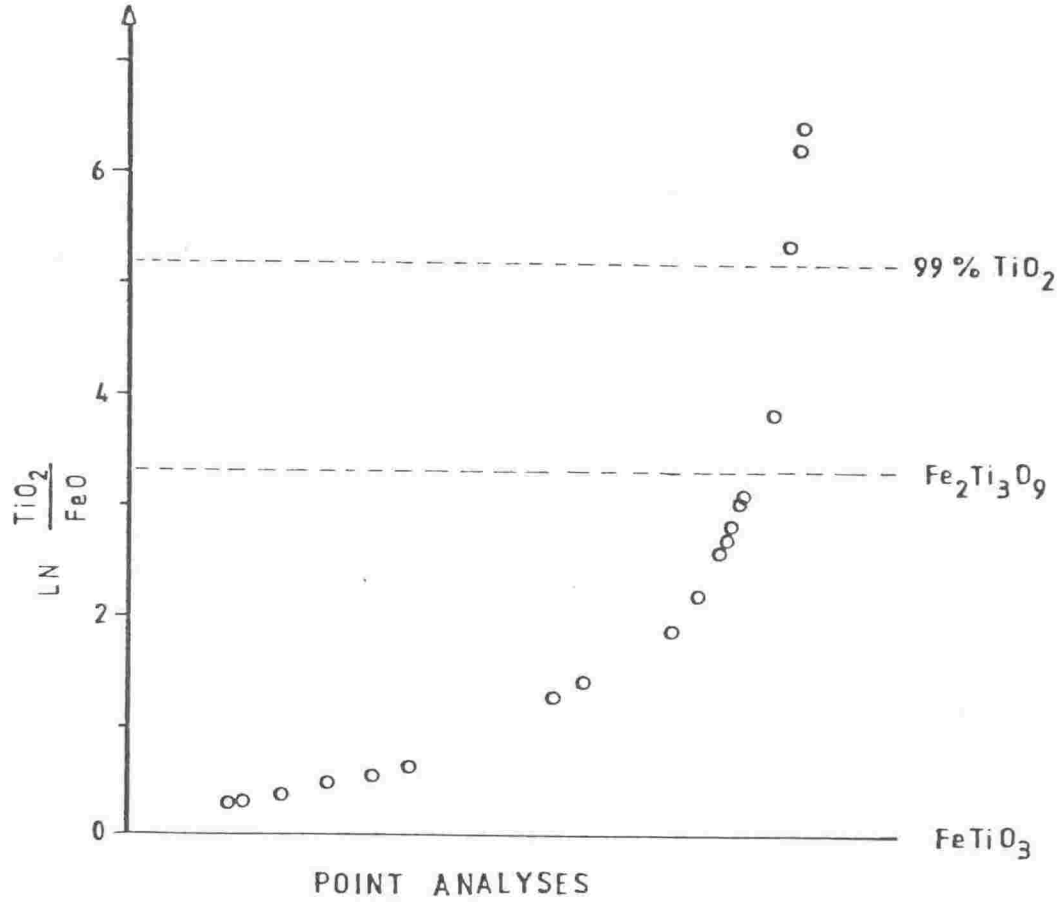

Fig. 5.4 Iron-titanium ratios from a range of analysis points, showing extreme variations in composition . Sample-HYTI68.

This broad compositional range is also revealed in polarized light optical microscopy (Fig. 5.5), however X-ray diffraction patterns (Fig. 5.6) show only the two end members of the ilmenite-rutile transition. The Australian ilmenite concentrates show a suggestion of pseudorutile from intensity variations in the (200), (111) and (210) rutile reflections.

The pattern of alteration in the high titanium concentrates reveals considerable similarity to the selective attack observed in acid dissolution of Tauranga Bay ilmenite. Titanium rich zones are developed around the grain surface and in parallel streaks through the interior (Fig. 5.5). Many highly altered grains still contain a core of unaltered material analysing close to stoichiometric ilmenite.

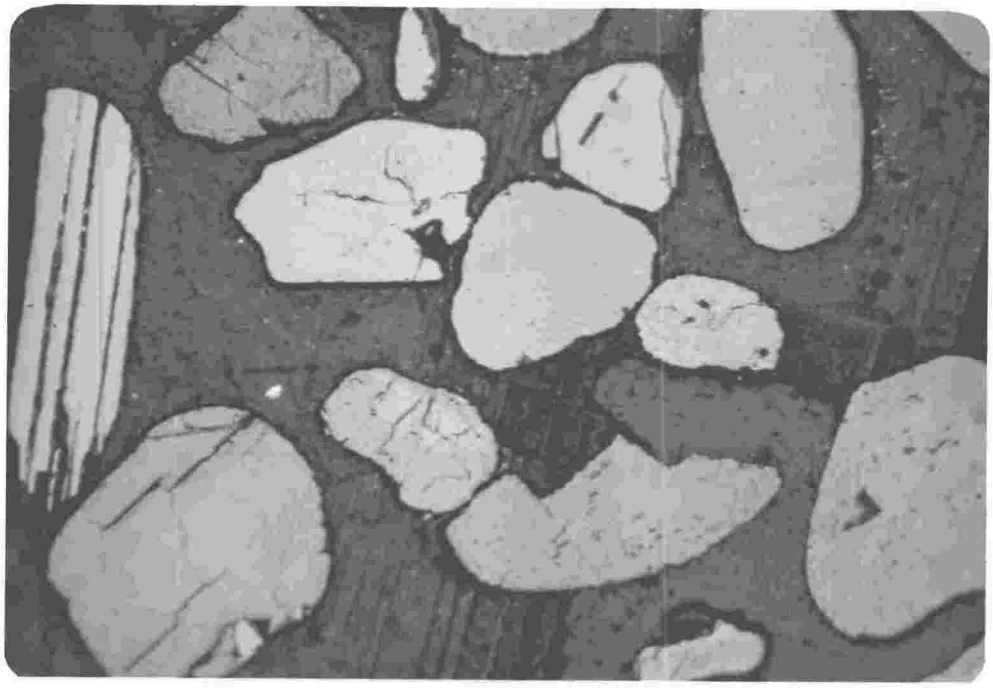

(a)

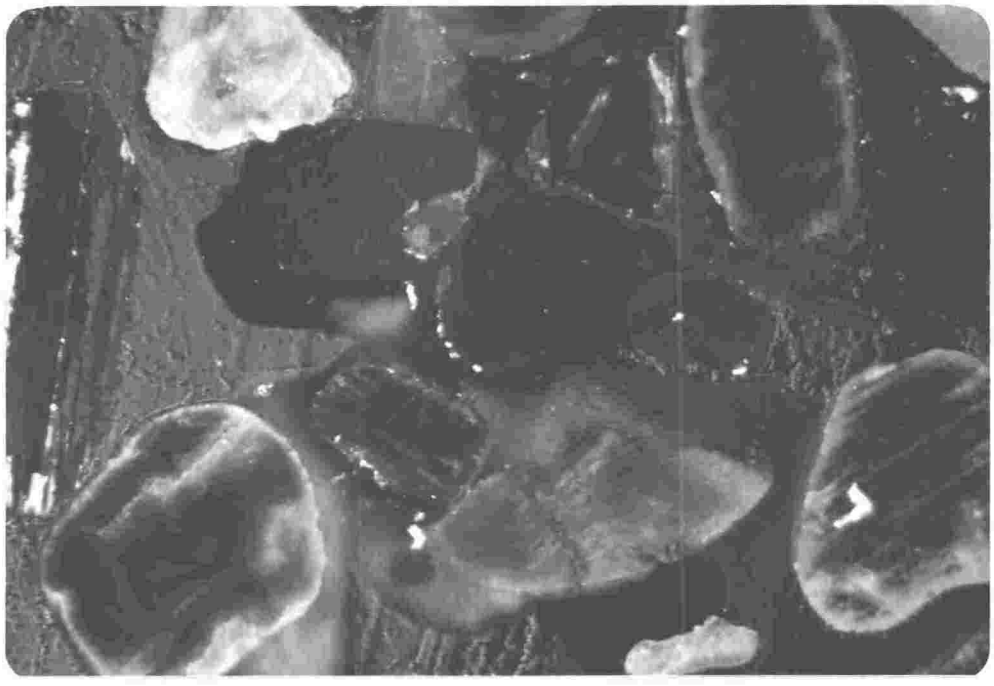

(b)

Fig. 5.5 Cross-section view of a cluster of altered ilmenite grains. The light zones around grain edges approach rutile in composition while darker zones approach ilmenite. (a) reflected light (b) crossed polarised light (Field of view = 420 μm) - Sample HYTI68.

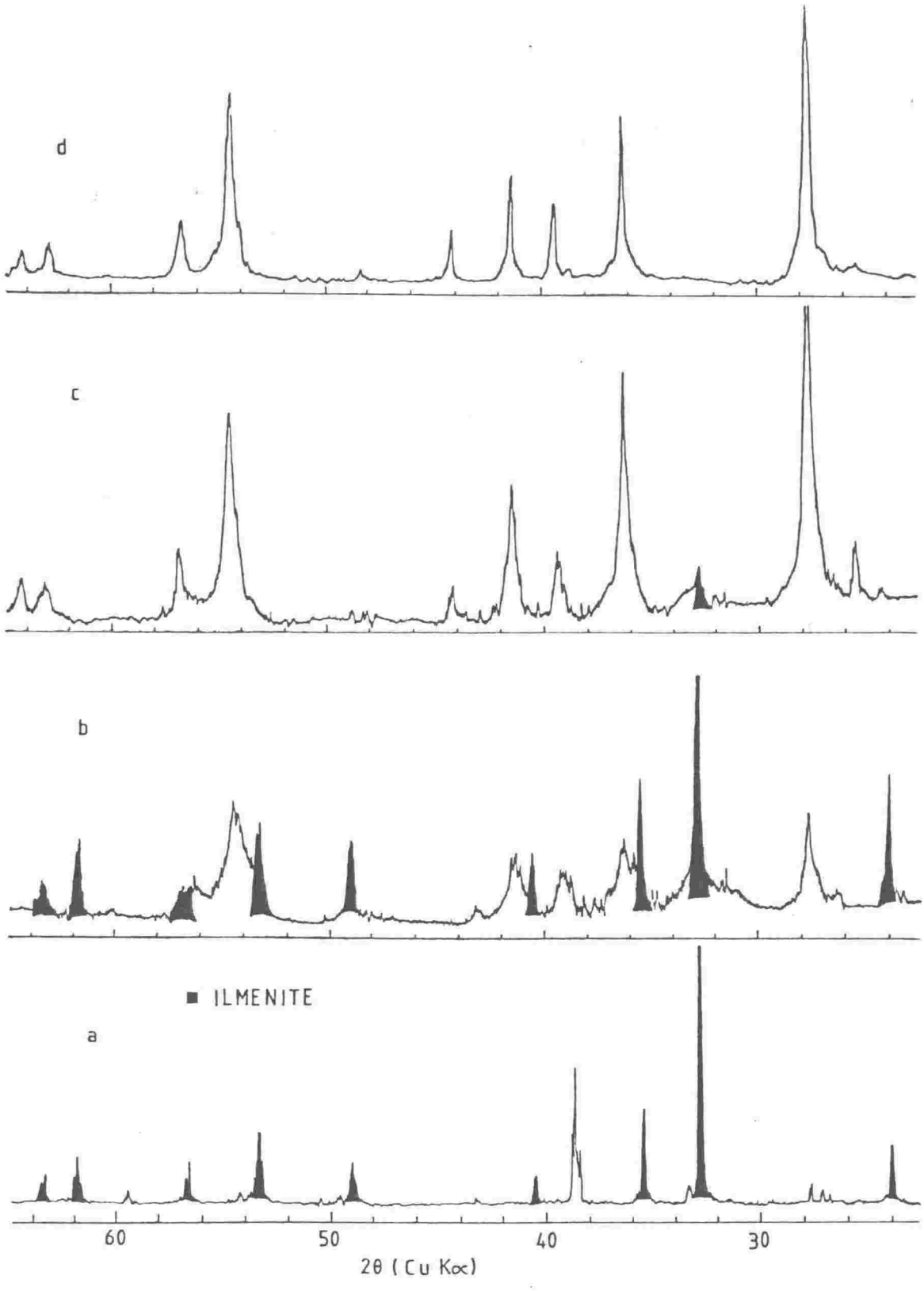

Fig. 5.6 X-ray powder diffraction patterns of New Zealand and Australian titanium ores, showing a progression from almost pure ilmenite to almost pure rutile.

(a) Manukau ilmenite
(b) Western Titanium ilmenite concentrate
(c) Westralian Sands HYTI68
(d) Westralian Sands HYTI75 (a near pure rutile diffraction pattern)

Mössbauer spectra of the samples reveal significant changes in the iron environment with degree of alteration. Spectra, along with the peaks from the best computer fits achieved (see section 3.4.6), are shown in figures 5.8-5.12. Parameters for the fitted spectra are compiled in Table 5.3.

The dominant doublet in the spectra of both New Zealand and Australian ilmenite concentrates is typical of high spin ferrous iron in an oxide structure and is consistent with reported parameter values for $FeTiO_3$ (see Table 4.9). The position of this doublet is invariant over the range of ilmenites considered, however the remaining components of the spectra are quite complex. All Australian samples considered showed a broadened doublet consistent with ferric iron in distorted octahedral symmetry. The two doublets fitted to the HYTI 75 spectrum, represent the extremes of the range of ferric sites contributing to the doublet. The peak broadening can be attributed to the normal Lorentzian curves becoming Gaussian in nature due to contributions from a range of ferric sites rather than a single resonance (J. H. Johnston pers. comm.).

The position of this broad ferric doublet is not consistent with published values for most of the iron-titanium oxides (Table 5.4).

The doublet appears to be due to ferric iron either in an altered ilmenite lattice or simply in a new structure formed as a weathering product. The accepted mechanism of ilmenite alteration (see section 2.2), requires no destruction of the oxide lattice - at least until the pseudorutile composition is reached (Grey and Reid 1975). Thus the observed ferric doublet can be attributed to a range of electronic environments, representing structures between ilmenite and pseudorutile.

Table 5.3 Mössbauer parameters of ilmenite spectra

Sample	Fig. No.	Peak Position (mm s^{-1})	Rel. Area	Chemical Isomer shift (mm s^{-1})	Quadrupole Splitting (mm s^{-1})	Component
Manukau ilmenite	5.8	-0.99±0.02	10	0.26±0.03	2.51±0.03	Inner doublet of 6 pk hematite
		-0.11±0.01	23	0.08±0.02	0.35±0.02	broadened ferric doublet
		0.24±0.01	30			
		0.51±0.01	95	0.85±0.02	0.68±0.01	Fe^{2+} - $FeTiO_3$
		1.19±0.01	100			
		1.52±0.01	15			
Bowentown ilmenite	5.9	-0.96±0.03	25	0.23±0.06	2.38±0.06	Inner two overlapping
		-0.10±0.01	33	0.07±0.02	0.33±0.02	doublets of magnetite
		0.23±0.01	32			broadened ferric doublet
		0.50±0.01	86	0.84±0.02	0.68±0.01	Fe^{2+} - $FeTiO_3$
		1.18±0.01	100			
		1.42±0.03	30			
Western Titanium ilmenite concentrate	5.10	-0.27±0.04	27			The broadened ferric doublet
		-0.10±0.02	70	0.09±0.06	0.5 ±0.1	above is enhanced and now
		0.37±0.02	50			resolved into three peaks
		0.52±0.01	100	0.87±0.02	0.69±0.01	Fe^{2+} - $FeTiO_3$
		1.21±0.01	90			
Westralian Sands ilmenite concentrate	5.11	-0.32±0.05	18			Broadening ferric resonance
		-0.12±0.02	95	0.15±0.08	0.6 ±0.1	from a range of sites, again
		0.43±0.01	100			resolved into three peaks
		0.54±0.01	70	0.87±0.02	0.67±0.01	Fe^{2+} - $FeTiO_3$
		1.21±0.01	73			
Westralian Sands HYTI 75	5.12	-0.25±0.02	100			Two doublets showing the
		-0.09±0.01	84	0.15±0.04	0.65±0.04	end members of the range of
		0.40±0.01	80			ferric sites in alteration
		0.56±0.03	98			products

The spectra of New Zealand ilmenites show the same Gaussian ferric resonance but to a far lesser degree, consistent with the relatively unweathered nature of the materials. Spectra are complicated by the presence of other iron-containing phases such as hematite (Manukau ilmenite) and magnetite (Bowentown ilmenite). The presence of hematite in the spectrum of Manukau ilmenite was confirmed by obtaining a spectrum using a velocity range of ±10 mm s^{-1}, where the six peak magnetic hyperfine hematite spectrum is observed (Fig. 5.13). Peak area comparison indicates that hematite accounts for approximately 20% of the total iron in the Manukau ilmenite sample.

Table 5.4 Mössbauer parameters for iron-titanium oxides

	Chemical isomer shift* (mm s^{-1})	Quadrupole splitting (mm s^{-1})	Reference
$FeTiO_3$ (Ilmenite)	0.86	0.70	Gibb et al 1969
Fe_2TiO_4 (Ulvospinel)	0.76	1.7	Avrahami & Golding 1969
Fe_2TiO_5 (Pseudobrookite)	0.05	0.75	Gibb et al 1969
$FeTi_2O_5$	0.88	1.62	Grey & Ward 1973

*Relative to Cu

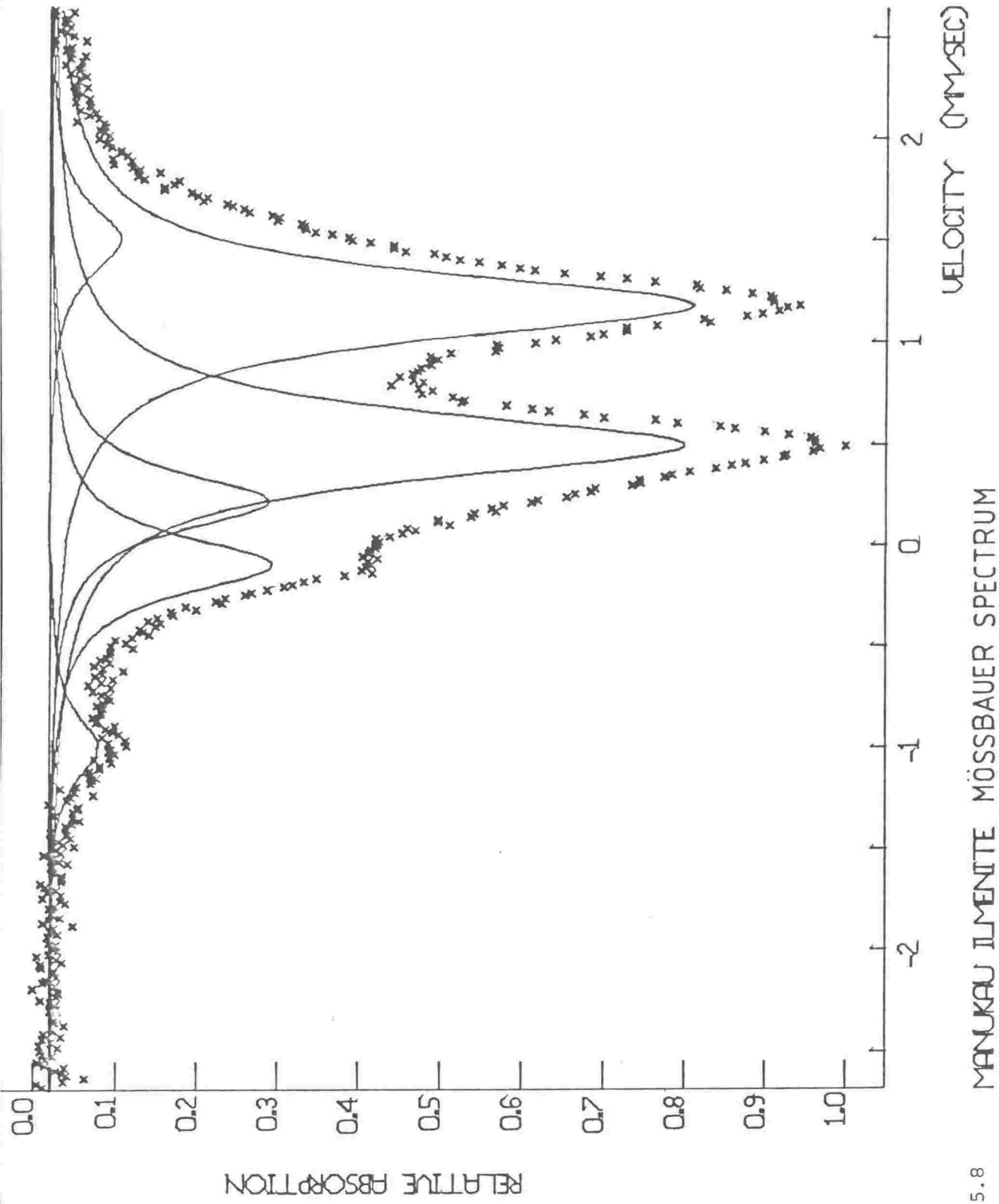
MANUKAU ILMENITE MÖSSBAUER SPECTRUM
RELATIVE ABSORPTION
VELOCITY (MM/SEC)
0.0
0.1
0.2
0.3
0.4
0.5
0.6
0.7
0.8
0.9
1.0
-2
-1
0
1
2

Fig. 5.8

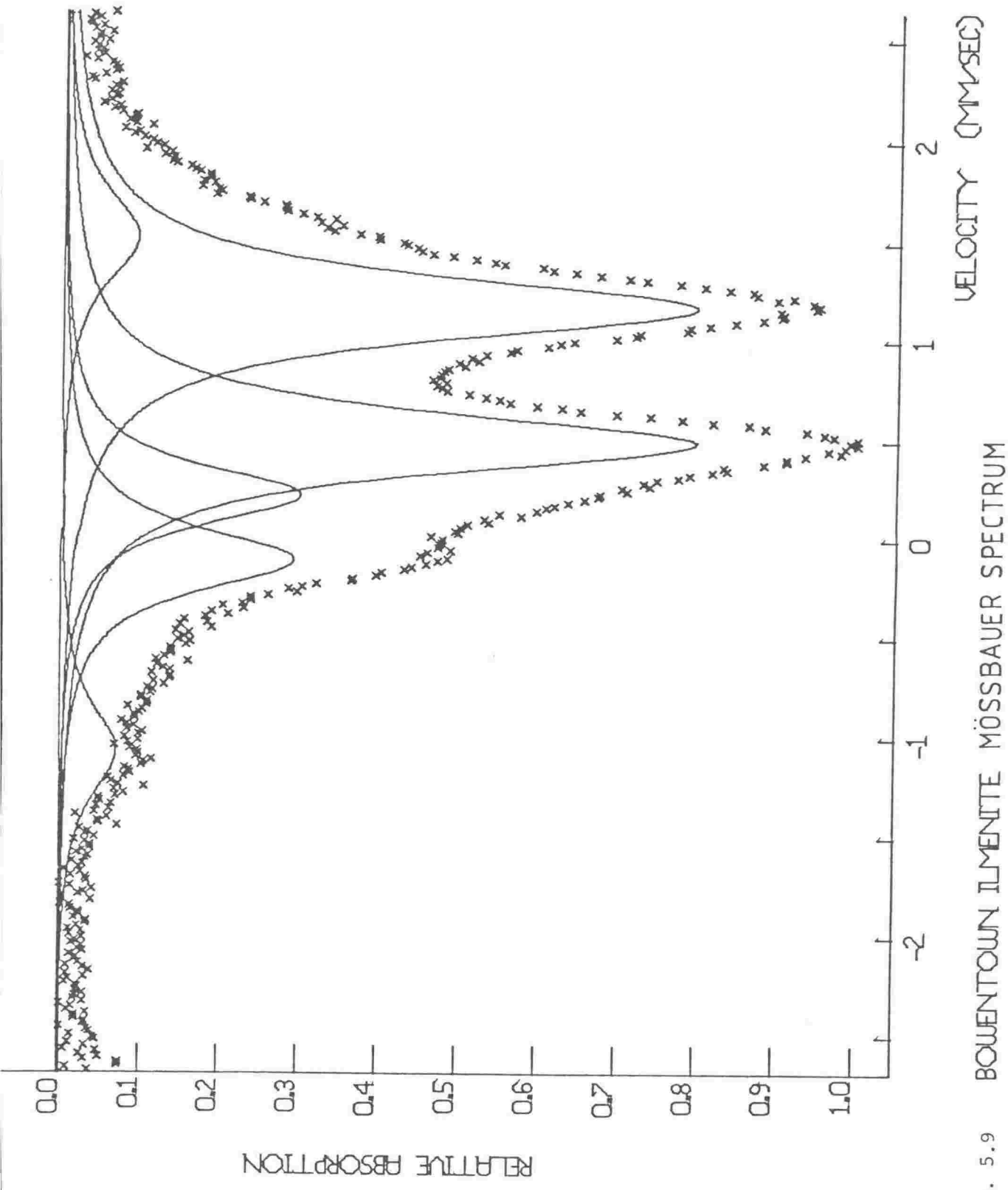
BOWENTOWN ILMENITE MÖSSBAUER SPECTRUM
RELATIVE ABSORPTION
VELOCITY (MM/SEC)
0.0
0.1
0.2
0.3
0.4
0.5
0.6
0.7
0.8
0.9
1.0
-2
-1
0
1
2

Fig. 5.9

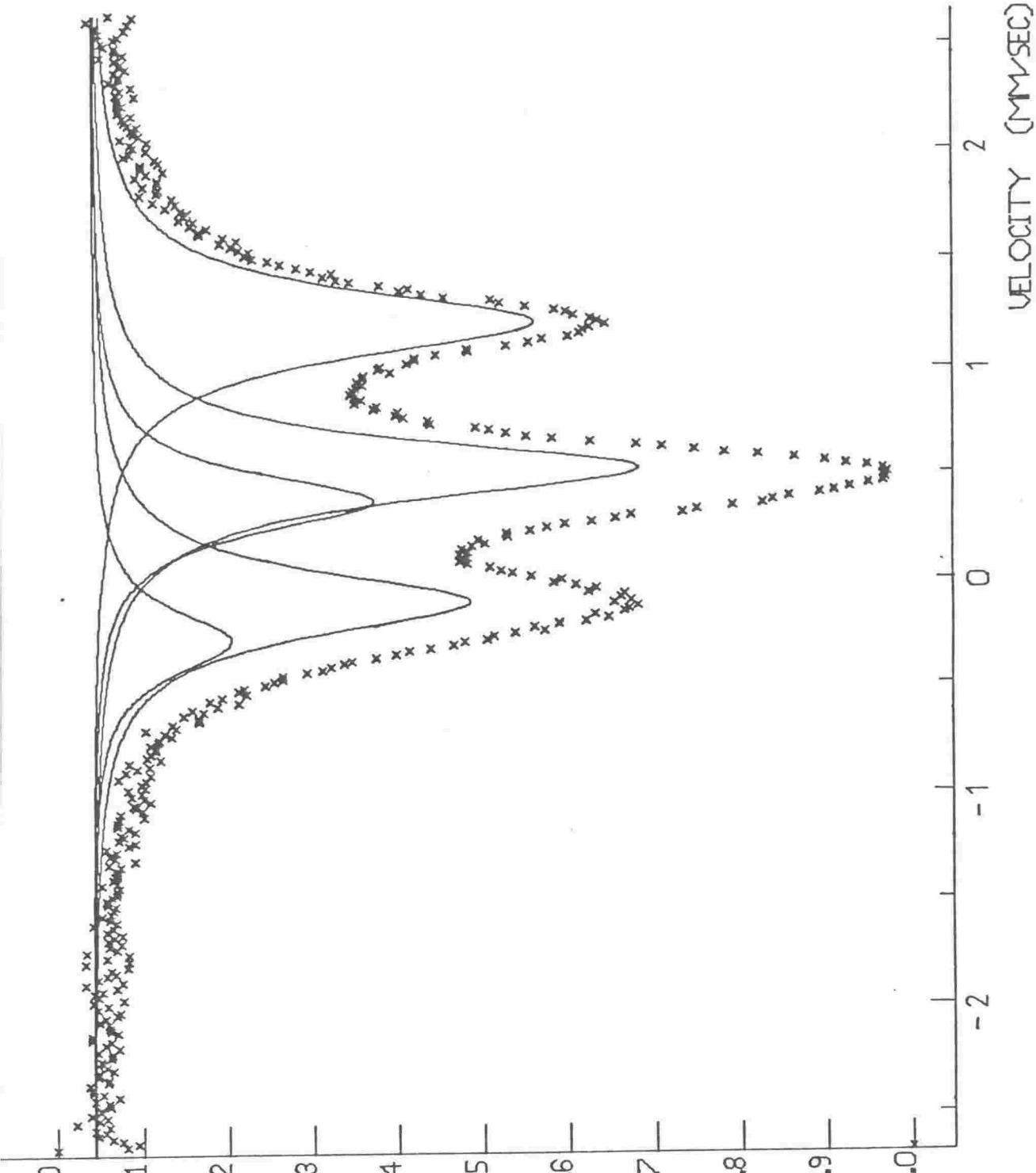
RELATIVE ABSORPTION
0.0
0.1
0.2
0.3
0.4
0.5
0.6
0.7
0.8
0.9
1.0
-2
-1
0
1
2
VELOCITY (MM/SEC)
WESTERN TITANIUM ILMENITE CONCENTRATE

Fig. 5.10

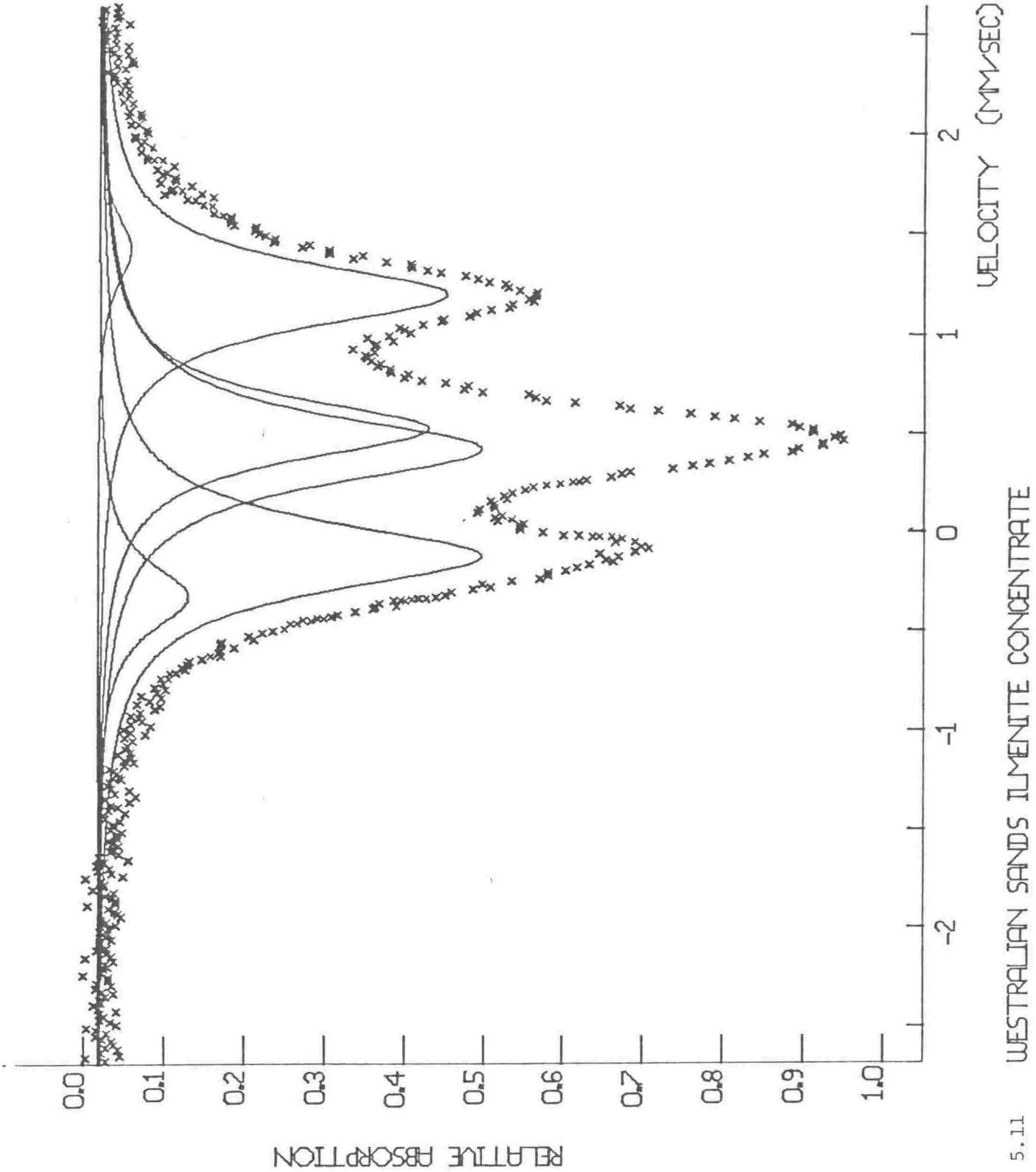

Fig. 5.11 WESTRALIAN SANDS ILMENITE CONCENTRATE

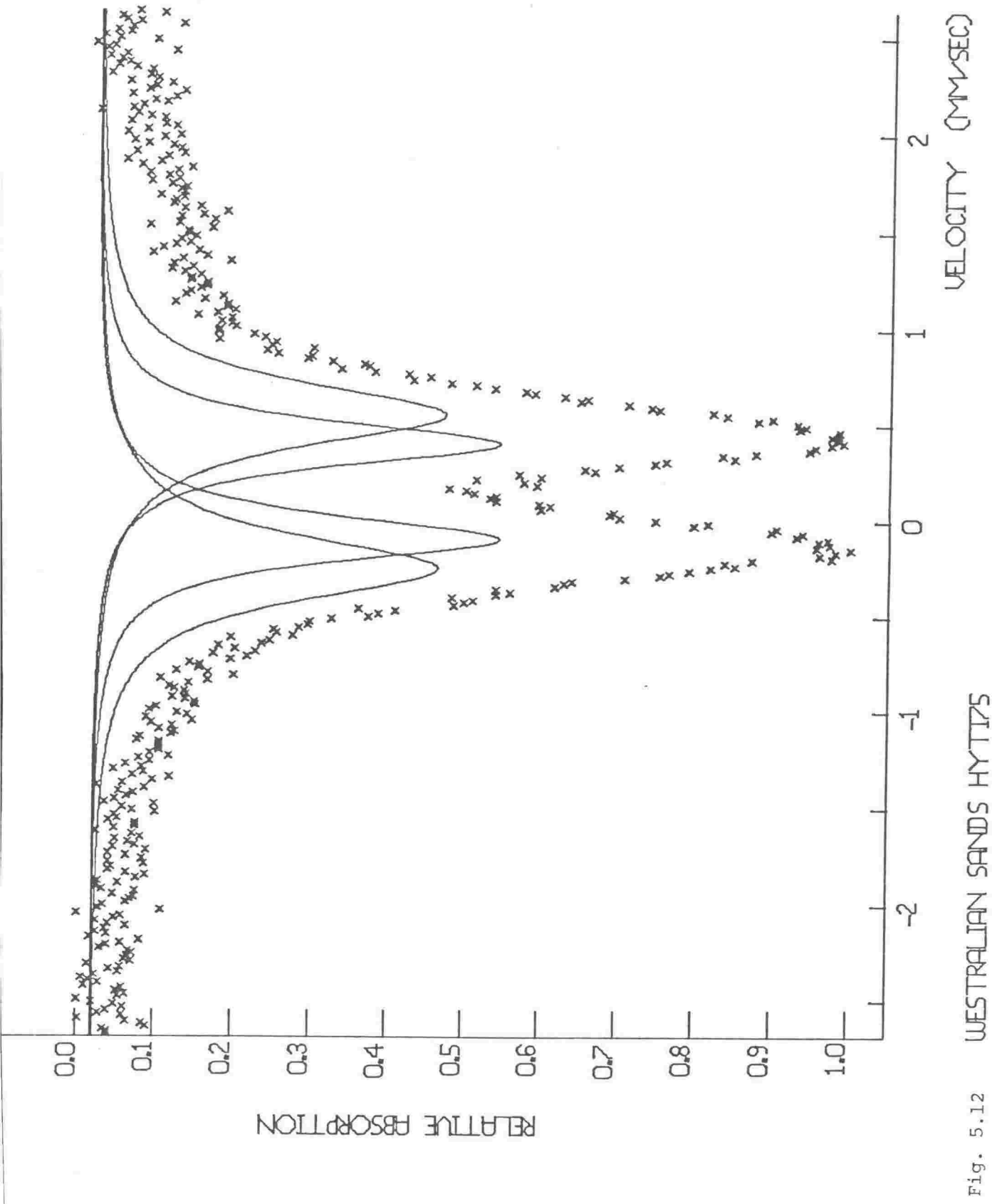
RELATIVE ABSORPTION
0.0
0.1
0.2
0.3
0.4
0.5
0.6
0.7
0.8
0.9
1.0
-2
-1
0
1
2
VELOCITY (MM/SEC)
WESTRALIAN SANDS HYTIPS

Fig. 5.12

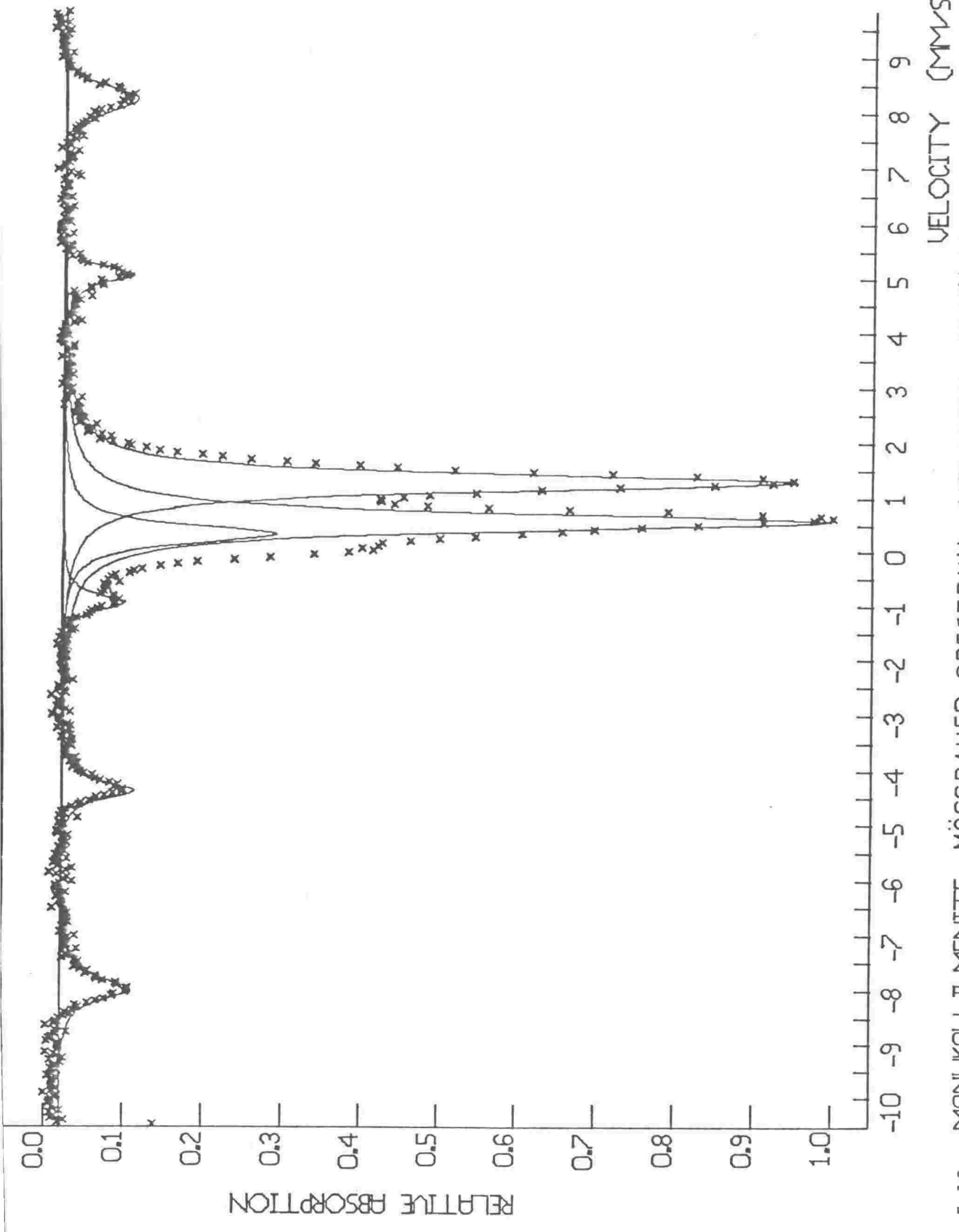

Fig. 5.13 MANUKAU ILMENITE MÖSSBAUER SPECTRUM - VELOCITY ±10 MM/S.

Chapter 6

SUMMARY AND CONCLUSIONS

6.1 Introduction

The purpose of this study was to investigate the factors influencing the reactivity of New Zealand ilmenites toward acid dissolution. Tauranga Bay ilmenite was used as the major raw material for study, as it is typical of the highly reactive South Island ilmenites and is extremely homogeneous by comparison to the other materials investigated.

Acid attack on ilmenite is a much exploited but only partially understood heterogeneous reaction:

$$Fe^{II}Ti^{IV}O_3 + 4H^+ \rightarrow Fe^{2+} + TiO^{2+} + 2H_2O$$

McConnel (1978) showed that the reaction was chemically controlled under the conditions he employed. However the reaction shows significantly different behaviour when low acid:ilmenite ratios are employed as in the work of Jain and Jena (1977) and in this work, which sought to resolve these discrepancies. The following conclusions were reached from experiments undertaken in the course of this study.

6.2 Mechanistic Conclusions

The dissolution of Tauranga Bay ilmenite in 1→10 M HCl occurs initially by proton attack at the ilmenite surface. There is evidence for the rapid dissolution of a ferric containing phase derived from both altered ilmenite and exsolution hematite. Dissolved iron is always dominant

over titanium in solution from the earliest stages of reaction, with the iron:titanium ratio directly related to acid strength.

Attack in the early stages of reaction is selective, with the formation of pores and channels parallel to the basal plane and to a lesser extent parallel to the $(10\bar{1}1)$ parting plane. This selective attack is not common to all grains and appears to relate to structural defects commonly observed in these planes in mineral ilmenite (see section 5.3.1).

The initial period of rapid and selective attack is not sustained and reaction rate declines, rapidly in medium strength (1→4 M) HCl and more slowly in strong (7→10 M) HCl. This decline is closely related to the extent of pore formation, which is largely complete within the first few hours of reaction.

The linearity of concentration versus $t^{\frac{1}{2}}$ plots over the first 1→2 hr of reaction, supports diffusion controlled dissolution over this period. It was proposed that the diffusion of polymeric titanium species through the porous solid is rate controlling during the period of pore and cavity formation. Titanium polymers may reach colloidal size and precipitate, with stabilization of the dissolved titanium determined by free acid and anion concentration. This explains why the decline in reaction rate is rapid at low acid strengths and more gradual in higher acid concentrations.

The titanium polymerisation problem is not prevalent in hydrochloric acid solutions if the titanium concentration is below $\approx 1\times10^{-2}$ M. In sulphuric acid solutions, this limit is considerably higher. Thus the type of behaviour outlined above is not significant when high acid:ilmenite ratios are used.

Dependence of the reaction on titanium concentration is clearly demonstrated in dissolution experiments where additional titanium was placed

in the acid solution before reaction. Reaction rate and ilmenite conversion were markedly impaired, whereas corresponding addition of iron had a negligible effect. The behaviour of dissolved titanium can also be regulated by the addition of other interferring reagents. Added phosphate causes titanium precipitation within and on the surface of the ilmenite grains, dramatically reducing dissolution rate. Added fluoride causes an immediate acceleration of dissolution rate, attributed to the stability of fluoride/titanium complexes which effectively prevent titanium polymerisation and/or hydrolysis.

Bulk and electron-microprobe analyses of the residual ilmenite show the dissolution reaction itself proceeds with near stoichiometric removal of iron, titanium and manganese, the cationic components of the ilmenite phase, in spite of the iron:titanium imbalance observed in the solution. Soluble inclusions such as apatite, dissolve within the first hour of reaction and the ilmenite residue becomes progressively enriched in acid resistant gangue minerals, mainly quartz and feldspars.

Activation energies for the dissolution reaction were determined from the temperature dependence of reaction rate, using both high and commercial level acid:ilmenite ratios. Values obtained were consistent with those reported by other workers and support chemical control of the reaction. However the curvature of concentration/time plots when using commercial level acid:ilmenite ratios makes even zero-time rates difficult to determine and indicates only chemical control at this stage, irrespective of the control mechanism later in the dissolution.

6.3 Other Ilmenites

The study of a range of other ilmenite concentrates was limited to the study of composition and structure. Weathered Australian concentrates show in cross-section a pattern of alteration zones resembling the pores and cavities observed in the early stages of acid dissolution. Alteration, like acid attack, occurs preferentially parallel to the basal plane and many altered grains show a streaked appearance in cross-section. In natural weathering, the titanium is retained within the oxide lattice which remains largely intact in the early stages.

Mössbauer spectroscopy reveals a shift in iron occupancy during weathering, from the unique ilmenite ferrous site, to a range of distorted octahedral ferric sites which have been proposed in this work, to represent lattice environments between an essentially ilmenite lattice and a pseudorutile type structure. High titanium concentrates show only this broad ferric resonance, while at the other end of the scale, unweathered New Zealand ilmenites show the dominant ferrous doublet with only traces of the ferric resonance.

6.4 Commercial Prospects

South Island New Zealand ilmenites are particularly reactive toward acid dissolution by comparison with more weathered overseas concentrates. Thus although these materials are relatively low grade in terms of titanium content ($\approx$46% TiO_2), they offer interesting possibilities for either upgrading to a rutile substitute, or pigment manufacture by the sulphate route. Hydrochloric acid dissolution offers distinct advantages over a sulphuric acid process, in terms of acid recovery and saleable by-products,

such as high grade Fe_2O_3. The problem is one of balancing the increased reactivity of this New Zealand ilmenite with the decreased effectiveness of hydrochloric acid as a dissolution medium, particularly as acid recovery is suited to medium strength acid (≈6 M).

This work has shown that to effect rapid dissolution of ilmenite, the acid solution must stabilize the dissolved titanium. In the absence of titanium polymerisation and hydrolysis, optimum dissolution rates can be achieved. The tendency of Cl^- ions to promote polymerisation makes hydrochloric acid an inherently inferior dissolution medium by comparison with sulphuric acid. The effectiveness of both acids can be improved by the addition of small amounts of fluoride, one of the few agents which complexes with Ti^{4+} and is stable under the conditions of acidity and temperature employed in ilmenite dissolution.

Fluoride addition has however, a number of undesirable side effects, particularly in plant design and corrosion levels. It also causes major difficulties in the recovery of dissolved titanium. The crude titanium product is generally recovered from solution after iron removal, by controlled hydrolysis, a reaction severely inhibited by titanium complexing. It is therefore desirable to remove the complexing agent following the dissolution step. This means that the conditions necessary for optimum dissolution i.e. Ti^{4+} stabilization, are counter-productive at the next stage of the titanium recovery process.

One potentially useful aspect of the dissolution reaction is the pattern of selective attack. The fresh surface exposed by grinding after partial dissolution, has been shown to markedly improve dissolution rate. Furthermore, the pore ridden appearance of many grains suggests that an intermittent regrinding of the partially dissolved ilmenite would be considerably more energy efficient than extensive grinding before reaction.

It is also apparent that column leaching of the ilmenite offers a means of avoiding titanium build-up in the solution during digestion. Jain and Jena (1977) found the same quantity of acid showed greater efficiency in leaching when passed through a column of ilmenite than when used in a single stage digestion. Although a multistage mixer cascade system has been studied for sulphuric acid digestion of ilmenite (Walker et al 1975), it appears that this type of process is worthy of further investigation, particularly with regard to hydrochloric acid digestion.

References

Anfinger E.M., Chervyakov P.I., Kamyshev A.K., Chernov B.I. and Sysolyatin S.A. (1973) Sb. Nauch. Tr. Omsk. Gos. Pedagog. 74, 83-8. Chem. Abs. Vol. 81, 141669.

Appleton D.E., Handwerker D.S. and Evans H.T. (1963) The Least Squares Refinement of Crystal unit cell data with Powder Diffraction data by automatic computer indexing method. Abstracts from Program of the annual meeting of the American Crystallographic Society.

Avrahami M. and Golding R.M. (1969) Mössbauer Spectroscopy as a tool in Analytical Chemistry. N.Z.J. Sci. 12, 594-605.

Bailey S.W., Cameron E.N., Spedden H.R., and Weege R.J. (1956) The Alteration of Ilmenite in beach sands. Econ. Geol. 51, 263-279.

Bancroft G.M. (1973) Mössbauer Spectroscopy (McGraw-Hill, London).

Barksdale J. (1949) Titanium (Ronald Press, New York).

Barraclough C.G., Lewis J. and Nyholm R.S. (1959). The stretching frequencies of Metal-Oxygen double bonds. J. Chem. Soc. Pt. 4, 3552-3555.

Barton A.F.M. and McConnel S.R. (1979) Dissolution behaviour of solids: the rotating disc method. Chemistry in Australia 46 (10), 427-433.

Barton A.F.M. and McConnel S.R. (1979) Rotating disc dissolution rates of ionic solids. Part 3 - Natural and synthetic ilmenite. Trans. Faraday Soc. I (4), 971-983.

Berner R.A., Sjöberg E.L., Velbel M.A. and Krom M.D. (1980) Dissolution of Pyroxenes and Amphiboles during weathering. Science 207 1205-1206.

Bertin E.P. (1978) Introduction to X-ray spectrometric analysis (Plenum-New York).

Beukemkamp J. and Herrington K.D. (1960) Ion exchange investigation of the nature of Titanium(IV) in sulphuric acid and perchloric acid. J. Am. Chem. Soc. 82, 3025.

Bircumshaw L.L. and Riddiford A.C. (1952) Transport control in heterogeneous reactions. Quart. Reviews 6, 157-185.

Bragina M.I. and Bobyrenko Yu Ya (1972) Infrared absorption spectra of sulphuric acid and hydrochloric acid solutions of titanium(IV). Russ J. Inorg. Chem. 17 (1), 61-64.

Cagliotti V., Ciavatta L. and Liberti A. (1960) Complexity of Titanium(IV) fluoride solutions. J. Inorg. Nucl. Chem. 15, 115-124.

Cotton F.A. and Wilkinson G. (1962) Advanced Inorganic Chemistry. (John Wiley and Sons).

Deer W.A., Howie R.A. and Zussman J. (1962) Rock forming minerals. Vol. 5. (Longmans - London).

Deer W.A., Howie R.A. and Zussman J. (1966) An introduction to the rock forming minerals. (Longmans - London).

Duncan J.F. and Richards R.G. (1976) Hydrolysis of titanium(IV) sulphate solutions. N.Z. J. Sci. 19, 171-178.

El-Hinniwai E.E. (1969) Electron-probe investigation of some intergrowths in iron-titanium minerals from Rosetta black sands. Contr. Mineral. and Petrol. 21, 332-337.

Elsdon R. (1975) Iron-Titanium oxide minerals in igneous and metamorphic rocks. Minerals Sci. Engng. 7 (1), 48-70.

Gibb T.C., Greenwood N.N. and Twist W. (1969). The Mössbauer spectra of natural ilmenites. J. Inorg. Nucl. Chem. 31, 947-954.

Glasstone S., Laidler K.J. and Eyring H. (1941) The theory of rate processes (McGraw-Hill, New York).

Goldanskii V.I. and Herber R.H. (1968) Chemical applications of Mössbauer Spectroscopy. (Academic Press).

Grey I.E. and Reid A.F. (1975) The structure of Pseudorutile and its role in the natural alteration of ilmenite. Am. Mineral. 60, 898-906.

Grey I.E. and Ward J. (1973) An X-ray and Mössbauer study of the $FeTi_2O_5$-Ti_3O_5 system. J. Solid State Chem. 7, 300-307.

Handbook of Chemistry and Physics (1974) R.C. Weast, Editor. CRC Press - Cleveland.

Imahashi M. and Takamatsu N. (1976) The dissolution of titanium minerals in hydrochloric and sulphuric acids. Bull. Chem. Soc. Japan 49 (6), 1549-1553.

Jackson J.S. (1975) A kinetic study of the dissolution of Allard Lake ilmenite in hydrochloric acid. Ph.D Thesis, University of Utah.

Jain S.K. and Jena P.K. (1977) Hydrochloric acid leaching of Gopalpur ilmenite. Ind. J. Technology 15, 398-402.

Johnston J.H. and Nixon J.E.A. (1971) Constant acceleration drive for Mossbauer experiments. N.Z. J. Sci. 14, 1107.

Judd B.T. and Palmer E.R. (1973) Production of Titanium dioxide from ilmenite of the West Coast, South Island, New Zealand. Proc. Australas. Inst. Min. Metall. 247, 23-33.

Judd B.T. (1977) The production of titanium dioxide from Westland ilmenite by hydrochloric acid leaching. N.Z. Dept Sci. Ind. Res. Report No. CD 2255.

Kennedy P.C., Roser B.P. and Palmer K. The analysis of major and trace elements by X-ray fluorescence spectrometry in the Analytical Facility, Victoria University of Wellington. Publ. Geol. Dept, Victoria University of Wellington, N.Z. (in prepn).

Lally J.S., Heuer A.H. and Nord G.L. (1976) Precipitation in the ilmenite-hematite system. From "Electron microscopy in mineralogy". Editor H.R. Wenk. Springer-Verlag, New York.

Levich V.G. (1962) Physicochemical Hydrodynamics (Prentice Hall - New Jersey).

Llewellyn W.B. and Crundell S.F.W. (1933) U.S. 1,876,065 from Chem. Abs 27, 170.

Lynd L.E. (1960) Study of the mechanism and rate of ilmenite weathering. Am. Inst. Mining, Metall. and Petrol. Eng. Trans. 217, 311-318.

Marshall T. and Finch J. (1967) High-titania slag smelting of New Zealand titanium ores. N.Z. J. Sci. 10, 193-205.

Martin W.R.B. (1955). The iron and titanium ores of New Zealand. N.Z. Eng. 10, 317-336.

McConnel S.R. (1978) Dissolution of ilmenite and related minerals in sulphuric acid. Ph.D Thesis, Murdoch University .

McPherson R.I. (1978) Geology of quaternary ilmenite-bearing coastal deposits at Westport. N.Z. Geol. Survey Bull. 87.

Minerals Research in CSIRO (1976) Ilmenite research in CSIRO - part 2. 12, 5-10.

Mott N.F. and Gurney R.W. (1948) Electronic processes in ionic crystals. Oxford Univ. Press, 2nd Edn.

Nabivanets B.I. and Kudritskaya L.N. (1967). A study of the polymerisation of titanium(IV) in hydrochloric acid solutions. Russ. J. Inorg. Chem. 12 (5), 616-620.

Nicholson D.S., Cornes J.J.S. and Martin W.R.B. (1958) Ilmenite deposits in New Zealand. N.Z. J. Geol. Geophys. 1, 611-616.

Nicholson D.S., Shannon W.T. and Marshall T. (1966) Separation of ilmenite, zircon and monazite from Westport beach sands. N.Z. J. Sci. 9, 586-598.

Overhault J.L., Vaux G. and Rodda J.L. (1950) The nature of arizonite. Am. Mineral. 35, 117-119.

Palmer E.R. and Judd B.T. (1973) The production of high-titania products from ilmenite by a sulphuric acid process. N.Z. Eng. 28 (8), 227-233.

Pogorelov V.I. and Boitenev N.A. (1974) The nature of chemical bonding in some titanium and iron minerals. Deposited Documents VINITI 1446-1474. Chem. Abs. 86, 132610.

Price W.J. (1972) Analytical Atomic Absorption Spectrometry. (Heyden and Son Ltd - London).

Raymond K.N. and Wenk H.R. (1971) Lunar ilmenite (refinement of the crystal structure). Contr. Mineral. and Petrol. 30, 135-140.

Richards R.G. (1975) Aspects of the hydrolysis of titanium(IV) sulphate solutions. Ph.D Thesis, Victoria University of Wellington.

Robinson R.A. and Harned H.S. (1941) Some aspects of the thermodynamics of strong electrolytes from electromotive force and vapour pressure measurements. Chem. Reviews 28, 419-476.

Robinson R.A. and Stokes R.H. (1959). Electrolyte Solutions. 2nd Edn. Butterworths - London.

Ruby S.L. and Shirane G. (1961). Magnetic anomaly in $FeTiO_3$-αFe_2O_3 system by Mössbauer effect. Phys. Review, 123 (4), 1239-1240.

Sakai N., Yoshikawa K., Suzuki M. and Kobashi S. (1961) The hydrolysis of titanium sulphate solutions. Kogyo Kagaku Zasshi 64 (4) 613. Chem. Abs. 57, 3077.

Sarver L.A. (1927) The determination of ferrous iron in silicates. J. Am. Chem. Soc. 49, 1472-1477.

Selbin J. (1964) Metal oxocations. J. Chem. Ed. 41, 86-92.

Shirane G., Cox D.E. and Ruby S.L. (1962) Mössbauer study of Isomer Shift, Quadrupole Interaction and Hyperfine Field in several oxides containing Fe^{57}. Phys. Review 125 (4), 1158-1165.

Shirane G., Cox D.E., Takei W.J. and Ruby S.L. (1962) A study of the magnetic properties of the $FeTiO_3$-αFe_2O_3 system by Neutron Diffraction and the Mössbauer Effect. J. Phys. Soc. Japan 17 (10), 1598-1611.

Singhvi A.K., Gupta D.K., Gokhale K.V.G.K., and Rao G.N. (1974) Mössbauer spectra of ilmenites from primary and secondary sources. Phys. Stat. Sol.(a) 23, 321-324.

Sinha N. H. (1973) Murso Process for producing rutile substitute. in 'Titanium Science and Technology'. Vol. 1, p.233 (Plenum Press - New York).

Sinibaldi M. (1973) J. Chromatog. 76 (1), 280.

Stone A.J. (1967) Least squares fitting of Mössbauer spectra. Appendix to Bancroft G.M., Maddock A.G., Ong W.K. and Prince R.H. Mössbauer spectra of iron(III) diketone complexes. J. Chem. Soc. A. 1966.

Temple A.K. (1966) Alteration of ilmenite. Econ. Geol. 61, 695-714.

Teufer G. and Temple A.K. (1966) Pseudorutile - a new mineral intermediate between ilmenite and rutile in the natural alteration of ilmenite. Nature 211, 179-181.

Thomas A.W. and Tai A.P. (1932) The nature of aluminium oxide hydrosols. J. Am. Chem. Soc. 54 (3), 841-855.

Walker B.V. (1967) Titanium dioxide from New Zealand titaniferous materials. N.Z. J. Sci. 10, 3-25.

Walker B.V., Judd B.T., Taylor B.A. and Kemp R.M. (1975) Experiments with a mixer-cascade for the sulphuric acid digestion of ilmenite. N.Z. Eng. 30 (4), 108-110.

Whitehead J., Williams F.R., Gosden D.V. and Woodhouse G. (1972) Processing of material containing iron and titanium. Ger. Offen 2,124,105. Chem. Abs. 76, 48580.

Zhukov A.I. and Nazarov A.S. (1964) Sorption of titanium(IV) by KU-1 cation-exchange resin. Russ. J. Inorg. Chem. 9 (6), 794-797.